CHEMICAL INTERACTIONS BETWEEN IRON AND ARSENIC IN WATER

Richard Johnston

A dissertation submitted to the faculty of the University of North Carolina at Chapel Hill in partial fulfillment of the requirements for the degree of Doctor of Philosophy in the Department of Environmental Sciences and Engineering, School of Public Health

Chapel Hill
2008

Approved by:

Philip C. Singer

Cass T. Miller

Larry Benninger

William Glaze

Dharni Vasudevan

Urs von Gunten

ABSTRACT

Richard Johnston: Chemical interactions between iron and arsenic in water
(Under the direction of Philip C. Singer)

This dissertation presents results from a series of experiments involving precipitation of ferrous arsenate, redox reactions between various Fe/As couples, and competitive adsorption. Batch and column experiments were made and interpreted quantitatively using geochemical modeling.

A new solubility constant was calculated for symplesite, a ferrous arsenate mineral, and geochemical modeling suggests that some arsenic-impacted groundwaters in Bangladesh are super-saturated with respect to this mineral. Oxidation experiments demonstrated that oxygenation of Fe(II) is much faster in the presence of inorganic buffers than when non-complexing organic buffers are used. Fe(II) oxidation was largely unaffected by the presence of the hydroxyl radical scavenger propanol. These findings call into question the classic formulation of Fe(II) oxygenation, and long-accepted kinetic rate constants.

During the oxygenation of Fe(II), As(III) competes with Fe(II) for reactive oxidizing species. As(III) oxidation is reduced in the presence of inorganic ligands, most likely because these ligands increase the reactivity of dissolved Fe(II).

Competitive adsorption experiments using goethite demonstrated relatively minor competitive effects between As(III) and As(V), and between As(III) and Fe(II). Batch experiments showed that much more Fe(II) was removed from solution than As(III) or As(V)

after contacting the goethite surface. This could be explained by the existence of sites which can adsorb Fe(II) but not As. However, surface complexation modeling with this approach could not capture some of the aspects of multi-component adsorption. An alternate explanation could be that upon adsorption Fe(II) transfers an electron into the bulk surface of the goethite, regenerating Fe(III) at the surface and allowing more adsorption to take place.

Column experiments were performed to simulate *in situ* removal of arsenic and iron, and demonstrated that an alternating push-pull configuration can lead to consistent retardation of both solutes. A 'ripening' effect, whereby the *in situ* process becomes increasingly efficient as more Fe(III) is emplaced on sediment surfaces, was observed at pH 8, where the process increased the amount of iron oxide in the column by more than 50%, even though the column iron oxide concentration was lower than in naturally arsenic-impacted aquifers such as Bangladesh, implying that *in situ* treatment in such settings is feasible.

ACKNOWLEDGEMENTS

I would first of all like to thank my dissertation advisor, Professor Phil Singer, for allowing me to explore my interests in arsenic, even though it was not an area of active research for him, and for all the mentoring and guidance he has provided me over the years. I could never have set up the UNC laboratory experiments, especially that beautiful old AAS and all the column plumbing, without the assistance of Glenn Walters and Randy Goodman, and I thank Professor Dharni Vasudevan for the use of her glovebox and laboratory at Duke. I also thank the other members of my dissertation committee, Professors Casey Miller, Larry Benninger and Bill Glaze (Emeritus) at UNC, and Urs von Gunten at EAWAG, for their advice and patience. I greatly appreciate the fellowships provided by the UNC Graduate School and the National Science Foundation which made this work possible.

I am grateful to UNICEF for giving me the opportunity to work on arsenic mitigation in Bangladesh both before and after my time at UNC. It has been a privilege and a great learning experience, in spite of all the challenges. Thanks to my colleagues there for their friendship and support, and to my supervisor Paul Edwards for endorsing my request to take time off (during the monsoon flood season, even) to complete and defend this dissertation.

Thanks to my parents for all their encouragement and support over many years, even when email contact has slowed to a trickle. Finally, thanks most of all to my wife Heidi for making the space for me to work on this project, taking on more than her share of kid management during vacations and weekends, and tolerating countless late nights at the computer, without ever complaining.

TABLE OF CONTENTS

Page

LIST OF TABLES

Page

LIST OF FIGURES

Page

CHAPTER 1: INTRODUCTION

1.1 Background

Arsenic is a drinking water contaminant of great public health concern, as low levels of exposure can lead to a variety of cancer (skin, lung, bladder) and non-cancer (diabetes mellitus, vascular hypertension, dermal lesions) endpoints (WHO 2001). In 2001, the USEPA lowered its maximum contaminant level (MCL) for arsenic in drinking water from 50 to 10 µg/L (USEPA 2001b).

Widespread arsenic contamination of groundwater affects tens of millions of people in Asia and Latin America, with arsenic levels of over 1000 µg/L frequently reported. In the United States such gross contamination has been reported in only a few instances, but a large number of municipalities face low-level arsenic contamination, chiefly in their groundwater sources. It is estimated that 5% of U.S. municipalities will need to provide some kind of treatment to comply with the new MCL (USEPA 2001b). The vast majority of affected systems are small utilities servicing fewer than 10,000 people. Estimates of annualized compliance costs in the U.S. range widely, from 180 million dollars (USEPA 2000) to 955 million dollars (Frey, Owen et al. 1998), but the arsenic rule will be expensive by any standard.

Most arsenic removal technologies take advantage of the strong attraction between arsenic and metal oxides, particularly iron oxides. Coagulation with alum or ferric chloride followed by settling and filtration is the most commonly applied technology, though fixed-

bed adsorption onto granular ferric hydroxide is gaining in popularity. Ion exchange and reverse osmosis are also potential treatment technologies, but have not found as wide application. Most of these treatment trains require pre-oxidation, since arsenate [As(V)] is much easier to remove than arsenite [As(III)]. Small systems often have no treatment apart from chlorination and corrosion control, so adding an arsenic removal train will require considerable infrastructure modifications and training.

Subsurface immobilization of arsenic might be an effective alternative to above-ground treatment (Rott and Friedle 2000). *In situ* immobilization of ferrous iron has been practiced effectively for decades, chiefly in Europe (e.g. Braester and Martinell 1988b; Mettler, Abdelmoula et al. 2001; Mettler 2002). In this technology, a volume of oxygenated water (usually groundwater that has been extracted and saturated with dissolved oxygen or air) is injected into the subsurface where it oxidizes native ferrous iron to form an insoluble ferric hydroxide coating on mineral surfaces. Iron-free water can then be withdrawn from the aquifer for extended periods before dissolved iron breaks through. The efficiency of the process, defined as the volume ratio of groundwater abstracted to oxidized water injected, ranges from about 3 to 12 (Appelo, Drijver et al. 1999) and typically increases with time. Since ferric hydroxide is a strong scavenger of arsenic, and arsenic-impacted groundwater often has high levels of ferrous iron (Nickson, McArthur et al. 2000), it might be possible to take advantage of the freshly precipitated ferric oxide to adsorb arsenic from solution. The concept has only been examined in a handful of pilot plants, but results seem encouraging (Welch, Stollenwerk et al. 2000; Sarkar and Rahman 2001; Rott, Meyer et al. 2002).

In situ treatment for arsenic control offers several obvious advantages relative to above-ground treatment: minimal new infrastructure is required, no hazardous chemicals are

used, and since operation is simple and requires no special scientific or technical background, recurring costs are low. Water quality would be improved by removing iron and possibly manganese along with arsenic. Another advantage in the case of arsenic removal is that no arsenic-rich wastes are produced at the surface – management of such residuals in traditional treatment plants can add a significant burden to utilities.

Although *in situ* arsenic removal has been demonstrated in several pilot studies, the mechanisms controlling removal are not well understood. It is not clear why arsenic removal varies widely, from 50% (Sarkar and Rahman 2001) to over 90% (Rott, Meyer et al. 2002). Key mechanisms at work include competitive adsorption of both iron and arsenic onto ferric oxide surfaces, and heterogeneous oxidation of iron and possible arsenic. Authigenic precipitation of minerals containing ferrous iron and/or arsenic could also play a controlling role in subsurface transport.

1.1.1 Geochemistry of arsenic and iron

1.1.1.1 Arsenic

In natural waters arsenic is found in the +III and +V oxidation states. Arsenite [As(III)] is uncharged at environmental pH, while arsenate [As(V)] is usually present as an anion with a charge of minus one or two (see Figure 1-1 and Table 1-1). Arsenate is thermodynamically favored under oxidizing conditions, while arsenite should prevail in reduced settings such as groundwater. Because of slow redox kinetics, arsenic is often out of redox equilibrium in natural systems. Complexation with inorganic cations or organic matter can also change oxidation kinetics.

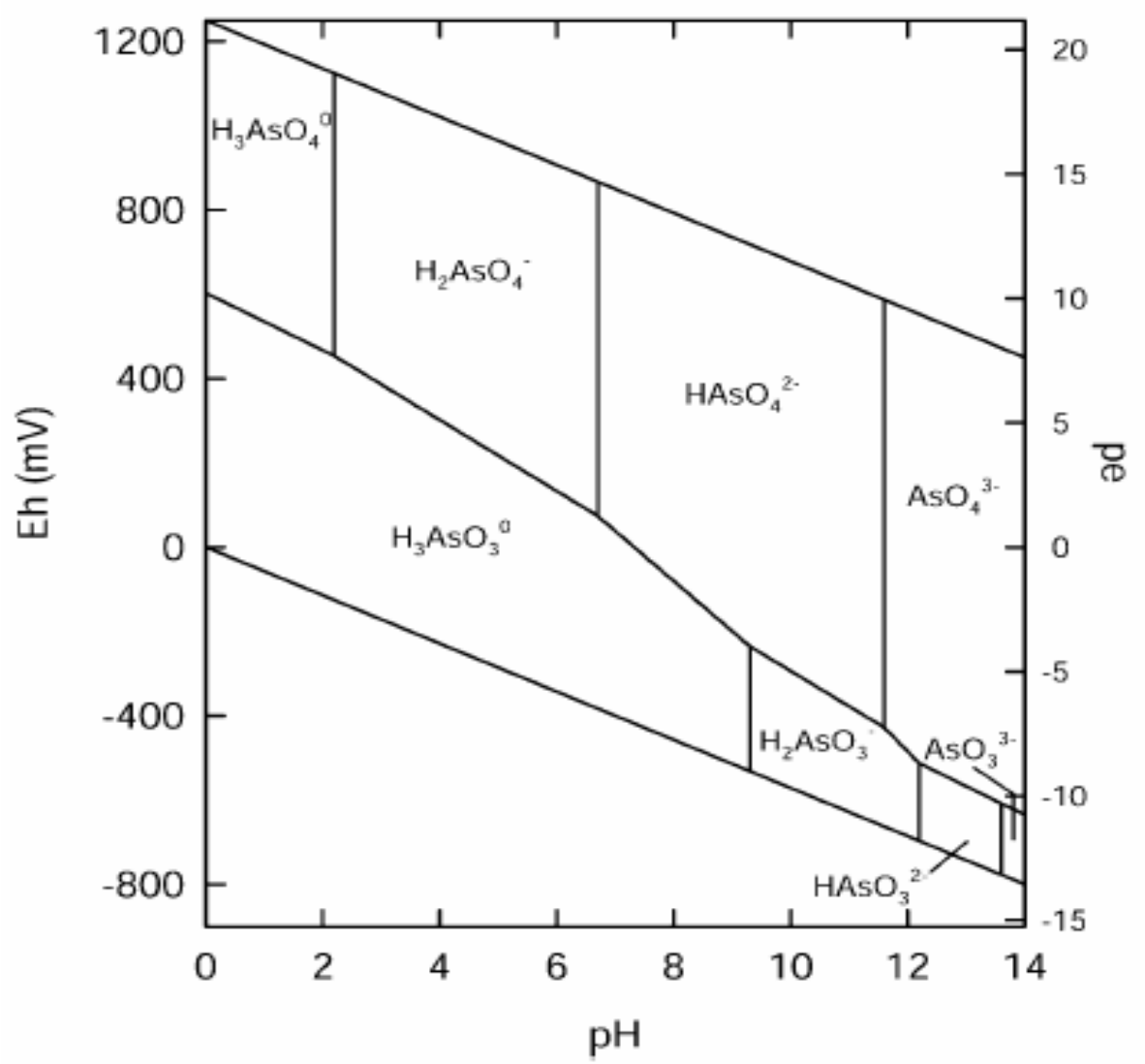

Figure 1-1: pe-pH diagram for arsenic at 25 °C (Smedley and Kinniburgh 2002)

Table 1-1: Acidity constants for arsenate and arsenite (Smith and Martell 2001)

Reaction	-log K
Arsenate (arsenic acid)	
$H_2AsO_4^- + H^+ = H_3AsO_4$	2.24
$HAsO_4^{-2} + H^+ = H_2AsO_4^-$	6.96
$AsO_4^{-3} + H^+ = HAsO_4^{-2}$	11.50
Arsenite (arsenious acid)	
$H_2AsO_3^- + H^+ = H_3AsO_3$	9.22
$HAsO_3^{-2} + H^+ = H_2AsO_3^-$	12.11
$AsO_3^{-3} + H^+ = HAsO_3^{-2}$	13.41

Arsenic levels in groundwaters vary widely, depending on the mineral or sediment type and geochemical conditions. Minerals, especially iron oxides, are thought to control arsenic mobility. Arsenic concentrations are typically below 10 µg/L, but widespread areas have been found (e.g. in China, India, Bangladesh, Taiwan, Argentina, Mexico and Hungary) where concentrations can reach up to 5000 µg/L (Smedley and Kinniburgh 2002). Arsenic levels are lower in the USA, with only a handful of municipalities reported concentrations greater than 50 µg/L. However, individual US wells can contain extreme concentrations of arsenic (up to 12 mg/L) in rare cases (Schreiber, Simo et al. 2000), and levels of 10-50 µg/L are not uncommon (Chen, Frey et al. 1999; Welch, Westjohn et al. 2000).

In groundwaters not impacted by acid mine drainage or geothermal waters, there are two main geochemical environments that can lead to arsenic mobilization: anoxic conditions, and arid oxidizing environments (Smedley and Kinniburgh 2002; Ravenscroft 2008). In both cases, a significant portion of the mobilization is due to the failure of iron oxide minerals to retain arsenic. Under anoxic conditions, iron oxides undergo reductive dissolution, liberating any adsorbed trace elements. In arid oxidizing environments, groundwater is often alkaline, which decreases the positive charge on oxide surfaces, making adsorption of anions such as arsenate less favorable. Since iron oxides typically have points of zero charge near pH 7 or 8 (Schwertmann and Cornell 2000), they may actually bear a negative charge in these environments.

A third mechanism for arsenic mobilization is through oxidation of arsenic-bearing sulfidic minerals, especially pyrite and arsenopyrite. This mechanism is mainly found in areas of precious metal mining, though it may occur to a limited extent in reducing aquifers as well (Smedley and Kinniburgh 2002; Ravenscroft 2008).

In sediments, the element which correlates best with arsenic levels is frequently iron, and arsenic-rich groundwater often has high levels of dissolved iron, especially under reducing conditions (Smedley and Kinniburgh 2002).

1.1.1.2 Iron

Dissolved iron in groundwater is a much more pervasive problem than dissolved arsenic. There are no negative health impacts of dissolved iron in drinking water, but because of the aesthetic problems caused by iron, including taste, color and staining, the USEPA has set a secondary maximum contaminant level (SMCL) of 0.3 mg/L. SMCLs are not enforced by EPA, but iron removal is common in order to satisfy consumer expectations.

Fe(III) (ferric iron) is practically insoluble above pH 3 (see Figure 1-2), though ferric colloids can contribute to iron in drinking water. Iron speciation in groundwater is dominated by dissolved Fe(II) (ferrous iron). Due to microbial reduction of FeOOH, where FeOOH is the terminal electron acceptor, dissolved Fe(II) frequently exceeds 10^{-4} M (5.5 mg/L) or even 10^{-3} M (55 mg/L) in groundwater (Tyrrel and Howsam 1997).

The solubility of both ferrous and ferric iron is limited by a number of minerals, most of which are more soluble under acidic conditions (Table 1-2). The more crystalline ferric minerals (goethite, hematite) are much less soluble than the amorphous ferrihydrite.

Ferric minerals may include oxides (hematite), oxyhydroxides (goethite), and hydroxides (ferrihydrite), all of which can be present in natural systems. Most iron oxides have a point of zero charge (pH_{PZC}) in the range of pH 7 to 8 (Table 1-3), so they could be either positively or negatively charged in natural waters.

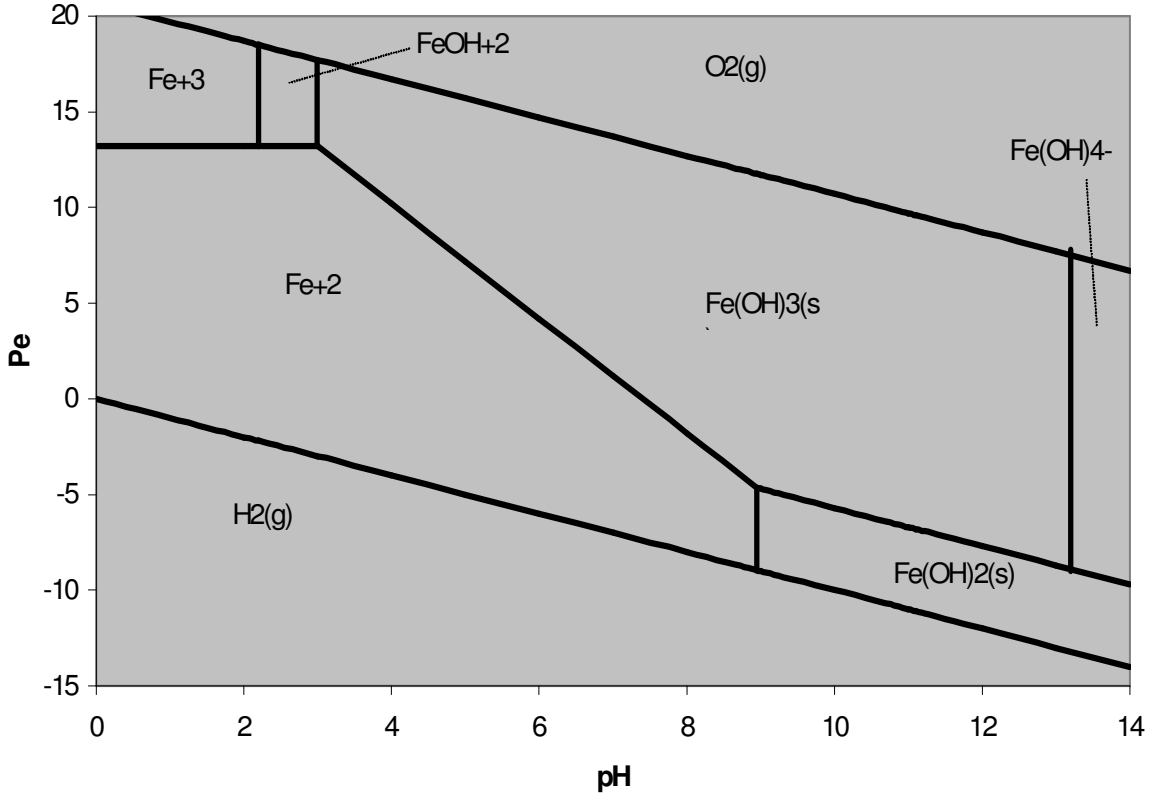

Figure 1-2: pe-pH stability diagram for 10^{-5} M iron, 25°C (after Stumm and Morgan 1996)

Table 1-2: Solubility of Fe(II) and Fe(III) minerals (Stumm and Morgan 1996; Parkhurst and Appelo 1999)

Mineral name	Dissolution reaction	log K_{so}
Ferrous iron		
Siderite	$FeCO_3 = Fe^{+2} + CO_3^{-2}$	-10.89
Pyrite	$FeS_2 + 2H^+ + 2e^- = Fe^{+2} + 2HS^-$	-18.48
Ferrous sulfide (amorphous)	$FeS + H^+ = Fe^{+2} + HS^-$	-3.92
Mackinawite	$FeS + H^+ = Fe^{+2} + HS^-$	-4.65
Ferric iron		
Ferrihydrite	$Fe(OH)_3 + 3H^+ = Fe^{+3} + 3H_2O$	3.0 – 5.0
Goethite	$FeOOH + 3H^+ = Fe^{+3} + 2H_2O$	-1.0
Hematite	$Fe_2O_3 + 6H^+ = 2Fe^{+3} + 3H_2O$	-4.0
Mixed valence iron		
Magnetite	$Fe_3O_4 + 8H^+ = 2Fe^{+3} + Fe^{+2} + 4H_2O$	3.74

Table 1-3: Points of zero charge for common iron oxides

Mineral Name	Formula	pH_{PZC}	Source
Goethite	α-FeOOH	7.0 – 8.0	(Sposito 1989)
		7.55	(Atkinson, Posner et al. 1967)
		8.5	(Peacock and Sherman 2004)
		8.7	(Manning and Goldberg 1996)
		8.9	(van Geen, Robertson et al. 1994)
Akaganeite	β-FeOOH	7.3	(Solozhenkin, Deliyanni et al. 2003)
		7.5	(Lazaridis, Bakoyannakis et al. 2005)
Lepidocrocite	γ-FeOOH	7.3	(Zhang, Charlet et al. 1992)
		7.7	(Peacock and Sherman 2004)
Ferrihydrite	$Fe(OH)_3$[1]	8.1	(Dzombak and Morel 1990)
Hematite	α-Fe_2O_3	8.0 – 8.5	(Sposito 1989)
		8.8	(Peacock and Sherman 2004)
		8.5 – 9.3	(Atkinson, Posner et al. 1967)

1.1.2 Adsorption onto iron oxides

1.1.2.1 Surface complexation theory

The concentration of many trace elements, including arsenic, in natural waters is limited by the availability of surface sites for adsorption. In natural sediments, natural organic matter (NOM), clays, and metal oxides can all complex trace constituents, but the oxides, particularly of iron, are thought to play the most important role (Dzombak and Morel 1990).

The binding of dissolved ions with functional groups at a surface can be considered as analogous to reactions that occur in solution, such as the formation of metal-ligand or proton-

[1] The term "ferrihydrite" is often used to describe an amorphous ferric solid with approximate formula $Fe(OH)_3$. Sometimes the alternate formulas Fe_5HO_8-$4H_2O$ or Fe_2O_3-H_2O are also used. The solid is also referred to as "amorphous ferric hydroxide" or "hydrous ferric oxide" in the literature.

base complexes. The adsorption of metals results in the displacement of protons from the surface:

$$>Fe(III)OH + M^{+2} = >Fe(III)OM^{+} + H^{+} \quad \text{(Equation 1-1)}$$

where > represents the oxide surface. Anion adsorption results in ligand exchange with surface hydroxyl groups:

$$>Fe(III)OH + A^{-2} = >Fe(III)A^{-} + OH^{-} \quad \text{(Equation 1-2)}$$

Surface complexation modeling (SCM), as developed by Stumm and co-workers (Singer and Stumm 1970; Schindler and Stumm 1987; Stumm 1992), involves the quantification of these adsorption reactions with equilibrium constants. For example, for the anion A^{-2}, the equilibrium relationship is:

$$K^{app} = \frac{\{>Fe^{III}A^{-}\}\{OH^{-}\}}{\{>Fe^{III}OH\}\{A^{-2}\}} \quad \text{(Equation 1-3)}$$

where K^{app} is the apparent equilibrium constant, and { } represents activity. Activities of surface species are commonly assumed to be proportional to their concentration (Stumm and Morgan 1996) for low ionic strength conditions.

In classical surface complexation modeling, the iron oxide surface is considered to consist of a single type of surface hydroxyl group, which can protonate or deprotonate, resulting in a local surface charge of –1, 0, or +1 (Dzombak and Morel 1990):

$$>Fe(III)OH + H^+ = >Fe(III)OH_2^+ \quad \text{(Equation 1-4)}$$

$$>Fe(III)OH = >Fe(III)O^- + H^+ \quad \text{(Equation 1-5)}$$

Surface complexation modeling recognizes that the surface can be charged, and that ions will need to diffuse across an electrostatic gradient before binding at the surface. The apparent adsorption constant can be broken up into an intrinsic term, describing the formation of a chemical bond with a hypothetical uncharged surface, and a Coulombic term, describing the electrostatic effect of the charged surface.

$$K^{app} = K^{int} \exp(\Delta Z F \Psi / RT) \quad \text{(Equation 1-6)}$$

where K^{int} is the intrinsic equilibrium constant, ΔZ is the net change in surface charge, F is Faraday's constant, Ψ is the surface potential, R is the gas constant, and T is the absolute temperature.

Clearly, a charged surface will repel ions of like charge and attract oppositely charged ions, so adsorption is favored at high pH for metals and low pH for anions. However, the intrinsic chemisorption term can overcome a Coulombic repulsion: adsorption of metals onto metal oxides below the point of zero charge is well-known (Stumm and Morgan 1996). Surface charge must be balanced by counterions in the solution phase. This can be modeled in a number of different ways, the most common of which are the diffuse layer, constant capacitance and triple layer models (Davis and Kent 1990; Dzombak and Morel 1990).

A number of proprietary or free surface complexation codes are available; the most commonly used are USEPA's MINTEQA2 (Allison, Brown et al. 1991) and USGS's PHREEQC (Parkhurst and Appelo 1999). In this work, PHREEQC is used, since it has the ability for simple one-dimensional transport with advection and diffusion, unlike MINTEQA2, which is purely an equilibrium speciation model. A related program, PHAST (Parkhurst, Kipp et al. 2008), extends PHREEQC's transport abilities into three dimensions by using the transport code HST3D. PHREEQC was revised in 1999, and contains kinetic modeling options not available in MINTEQA2.

All of the surface complexation codes make use of the Dzombak and Morel compilation (1990) of adsorption constants onto ferrihydrite. Constants are available for 12 cations (Ag^{+}, Ba^{+2}, Ca^{+2}, Cd^{+2}, Co^{+2}, Cr^{+3}, Cu^{+2}, Hg^{+2}, Ni^{+2}, Pb^{+2}, Sr^{+2}, Zn^{+2}), 8 anions (AsO_4^{-3}, CrO_4^{-2}, PO_4^{-3}, SO_4^{-2}, $S_2O_3^{-2}$, SeO_3^{-2}, SeO_4^{-2}, VO_4^{-3}) and 2 uncharged species (H_3AsO_3, H_3BO_3). The compilation lacks constants for ferrous iron and carbonate, both of which are required for this dissertation. Other researchers have published binding constants for ferrous iron (Coughlin and Stone 1995; Liger, Charlet et al. 1999; Appelo, Van der Weiden et al. 2002) and carbonate (Zachara, Girvin et al. 1987; van Geen, Robertson et al. 1994; Villalobos and Leckie 2000; Wijnja and Schulthess 2001; Appelo, Van der Weiden et al. 2002), using new experimental evidence or linear free energy relationships.

A similar compilation of adsorption constants onto goethite has recently been published (Mathur and Dzombak 2006), with constants available for 9 cations (Ca^{+2}, Cd^{+2}, Co^{+2}, Cr^{+3}, Cu^{+2}, Hg^{+2}, Ni^{+2}, Pb^{+2}, Zn^{+2}), and 9 anions (CrO_4^{-2}, $C_2O_4^{-2}$, F^{-}, PO_4^{-3}, SO_4^{-2}, SeO_3^{-2}, SeO_4^{-2}, phthalic acid, and chelidalmic acid). Like the ferrihydrite compilation, constants are

lacking for ferrous iron and carbonate. Unfortunately, constants are also lacking for arsenite and arsenate.

1.1.2.2 Adsorption of arsenic

Arsenate is relatively easy to remove from water using coagulation methods, since it bears a negative charge in natural waters above pH 2.2 (see Figure 1.1), and is electrostatically attracted to the positive charge on metal hydroxide surfaces. Fresh, preformed ferrihydrite has a reported arsenate adsorption capacity in the range of 0.1 M As/M Fe. Preformed hydroxides only remove arsenic through adsorption, while *in situ* coagulation leads to coprecipitation as well, and yields much higher capacities, in the vicinity of 0.5 to 0.6 M As/M Fe. (Edwards 1994).

Arsenate adsorption is theoretically favored at a pH below a sorbent's point of zero charge (see Table 1.3). Arsenite is uncharged in most natural waters (see Figure 1.1) and as such is more difficult to remove, since there is no electrostatic attraction to charged solids. Nonetheless, coprecipitation experiments have shown excellent removal of arsenite with ferric salts, with reported maximum surface densities on preformed ferrihydrite ranging up to 0.4 M As/M Fe (Edwards 1994). Most researchers, however, have reported arsenite removal with ferrihydrite to be somewhat less effective than arsenate removal. Adsorption of arsenite onto ferrihydrite is relatively insensitive to pH within most natural waters, and is theoretically favored from about pH 5 to 8 (see Figure 1.3b), below the pHpzc of ~8 (Dzombak and Morel 1990) . Ferrihydrite has a much higher surface area (ca. 600 m^2/g) than the crystalline oxides (typically 10-100 m^2/g), so adsorption capacities of the crystalline oxides are much lower.

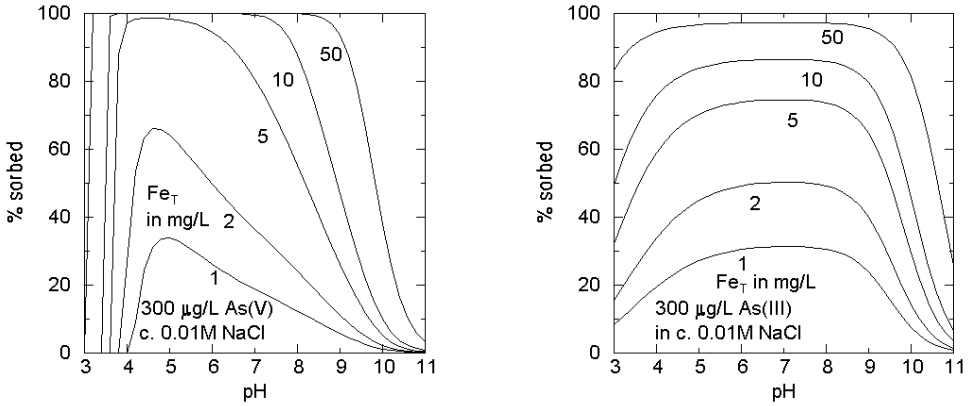

Figure 1-3: Adsorption of arsenate (a) and arsenite (b) onto ferrihydrite (DPHE/BGS/MML 2000)

Arsenic adsorption will be affected by the presence of other anions and cations. Some anions will impede adsorption by competing with arsenic for surface sites and lowering the surface charge. Cations, in contrast, can increase the positive surface charge, and enhance arsenic adsorption (Dzombak and Morel 1990).

The mechanisms of adsorption are understood better for arsenate than for arsenite. Indirect evidence (e.g. lack of sensitivity to ionic strength) and direct spectroscopic evidence both indicate that arsenate forms inner-sphere complexes at iron oxide surfaces. Evidence of an inner-sphere bidentate binuclear surface complex has been found with extended X-ray absorption fine structure (EXAFS) spectroscopy (e.g. Waychunas, Rea et al. 1993; Waychunas, Davis et al. 1995; e.g. O'Reilly, Strawn et al. 2001), wide angle X-ray scattering (WAXS) (Waychunas, Fuller et al. 1996), and Fourier transform infrared (FTIR) spectroscopy (Hering, Chen et al. 1996). Several different surface species can form: a monodentate complex is favored at low surface coverages typical of natural waters, and bidentate complexes at moderate to high surface loadings (Fendorf, Eick et al. 1997). Bidentate complexes have bonds between the arsenic atom and two separate surface

hydroxyls; these can be mononuclear or binucleaer, depending on whether the hydroxyls are coordinated to the same or different iron atom in the oxide. O'Reilly et al. (2001) found further EXAFS evidence of a bidentate binuclear structure at the As(V)-goethite surface, and showed that adsorption was rapid, with 93% of adsorption occurring within the first 24 hours. Arsenate desorption in a phosphate solution was initially rapid, but reached a plateau after ~35% of arsenic had been desorbed. Even after 5 months of phosphate extraction, a significant amount of arsenate remained adsorbed.

EXAFS (Manning, Fendorf et al. 1998) and FTIR (Sun and Doner 1998) studies of arsenite at the goethite surface suggest an inner-sphere bidentate binuclear bridging complex, similar to that of arsenate.

Information on the structure of arsenic surface complexes gleaned from spectroscopic studies can be used to inform surface complexation modeling; the above studies suggest that in most cases arsenic surface complexes should be modeled as bidentate binuclear species.

1.1.2.3 Adsorption of ferrous iron

Adsorption of trace metals onto iron oxides has been extensively studied, but relatively little research has been done on ferrous iron adsorption, because of the difficulties in prevention of Fe(II) oxidation, especially at higher pH. Recently more attention has been paid to ferrous iron adsorption, since the adsorbed ferrous ion is a strong reductant and can chemically reduce a number of compounds that are otherwise nonlabile.

A number of studies have examined and attempted to model Fe(II) adsorption onto goethite. In most cases, surface complexation is done with site densities ranging from 1-2.5 sites/nm^2 (Liger, Charlet et al. 1999; Amonette, Workman et al. 2000; Dixit and Hering 2006), though earlier models used higher densities near 7.0 sites/nm^2 (Hayes and Leckie

1986; Coughlin and Stone 1995). The density of sites accessible to Fe(II) has been estimated at 1.6 to 2.9 sites/nm^2 from isotherms made at near pH 7.0 (Coughlin and Stone 1995; Amonette, Workman et al. 2000; Mettler 2002), similar to the generic density of 2.3 sites/nm^2 recommended for all minerals (Davis and Kent 1990). However, maximum adsorption capacity is pH-dependent: Mettler (2002) found a maximum capacity of 10.2 sites/nm^2 at pH 8, compared to 2.9 sites/nm^2 for the same goethite at pH 7. Vikesland and Valentine (2002) could model adsorption of Fe(II) below pH 7 and in the absence of carbonate using standard site densities, but needed to invoke a site density of 13 sites/nm^2, citing the precedent of Davies and Morgan (1989), in order to match Fe(II) adsorption at higher pH and in the presence of carbonate.

Several studies have shown incomplete recovery of adsorbed Fe(II) upon acidification (Coughlin and Stone 1995; Jeon, Dempsey et al. 2001). Recent work has shown that adsorbed Fe(II) is re-worked into the interior of the goethite matrix through an electron transfer process (Coughlin and Stone 1995; Jeon, Dempsey et al. 2001; Jeon, Dempsey et al. 2003):

$$>Fe(III)OH + Fe(II) \rightarrow >Fe(III)OFe(II)OH \rightarrow >Fe(II)OFe(III)OH \qquad \text{(Equation 1-7)}$$

This reaction regenerates reactive ferric surface sites, greatly increasing the "apparent" adsorptive capacity of the surface. Fe(II) atoms within the bulk matrix might not be recovered during acid extractions. Spectroscopic evidence for such an electron transfer reaction, occurring after one or more days of Fe(II) adsorption, has been shown recently (Williams and Scherer 2004; Silvester, Charlet et al. 2005).

1.1.3 Oxidation

Both arsenic and iron have two stable oxidation states in natural systems, with the reduced species being favored under the reducing conditions typical of groundwater, and the oxidized species dominating (at equilibrium) in the presence of oxygen.

When oxidants are introduced into the subsurface, they may be consumed by a number of reduced species. The chief desired target for the proposed *in situ* arsenic removal process is ferrous iron, in order to create fresh sorption sites, but arsenite oxidation may be an additional goal. Reduced manganese could also consume oxidants, but the main unintended sink for oxidants will most likely be organic material coating sediment grains.

1.1.3.1 Arsenite

Arsenite is a moderately strong reductant in acid solution (Cotton and Wilkinson 1988):

$$H_3AsO_4 + 2H^+ + 2e^- = H_3AsO_3 + H_2O \qquad E_H° = 0.56 \text{ V, (Equation 1-8)}$$

Oxidation of arsenite generally reduces its mobility in the subsurface, because intrinsic constants for adsorption of arsenate to oxide minerals are stronger than those for arsenite (e.g. Dixit and Hering, 2003). Arsenite is predominantly non-charged below pH 9.2, whereas arsenate is negatively charged and therefore tends to be adsorbed by minerals such as iron oxides which have points of zero charge in the range of pH 7 to 9 (Table 1-3).

In natural systems most mineral surfaces tend to be negatively charged, due either to low points of zero charge or sorption of NOM, and therefore anions tend to be much more mobile than cations.

Oxygen is a readily available oxidant in natural waters, and is thermodynamically favored to oxidize arsenite. However the oxygenation of arsenite is very slow, taking days to weeks (Pierce and Moore 1982). Cherry and others (1979) showed that even when distilled water spiked with arsenite (pH 7) is saturated with oxygen, arsenic speciation stays relatively unchanged for days. Eary et al. (1990) reported that arsenite oxygenation was slowest around pH 5, and developed an empirical rate equation to describe the reaction kinetics between pH 8 and 12.

Arsenite can also be directly oxidized by a number of strong oxidants, including chlorine, hypochlorite, ozone, permanganate, hydrogen peroxide, and Fenton's reagent (H_2O_2/Fe^{2+}). Some solids, such as manganese dioxide, can also oxidize arsenite. Ultraviolet radiation can catalyze the oxidization of arsenite in the presence of other oxidants, such as oxygen. Direct UV oxidation of arsenite is slow, but may be catalyzed by the presence of sulfite (USEPA 2001a), ferric iron (Emett and Khoe 2001), citrate and iron (Hug, Canonica et al. 2001) or TiO_2 (Bissen, Vieillard-Baron et al. 2001).

The fact that advanced oxidation processes can oxidize arsenite where oxygen cannot suggests that the hydroxyl radical is the actual oxidant. However, Hug et al. (2001) showed that arsenite oxidation in a UV-Fe(III)-citrate system was unaffected by the addition of hydroxyl radical scavengers. They postulate that other oxidants, such as higher-valence iron compounds, are the key oxidizing species.

Ferric iron solids are thermodynamically capable of oxidizing arsenite, but EXAFS studies have shown that arsenite is not oxidized upon adsorption to goethite (Manning, Fendorf et al. 1998) or lepidocrocite (Farquhar, Charnock et al. 2002).

Biologically mediated oxidation may be faster than chemical oxidation in natural systems. Wilkie and Hering (1998) showed that microbes catalyzed arsenite oxidation in a geothermally-impacted river, and packed beds inoculated with iron-oxidizing bacteria can achieve better arsenite removal than control packed beds (Katsoyiannis, Zouboulis et al. 2002).

1.1.3.2 Ferrous iron

Homogeneous oxidation of ferrous iron is very slow under acidic conditions, but increases rapidly with pH, showing a first-order dependence on iron and oxygen, and a second-order dependence on [OH^-] concentration in the pH range 5-9 (Stumm and Lee 1961; Singer and Stumm 1970).

$$-\frac{d\left[Fe^{II}\right]}{dt} = k\left[Fe^{II}\right]P_{O2}\left[OH^-\right]^2 = k^{app}\left[Fe^{II}\right] \qquad \text{(Equation 1-9)}$$

where p_{O2} is the partial pressure of oxygen, and k is the rate constant in units of $min^{-1}atm^{-1}M^{-2}$.

Davison and Seed (1983) reviewed the available literature and found reasonable agreement on the value of the rate constant k, and suggested a 'universal' rate constant of $10^{13.30}$ $min^{-1}atm^{-1}M^{-2}$. With excess oxygen the oxidation follows pseudo-first-order kinetics with an apparent rate constant k^{app}.

The most commonly invoked mechanism, originally proposed by Weiss (1935) for homogeneous oxidation, involves dissolved oxygen being reduced to water through four single-electron transfers, passing respectively through the intermediary stages of superoxide, hydrogen peroxide, and hydroxyl radical, which can oxidize an additional three Fe(II) atoms (Stumm and Morgan 1996):

$$Fe^{II}(OH)_{2,aq} + O_2 \overset{slow}{\rightarrow} Fe^{III}(OH)_2^+ + \cdot O_2^- \quad \text{(Equation 1-10)}$$

$$Fe^{II}(OH)_{2,aq} + \cdot O_2^- + 2H^+ \rightarrow Fe^{III}(OH)_2^+ + H_2O_2 \quad \text{(Equation 1-11)}$$

$$Fe^{II}(OH)_{2,aq} + H_2O_2 + H^+ \rightarrow Fe^{III}(OH)_2^+ + H_2O + \cdot OH \quad \text{(Equation 1-12)}$$

$$Fe^{II}(OH)_{2,aq} + \cdot OH + H^+ \rightarrow Fe^{III}(OH)_2^+ + H_2O \quad \text{(Equation 1-13)}$$

giving the net reaction

$$4Fe^{II}(OH)_{2,aq} + O_2 + 4H^+ \rightarrow 4Fe^{III}(OH)_2^+ + 2H_2O \quad \text{(Equation 1-14)}$$

Mineral surfaces are known to catalyze many reactions, including the oxygenation of ferrous iron. When ferrous iron is adsorbed inner-spherically at an oxide surface, the surface species is electronically similar to the labile hydrolyzed ferrous species in solution, so it is not surprising that the adsorbed species is a stronger reductant than free ferrous iron (Luther III 1990; Wehrli 1990).

Kinetics of heterogeneous oxidation have been studied for over thirty years (Tamura, Goto et al. 1976; Sung and Morgan 1980; Tamura, Kawamura et al. 1980), but active

research continues today. Modern research focuses on how the presence of ferrous iron in heterogeneous systems can reduce species which are otherwise stable in oxidized settings, such as chromate (Fendorf and Li 1996; Pettine, D'Ottone et al. 1998), uranyl (Lenhart and Honeyman 1999), nitrobenzenes (Klausen, Trober et al. 1995), carbamate pesticides (Strathmann and Stone 2001; Strathmann and Stone 2002), and halogenated organic compounds (Amonette, Workman et al. 2000; Pecher, Haderlein et al. 2002). There is also interest in how ferrous iron scavenges disinfectant residuals in drinking water distribution systems (Vikesland and Valentine 2000; Vikesland and Valentine 2002).

In the presence of surfaces, ferrous iron can be oxidized in solution or at the surface, leading to the following mixed rate expression (Tamura, Goto et al. 1976; Tamura, Kawamura et al. 1980):

$$-\frac{d\left[Fe^{+2}\right]_T}{dt} = k_{homo}\left[Fe^{+2}\right] + k_{hetero}\left[> Fe^{III}OFe^{+}\right] \qquad \text{(Equation 1-15)}$$

where $\left[Fe^{+2}\right]_T = \left[> Fe^{III}OFe^{+}\right] + \left[Fe^{+2}\right]$.

The work of Tamura et al. predates Millero's contributions (Millero 1985; Millero, Sotolongo et al. 1987) to the understanding of the importance of speciation in the second-order rate dependence on pH, and the rate constants are conditional with respect to pH. In a more recent examination of heterogeneous Fe(II) oxidation, Wehrli (1990) demonstrated a linear free energy relationship (LFER) between the oxidation reaction rate constant k and the equilibrium constant K for each of the Fe(II) species (see Table 1-4). The resulting slope of

one is consistent with the Marcus theory of electron transfer in outer-sphere reactions (Stumm and Morgan 1996, p. 689), and the LFER was used to estimate an equilibrium constant and oxidation potential for the adsorbed Fe(II) species, based on the experimentally observed rate constant. The adsorbed Fe(II) species was found to have a similar kinetic rate to that of $FeOH^+$.

Table 1-4: Log rate (k in $M^{-1}s^{-1}$) and equilibrium (K) constants for oxidation reactions (Wehrli 1990; Stumm and Sulzberger 1992)

Ferrous Oxidation Reaction	Log k	log K	$E_H°$ (V) for Fe(III)/Fe(II) half-reaction
$Fe^{+2} + O_2 = Fe^{+3} + O_2^-$	-5.1	-15.7	0.77
$Fe(OH)^+ + O_2 = Fe(OH)^{+2} + O_2^-$	1.4	-8.45	0.34
$Fe(OH)_{2,\,aq} + O_2 = Fe(OH)_2^+ + O_2^-$	6.9	-3.04	0.02
$(>Fe(III)O)_2Fe + O_2 = (>Fe(III)O)_2Fe^+ + O_2^-$	0.7	-9	0.36

Biological oxidation of ferrous iron can be an important or even dominant process in engineered iron removal plants (Mouchet 1992; Sharma, Petrusevski et al. 2005). In the presence of oxygen, abiotic oxygenation of Fe(II) is probably more important than biotic oxidation above pH 7, due to the rapid kinetics. Likewise, if ferrous iron, arsenite and natural organic matter are all competing for oxygen which is artificially introduced into an aquifer, it is likely that ferrous iron will be the kinetically dominant reductant. In slightly acidic waters, ferrous oxygenation is much slower, so there should be more competition for oxygen among the inorganic reductants, and biotic oxidation of iron could become an important process.

1.1.4 *In situ* water treatment

In situ treatment of drinking water is still relatively uncommon in the US, though it has been applied successfully in Europe for decades. *In situ* treatment has the great advantage

of not producing any wastes that must be disposed of, and often requires little or no chemical addition. It is operationally simple, requires minimal construction, and can be more economical than conventional above-ground treatment, both in capital and recurring costs. The most commonly applied *in situ* removal technologies are for removal of nitrate (Braester and Martinell 1988b; Braester and Martinell 1988a) and iron and manganese removal, reviewed below.

1.1.4.1 Iron and manganese

Although *in situ* iron removal has been practiced for decades, mostly in Europe (Grombach 1985; Jechlinger, Kasper et al. 1985; Braester and Martinell 1988b; Braester and Martinell 1988a; Maogong 1988) the mechanisms of iron removal are not well understood, and have only recently been examined rigorously.

In *in situ* iron treatment, a volume of water is saturated with oxygen and introduced into an aquifer through an injection well. The injectate is usually allowed to react for some time (a few hours to a day), before extracting groundwater from the aquifer. Iron-free water can then be withdrawn from the aquifer for extended periods before dissolved iron breaks through. Upon iron breakthrough, the process is repeated. The injection well can also be used for extraction (the "push-pull" configuration), or a series of satellite injection wells can surround a central extraction well [e.g. the Vyredox™ system (Braester and Martinell 1988b; Braester and Martinell 1988a; Maogong 1988)]. The efficiency of the process, defined as the volume ratio of groundwater abstracted to oxidized water injected, ranges from about 3 to 12 (Appelo, Drijver et al. 1999), and typically increases with time.

Since Fe(II) removal occurs during the extraction phase of the cycle, adsorption of Fe(II) onto ferric oxide surfaces is clearly one important mechanism at work. The mechanism

of Fe(II) oxidation during injection phases is somewhat controversial. Some attribute the oxidation to biological processes (Grombach 1985; Rott and Friedle 2000), while others consider heterogeneous oxidation at the ferric oxide surface (Mettler 2002) or homogeneous oxidation following displacement by divalent ions in the injectate (Appelo, Drijver et al. 1999) to be the key mechanisms. Recent work by Mettler and others (Mettler, Abdelmoula et al. 2001; Mettler 2002) suggests that at slightly elevated pH (characteristic of a calcareous aquifer), abiotic oxidation rates are so fast that biotic oxidation of Fe(II) is insignificant.

The rapid kinetics of ferrous oxygenation above pH 7 allow Fe(II) to be oxidized even in the presence of competing reductants such as Mn(II) or NOM (Mettler 2002). However, the oxidant-rich injectate can only occupy a certain volume of aquifer, so the limiting factor in iron removal may well be the amount of ferrous iron adsorbed to mineral surfaces (Appelo, Drijver et al. 1999). In this case, injection of stronger oxidants or the use of pure oxygen to saturate injectate, as recommended by some (Jechlinger, Kasper et al. 1985; Rott and Friedle 2000; Rott, Meyer et al. 2002), will likely lead to only marginal improvements in iron removal. Developing this idea, Appelo (1999) has made numerical experiments with the geochemical reactive transport code PHREEQC, and successfully modeled the observed behavior of *in situ* iron removal plants.

1.1.4.2 Arsenic

Since arsenic is often present in groundwater under reducing conditions, along with elevated levels of ferrous iron, it should be possible to apply an *in situ* iron removal process as described above, and adsorb much of the arsenic onto the resulting ferric solid. Very little experimental data is available to test this hypothesis:

- In Germany, in order to remediate an acidic aquifer containing high levels of arsenite and ferrous iron, Matthess (1981) injected 29 tons of potassium permanganate directly into 17 contaminated wells, and reduced mean arsenic concentrations from 13,600 to 60 µg/L.
- Welch et al. (2000) showed that in an alkaline (pH >9) basaltic aquifer As(V) levels could be lowered by about 30% by injecting an acidic ferric chloride solution, which both increased the number of ferric sorption sites and lowered the pH to below 8.
- Martin and Kempton (2000) sequentially injected ferrous sulfate and oxygen solutions into a column packed with unconsolidated sand. The resulting ferric precipitate retarded As(V) breakthrough by 30 pore volumes (and Cr(VI) breakthrough by 8).
- In Bangladesh, Sarkar and Rahman (2001) pumped anoxic groundwater containing ca. 150 µg/L arsenic (speciation unknown) into a storage tank, aerating the water with cascading filters. The tank was allowed to drain back into the well overnight, and when water was pumped out the following day, arsenic levels were initially below 20 µg/L, but rose rapidly to ~100 µg/L.
- Rott et al. (2002) made a similar experimental setup to that of Sarkar and Rahman, and were able to reduce arsenic concentrations (mostly as arsenite) *in situ* from approximately 35 to 5 µg/L, while iron and manganese levels were also lowered.

This handful of pilot studies shows that *in situ* treatment of arsenic can succeed, but that understanding of the removal process is lacking. Neither Matthess nor Sarkar and Rahman provide any information about relevant water parameters such as pH and iron

concentration, indicate how long low arsenic levels were maintained, or try to explain the mechanisms responsible for the observed arsenic reduction.

1.2 Research objectives

The goal of this dissertation research is to examine the factors affecting *in situ* arsenic removal, especially the interactions between iron and arsenic which are key factors for *in situ* treatment. This dissertation explores three different geochemical phenomena: precipitation, oxidation, and adsorption. Extensive research has been conducted on the importance of these chemical factors for conventional (above-ground) arsenic removal, but these findings have not been extended to subsurface treatment.

After batch studies on each of these three topics (precipitation, oxidation, and adsorption), a series of packed column experiments were performed to mimic an *in situ* arsenic removal scheme, using goethite-coated sand as a surrogate for aquifer sediments. In both batch and column experiments, the geochemical transport code, PHREEQC (Parkhurst and Appelo 1999), was used to model and interpret the chemical processes.

Findings from this research are expected to improve understanding of geochemical processes affecting arsenic mobility in the subsurface, and arsenic removal in engineered systems. In particular, the results have direct implications for the successful application of *in situ* removal of arsenic from groundwater. By better understanding the chemical interactions between arsenic and iron which take place in an *in situ* treatment scheme, it will be possible to predict under what circumstances the technique could be successfully applied, and how treatment might be optimized.

1.3 Organization of thesis

This thesis contains four papers, presented as Chapters 2 through 5. Chapter 2, published in the *Soil Science Society of America Journal* in 2007, is entitled "Solubility of symplesite (ferrous arsenate): implications for reduced groundwaters and other geochemical environments." This paper describes the precipitation of the vivianite analogue symplesite, $Fe(II)_3(As(V)O_4)_2(s)$. A new solubility constant for the mineral is calculated based on controlled laboratory precipitation experiments. Using geochemical modeling and a database of groundwater composition in Bangladesh, it is shown that some groundwaters are supersaturated with respect to symplesite. The manuscript concludes with a consideration of environments in which symplesite might control arsenic solubility, such as engineered arsenic removal systems.

Chapter 3, published in *Chemosphere* in 2007, is entitled "Redox reactions in the Fe–As–O_2 system." This paper examines the direct reduction of As(V) by Fe(II), and shows that the reaction occurs at low but measurable levels, and is enhanced at higher pH or higher Fe(II) concentrations. The reaction was not seen in the absence of goethite. The paper also examines the co-oxidation of As(III) and Fe(II) by dissolved oxygen. While As(III) is kinetically stable in the presence of oxygen at circumneutral pH, As(V) is generated when Fe(II) is also present. The paper considers conventional descriptions of Fe(II) oxygenation, and concludes that buffer effects have compromised the quantification of oxidation kinetic constants in classic papers on this subject. Furthermore, the classical formulation of Fe(II) oxidation involves oxidation by hydroxyl radical and hydrogen peroxide, which is inconsistent with oxidation rates noted, in this work and others, in the presence of radical scavengers.

Chapter 4, entitled "Competitive adsorption of As(III), As(V), and Fe(II) onto goethite," describes competitive adsorption effects seen between As(III) and Fe(II), and between As(III) and As(V) on goethite. Limited competition was observed between As(III) and As(V), and surface complexation modeling gave a good qualitative description of this competitive effect. However, the model under-predicted the adsorption of As(III) at all pH levels, suggesting that some surface sites are more selective for As(III) than for As(V). Isotherm experiments showed a much higher capacity of the goethite surface for Fe(II) than for either arsenic species. This was simulated with a surface complexation model by postulating the existence of two groups of surface sites, one accessible only to Fe(II). This two-site model could successfully describe single-component adsorption of As(III), As(V), and Fe(II), but gave poor predictions of multi-component adsorption. It is hypothesized that the apparent high capacity of the goethite surface for Fe(II) is due to interfacial electron transfer rather than the diversity of surface sites.

Chapter 5, entitled "*In situ* removal of Fe(II) and As(III): column studies," describes a series of packed column experiments designed to simulate an *in situ* arsenic removal scheme consisting of sequential injection of oxygen-rich water followed by the abstraction of water from an aquifer enriched in arsenic and ferrous iron. The experiments showed that removal of both Fe(II) and As(III) was more effective at higher pH and that removal efficiency increased over time at higher pH, as expected. At pH 8, the amount of Fe(III) in the column increased by more than 50% due to oxidation of adsorbed Fe(II). Surface complexation modeling simulations predicted some of the retardation effects seen, notably the major retardation of As(III) when Fe(II) is added to the influent. Model predictions using the two-

site model from Chapter 4 are contrasted with the more conventional 1-site model, which does not match the data as well.

Chapters 4 and 5 are planned for submission to *Science of the Total Environment*.

Chapter 6 gives a summary of the overall findings of the research, and makes recommendations for future work on the basis of this research.

CHAPTER 2: SOLUBILITY OF SYMPLESITE (FERROUS ARSENATE): IMPLICATIONS FOR REDUCED GROUNDWATERS AND OTHER GEOCHEMICAL ENVIRONMENTS[2]

2.1 INTRODUCTION

Over the past decade, it has become evident that naturally occurring arsenic in groundwater is much more widespread than previously thought. Following the recognition in the mid-1990s that much of the alluvial groundwater of Bangladesh was contaminated with high levels of arsenic – exceeding 1 mg/L in cases – water quality surveys have revealed the presence of geogenic arsenic in other Asian countries, including Vietnam, Cambodia, Nepal, Myanmar, and Afghanistan. India and China have longstanding recognized zones of arsenic contamination, but new contaminated areas within these countries are still being identified (e.g. Bihar state in India). Tens of millions of people are exposed to unsafe levels of arsenic in drinking water in these countries, and tens of thousands of arsenicosis patients have already been identified.

Arsenic mobility in the subsurface is thought to be controlled by adsorption onto aquifer materials, particularly oxide minerals and clays. High levels of dissolved arsenic can occur in anoxic aquifers, where partial or complete reductive dissolution of iron oxides is driven by bacterial consumption of organic matter (Aggett and Obrien 1985; Lovley 1991;

[2] This chapter was published, in slightly modified form, in the *Soil Science Society of America Journal* 71(1): 101-107, 2007.

Nickson, McArthur et al. 1998; Nickson, McArthur et al. 2000). Oxic aquifers may also contain significant levels of dissolved arsenic, especially under alkaline conditions where desorption of anions is favored (Smedley and Kinniburgh 2002).

Under the strongly reducing conditions typical of young, organic-rich aquifers, arsenic is typically found as As(III), while under oxidizing conditions the As(V) species are thermodynamically favored. However, redox transformations of As(III) to As(V) and vice versa are kinetically limited (Cherry, Shaikh et al. 1979) so that non-equilibrium distributions of As(III) and As(V) are often encountered in natural waters. For example, in Bangladesh the National Hydrogeochemical Survey measured arsenite and total arsenic, along with other analytes in 271 wells; 123 of these had measurable levels of dissolved arsenic but dissolved oxygen and nitrate were below detection limits (in most cases 0.1 and 0.3 mg/L, respectively) (DPHE/BGS/MML 2000). In 54% of these anoxic wells the As(III):As^{tot} ratio was less than 0.5; in 17% of the wells the ratio was below 0.1. Elsewhere, in a study of arsenic cycling in lakes, Aurillo *et al.* reported that in late summer/fall oxic surface waters from Upper Mystic Lake had an As(III):As^{tot} ratio of approximately 0.5 (Aurillo, Mason et al. 1994). Both of these studies illustrate As(III) levels far from thermodynamic equilibrium.

If the high levels of dissolved arsenic in reducing groundwaters are caused by reductive dissolution of iron oxides, one would expect a strong correlation between dissolved Fe and As levels in groundwater. While most high-As waters under these conditions have relatively high Fe, there is no clear correlation between the two elements in groundwater (DPHE/BGS/MML 2000; Nickson, McArthur et al. 2000; Ahmed, Bhattacharya et al. 2004). Furthermore, dissolved iron levels, while high, are not as high as would be expected from complete dissolution of Fe(III) phases. Some invoke re-oxidation of Fe(II) to account for the

missing Fe (Zheng, Stute et al. 2004) while others point to the possibility that solid ferrous iron phases such as ferrous sulfide, pyrite, siderite, vivianite, or green rusts may sequester significant amounts of Fe(II) in reducing groundwaters (Horneman, Van Geen et al. 2004). Geochemical modeling has shown that shallow groundwater in Bangladesh is often saturated with respect to calcite, siderite and vivianite (Nickson, McArthur et al. 2000; Ahmed, Bhattacharya et al. 2004), and a number of ferrous solids including pyrite (Nickson, McArthur et al. 2000), ferrous phosphate and ferrous silicate (Harvey, Swartz et al. 2002) have been identified in core sediments from arsenic-affected areas in Bangladesh.

In principle, solid phases could also limit arsenate solubility. Scorodite ($Fe(III)As(V)O_4 \bullet 2H_2O$) is a well-known mineral in arsenic-bearing ore deposits, but is only formed under strongly acidic conditions (Dove and Rimstidt 1985; Rochette, Li et al. 1998). Arsenates of various divalent metals (Ba, Ca, Cu, Mg, Mn, Ni, Zn) exist as analogues of vivianite ($Fe(II)_3(PO_4)_2 \bullet 8H_2O$) but most are too soluble to limit arsenate concentrations in natural systems (Essington 1988; Voigt, Brantley et al. 1996; Bothe and Brown 1999a; Bothe and Brown 1999b). Isomorphic substitution of divalent metals, or of PO_4 for AsO_4, occurs readily in these minerals and solid solutions among the vivianite analogues can be expected (Frost, Martens et al. 2003). Mineral identification is complicated by the fact that X-ray diffraction patterns are identical for many of the vivianite analogues (Frost, Martens et al. 2003).

Symplesite and parasymplesite are arsenate analogues of vivianite with the formula ($Fe(II)_3(As(V)O_4)_2 \bullet 8H_2O$) from triclinic and monoclinic crystal systems, respectively (Mori and Ito 1950; Roberts, Campbell et al. 1990). Relatively few studies have examined the properties of these minerals. A recent study explored the Raman and infrared spectra of

various arsenate minerals including symplesite (Frost, Martens et al. 2003), and a few studies have reported thermodynamic data for ferrous arsenate species (Hess and Blanchar 1976; Khoe, Huang et al. 1991; Sadiq 1997; Gonzalez and Monhemius 1998). In the metallurgical literature, Khoe et al. (1991) have reported a solubility product for ferrous arsenate of 4 ± 1 $x10^{-41}$. In laboratory microcosms, bacterial reduction of Fe(III) in scorodite reportedly produces an acidic ferrous arsenate phase ($Fe(II)HAs(V)O_4 \bullet xH_2O$), (Cummings, Caccavo et al. 1999), and traces of symplesite along with other unknown ferrous arsenate phases (Papassiopi, Vaxevanidou et al. 2003). But to our knowledge, precipitation of authigenic symplesite has not been documented in natural systems.

In this paper a solubility constant for symplesite is reported based on controlled laboratory experimental data, and geochemical modeling is conducted, which suggests that this phase might occur in natural systems, as well as under more extreme conditions.

2.2 MATERIALS AND METHODS

2.2.1 Chemicals

All chemicals were of Certified ACS grade, and were used without further purification. Stock solutions of Fe(II) and As(V) were made by dissolving $Fe(II)(NH_4)_2(SO_4)_2$ and $NaH_2As(V)O_4$ in de-ionized water. $NaNO_3$ was used for ionic strength control. All solutions were prepared inside an anaerobic glove box (Coy Laboratory Products Inc., 2% hydrogen atmosphere) using de-ionized water that had been deaerated by boiling under a nitrogen atmosphere outside the glove box for 30 minutes. Strong acid (HNO_3) and base (KOH) were used for pH adjustment.

2.2.2 Experimental and analytical methods

An acidic solution containing 1.00 mM Fe(II) and 0.50 mM As(V) in dilute nitric acid (pH ~4.5) was prepared from stock solutions of ferrous ammonium sulfate and sodium dihydrogen arsenate in a background electrolyte of 100 mM $NaNO_3$. The solution was continuously mixed with a magnetic stirrer in a 500 mL reactor inside the glove box. Strong base (100 mM KOH) was added dropwise, resulting in the steady increase of pH (measured with an Orion probe) until the onset of precipitation at approximately pH 7.0, which was marked by a drop in pH and the appearance of a white precipitate. Precipitation was allowed to proceed for one hour, after which 10 mL aliquots were transferred in duplicate to 15 mL polypropylene centrifuge tubes (Falcon). Variable amounts of KOH were then added to the precipitation reactor, and pH was recorded after each addition. After an increase of approximately 0.2-0.3 pH units, duplicate aliquots were transferred to centrifuge tubes. The tubes were placed on an end-over-end shaker in the glove box, and equilibrated for 6-8 hours. Temperature in the anaerobic chamber ranged from 26.2°C to 27.0°C over the course of the experiment.

After equilibration, samples were filtered through pre-rinsed 0.2 μm nylon syringe filters for analysis of Fe(II) and As, and the final pH was recorded. Fe(II) was measured in the glove box using a modified Ferrozine method (Stookey 1970), while arsenic samples were acidified and measured within two days using graphite furnace atomic absorption spectroscopy (GFAAS, Perkin-Elmer 5100 with Zeeman correction).

In a separate experiment, a larger quantity of precipitate was prepared by mixing 5 mM Fe(II) with 3 mM As(V), and raising the pH with KOH to ~7.5, which calculations indicated to be below the saturation point for ferrous hydroxide. This experiment was done

with no inert electrolyte, to simplify precipitate identification. After stirring magnetically for one hour, the resulting precipitate was allowed to settle overnight in the glove box. A small amount of precipitate was dissolved in dilute nitric acid to allow measurement of the Fe(II):As(V) ratio. Approximately 20 mL of slurry was collected, dewatered using a nylon syringe filter (0.2 μm), and dried in a dessication chamber under anoxic conditions. The crystal structure of the precipitate was analyzed using X-ray powder diffractometry (Rigaku Multiflex) with a Cu-Kα radiation source (λ = 1.5418 Å, 40 mA current). The precipitate was mounted on a glass slide and immediately covered with a drop of glycerol to prevent oxidation. The scan range was from 5-60° (2θ) with a speed of 1° per second.

2.3 RESULTS

In all samples, a white precipitate was clearly visible, which was subsequently identified by X-ray diffraction analysis as ferrous arsenate [symplesite, $Fe(II)_3(As(V)O_4)_2$ (s)]. Fe(II) and As(V) concentrations dropped dramatically during equilibration, with the greatest reductions occurring at higher pH (see Figure 2-1). The solid lines shown are model predictions (discussed below). The pH also decreased, by as much as 1.4 units. As(V) precipitated in accordance with Equation 2-1:

$$3Fe^{2+} + 2HAsO_4^{-2} = Fe_3(AsO_4)_2(s) + 2H^+ \qquad \text{(Equation 2-1)}$$

The precipitation reaction shown liberates protons from the dissolved arsenic species, causing the pH to fall. At pH 8.5, dissolved arsenic levels were reduced by more than 99.9%, from an initial concentration of 500 μM (37.5 mg/L) to 0.32 μM (24 μg/L).

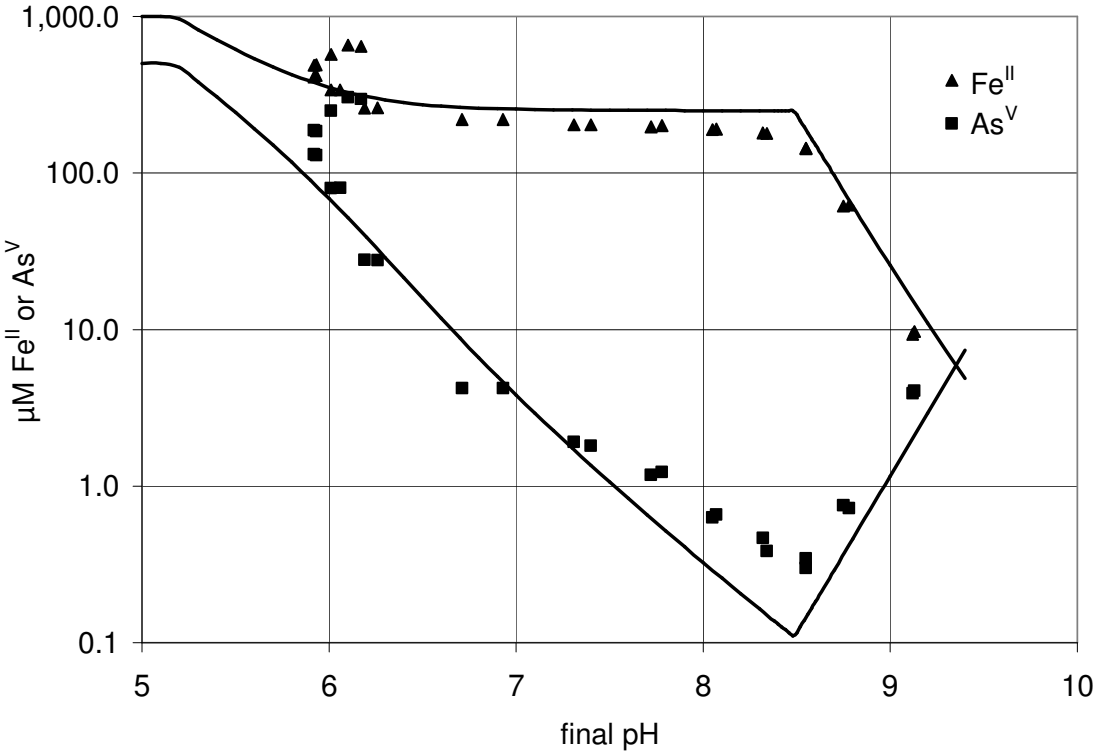

Figure 2-1: Precipitation of ferrous arsenate. Initial conditions, 1000 uM Fe(II), 500 uM As(V), 0.1 M $NaNO_3$. Solid lines represent model predictions.

Above pH 8.5, precipitation of ferrous hydroxide was observed (see Equation 2.2), which resulted in a further drop in dissolved Fe(II) levels and production of a bluish-green precipitate. Equilibrium As(V) levels began to rise above pH 8.5, as Fe(II) was increasingly sequestered in ferrous hydroxide.

$$Fe^{2+} + 2OH^- = Fe(OH)_2(s) \qquad \text{(Equation 2-2)}$$

Figure 2-1 shows good agreement between replicate samples, though the pH in some cases varied by as much as 0.2 units. This variation is not surprising given the lack of a pH buffer in the system, apart from the As(V) system itself.

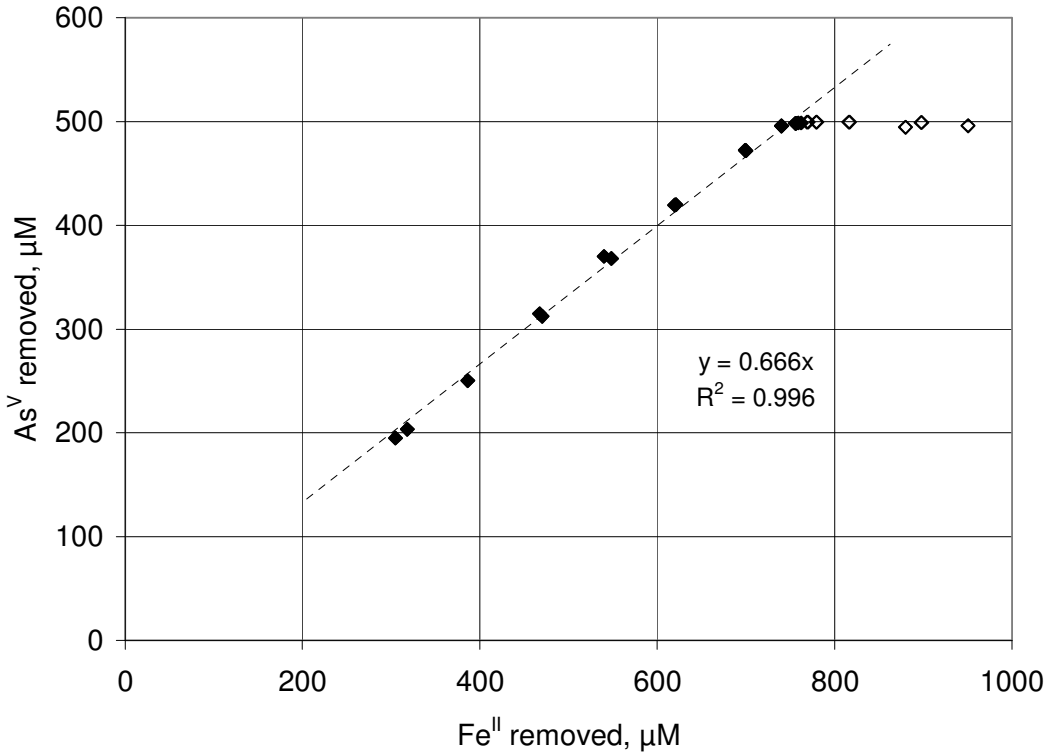

Figure 2-2: Ferrous arsenate stoichiometry. Open symbols represent conditions of oversaturation with respect to $Fe(OH)_2(s)$.

The stoichiometry of the precipitate was assessed by measuring the amounts of dissolved Fe(II) and As(V) removed from solution. Linear regression (Figure 2-2) shows that for every mole of Fe(II) removed, 0.666 moles of As(V) were lost, consistent with Equation 2-1. This stoichiometry was confirmed by precipitate dissolution and elemental analysis of the resulting solution, which yielded an Fe(II):As(V) ratio of 0.62. X-ray diffraction patterns showed clear peaks (d = 6.602, 2.329, 7.823, 3.206 and 1.665 Å, in order

of decreasing intensity) which matched the main peaks of the reference spectrum of symplesite, $Fe(II)_3(As(V)O_4)_2 \cdot 8(H_2O)$. Sample and reference spectra are shown in Appendix A.

PHREEQC (Parkhurst and Appelo 1999) was used to determine the ion activity product (IAP) for samples taken from the precipitation experiment. Activity coefficients were calculated using the Davies equation. The relevant equilibrium constants used in the calculations are shown in Table 2-1. Reactions involving ferrous sulfate species are included since the Fe(II) stock was prepared from ferrous ammonium sulfate, and significant formation of ferrous sulfate species could affect formation of ferrous arsenate complexes. For modeling purposes, redox transformations of Fe(II) and As(V) were blocked.

Table 2-1: PHREEQC model parameters for dissolved species

Reaction	*Log K*	*Source*
$Fe^{+2} + OH^- = FeOH^+$	4.5	(Morel and Hering 1993)
$Fe^{+2} + 2OH^- = Fe(OH)_{2,\,aq}$	7.4	(Morel and Hering 1993)
$Fe^{+2} + SO_4^{-2} = FeSO_4$	2.25	(Parkhurst and Appelo 1999)
$Fe^{+2} + HSO_4^- = FeHSO_4^+$	1.08	(Parkhurst and Appelo 1999)
$H_3AsO_4 = H_2AsO_4^- + H^+$	-2.24	(Ball and Nordstrom 1991)
$H_3AsO_4 = HAsO_4^{-2} + 2H^+$	-9.00	(Ball and Nordstrom 1991)
$H_3AsO_4 = AsO_4^{-3} + 3H^+$	-20.60	(Ball and Nordstrom 1991)

The ion activity products calculated for symplesite and ferrous hydroxide are shown in Figure 2-3. The eight samples with the lowest initial pH values (6.40 to 7.10 at the beginning of equilibration), have significantly higher IAPs for symplesite than other samples; these samples most likely remained oversaturated because of relatively slow precipitation kinetics under these conditions. At higher pH, precipitation is more rapid and an equilibrium value seems to be reached within the equilibration period of 6-8 hours. Averaging the sixteen data points which are considered to be at equilibrium with ferrous arsenate (closed

symbols in Figure 2-3), a solubility product, pK_{so}, of 33.25 (± 2σ = 0.46) is calculated for symplesite. Figure 2-3 also shows ferrous hydroxide precipitation occurring at approximately pH 8.5. The average IAP above this point is $10^{-15.2}$, which is in excellent agreement with the reported pK_{so} of 15.1 for ferrous hydroxide (Stumm and Morgan 1996). This serves as a validation of the quality of the Fe(II) and pH measurements, as well as the modeling analysis.

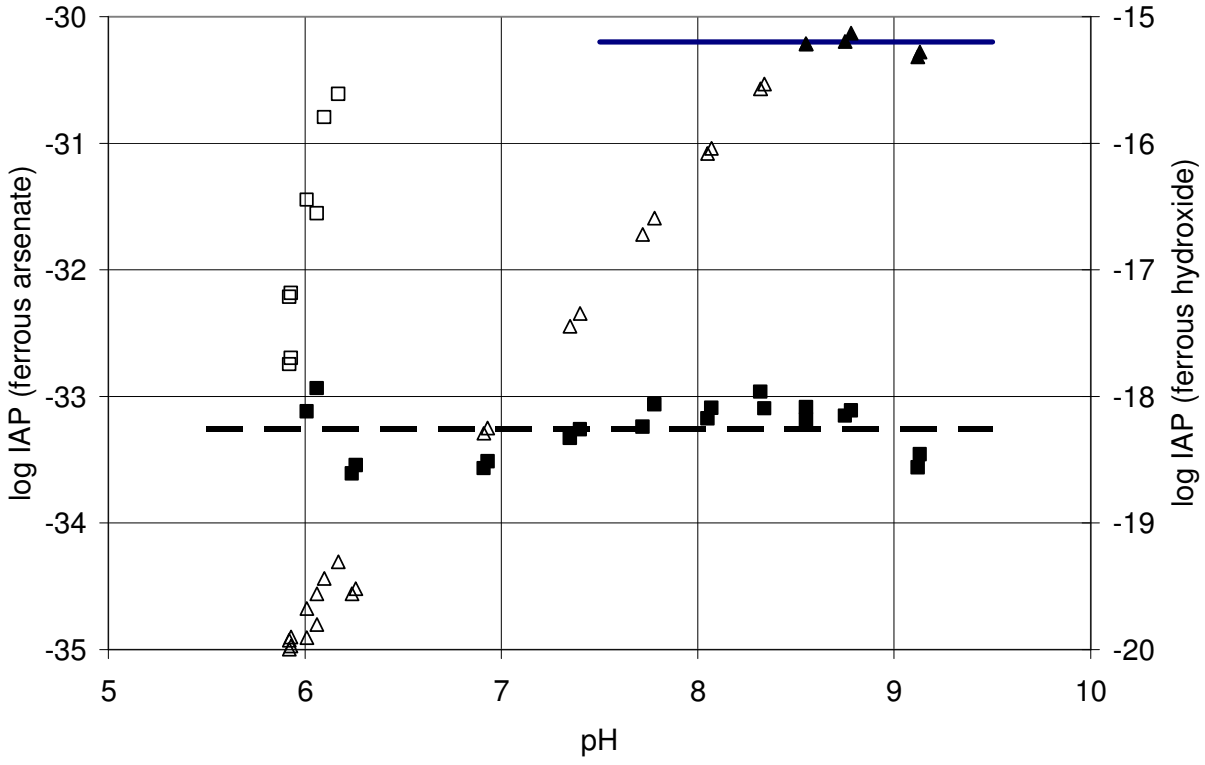

Figure 2-3: Log ion activity products for ferrous arsenate (squares, left axis) and ferrous hydroxide (triangles, right axis). Dashed and solid lines represent equilibrium solubility products for ferrous arsenate and ferrous hydroxide, respectively. Filled symbols are used for samples considered to be at equilibrium with ferrous arsenate or ferrous hydroxide phases.

In Figure 2-1, the solid lines show model predictions of dissolved Fe(II) and As(V) given the initial conditions of 1000 uM Fe(II) and 500 uM As(V) and the experimentally determined solubility product. The model matches observed concentrations well, and

correctly predicts the increase in As(V) and drop in Fe(II) as ferrous hydroxide precipitates above pH 8.5.

This new solubility constant for symplesite is several orders of magnitude larger than that reported by Khoe et al. (1991), of approximately $10^{-41.2}$. The reason(s) for this large difference are not clear. The difference could be explained by non-equilibrium conditions in these experiments, or by the possible passage of colloidal symplesite through the 0.2 micron nylon filters used in our system, but these potential explanations seem unlikely. It is also possible that different ferrous arsenate solids, having the same Fe(II):As(V) ratio, are formed under acidic and neutral conditions. The Khoe et al. experiments were based on precisely measuring the pH at the onset of precipitation (near pH 2) while these experiments measured soluble Fe(II) and As(V) in the presence of precipitate from pH 6-9. Further work is required to resolve the discrepancy between these reported solubility constants; ideally the solubility constant should be calculated from both oversaturated and undersaturated conditions.

It was hypothesized that a linear free energy relationship might exist between divalent metal precipitates of phosphate and arsenate of the form $Me(II)_3(YO_4)_2 \cdot 8(H_2O)$, where Y represents As(V) or P, since the two oxyanions are structurally similar. Published constants were found for many solids, but in only four cases were both arsenate and phosphate solubility products available (Table 2-2). No clear relationship is evident from these four sets of data, but in the case of Cd(II) and Fe(II), the solubility products for both oxyanions are very close.

Table 2-2: Thermodynamic solubility products (pK_{so}) for $Me(II)_3(YO_4)_2 \bullet 8(H_2O)$

Me(II)	*Y = As*	*Source*	*Y = P*	*Source*
Cd	32.66	(CRC 2005)	32.60	(CRC 2005)
Co	28.17	(CRC 2005)	34.69	(CRC 2005)
Cu	35.10	(CRC 2005)	36.85	(CRC 2005)
Fe	33.25	This study	33.06	(Singer 1972)

2.4 DISCUSSION

2.4.1 Bangladesh

Using the PHREEQC model and its associated database, modified to include arsenic compounds, equilibrium speciation can be computed for complex mixtures. Figure 2-4 is a simulated stability diagram for symplesite, indicating total dissolved As(V) concentrations in equilibrium with symplesite for various Fe(II) concentrations. The calculations are made for two ionic strengths representative of those in Bangladesh groundwaters. The figure shows that drinking water meeting the World Health Organization (WHO) Guideline Value for arsenic of 10 μg/L (WHO 2004) is unlikely to be saturated with respect to symplesite unless the Fe concentrations are unrealistically high. However, in reduced groundwaters, such as those found in Bangladesh, it is not uncommon to find water containing 100-1000 μg/L arsenic and significant amounts of dissolved iron (10% of samples in the National Hydrogeochemical Survey exceeded 10 mg/L), at circumneutral pH (DPHE/BGS/MML 2000). Symplesite might represent a significant sink for arsenate and ferrous iron in these systems.

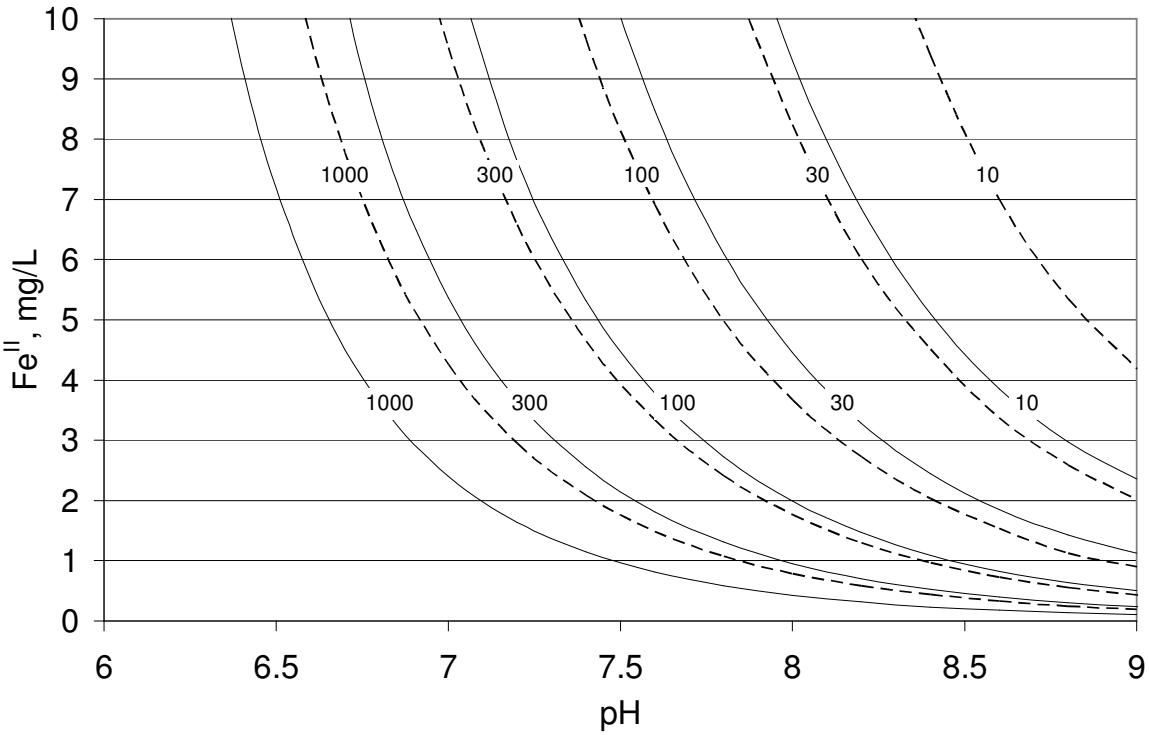

Figure 2-4: Stability field for symplesite. Isopleths represent total arsenate concentration in µg/L. Solid lines are calculated with an ionic strength of 0.01, while dotted lines have an ionic strength of 0.05. Areas to the right of the isopleths are oversaturated with respect to symplesite.

In Bangladesh groundwaters, dissolved arsenic is predominantly present as As(III) (Bhattacharya, Jacks et al. 2002), but As(V) is dominant in sediments near the water table, where highly enriched bands of ferric iron are found (Breit, Lowers et al. 2005). These are thought to be caused by repeated fluctuations of the water table: when submerged, arsenic and Fe(II) adsorb to ferric oxide surfaces, which may also partially dissolve due to dissimilatory reduction by bacteria. Bacterial reduction of ferric hydroxide would liberate arsenic to solution, without necessarily reducing As(V) to As(III) (Cummings, Caccavo et al. 1999). When water levels drop again, the adsorbed Fe(II) is oxidized, creating fresh ferric

hydroxide adsorption sites. Adsorbed Fe(II) is more easily oxidized than the free species (Stumm and Lee 1961), and reactive intermediary species produced during the oxygenation of Fe(II) can oxidize As(III) to produce As(V) (Roberts, Hug et al. 2004; Johnston and Singer 2007a).

In Bangladesh, a number of researchers have conducted geochemical surveys measuring arsenic and other parameters in groundwater. One of the most extensive is the National Hydrogeochemical Survey (NHS) (DPHE/BGS/MML 2000), which analyzed 271 wells in three Special Study Areas for a broad suite of parameters. Samples were filtered at collection through 0.2 μm acetate filters. Iron was not speciated, but is assumed to be completely present as ferrous species, since the solubility of ferric iron at neutral pH is negligible. Other researchers have reported very high $Fe(II)/Fe_{tot}$ ratios in Bangladesh groundwater (Horneman, Van Geen et al. 2004).

Concentrations of major ions (Ca^{2+}, Cl^-, F^-, Fe^{2+}, HCO_3^-, K^+, Mg^{2+}, Mn^{2+}, Na^+, NH_4^+, NO_3^-, PO_4^{-3}, $H_3SiO_3^-$, SO_4^{-2}) from this dataset were used along with As(V), As(III), pH and temperature to model geochemical speciation. Arsenic and iron redox transformations were blocked by decoupling the species in PHREEQC. Only the 256 records where pH data were available were used in the analysis. Solubility products for solid phases used in the model are listed in Table 2-3.

As a check on the input data, a charge balance was performed for each sample. A consistent positive bias was noted, with a median value of +8.7%. This suggests that cations are systematically overestimated, or that anions are missing or underestimated in the NHS database. However, the bias is not gross: 97% of samples had an error of less than +20%.

Table 2-3: Solubility products used for geochemical modeling

Solid phase	*Reaction*	*Log K*	*Source*
Calcite	$CaCO_3(s) = CO_3^{-2} + Ca^{+2}$	-8.48	(Parkhurst and Appelo 1999)
Rhodochrosite	$MnCO_3(s) = Mn^{+2} + CO_3^{-2}$	-11.13	(Parkhurst and Appelo 1999)
Siderite	$FeCO_3(s) = Fe^{+2} + CO_3^{-2}$	-10.89	(Parkhurst and Appelo 1999)
Vivianite	$Fe_3(PO_4)_2(s) = 3Fe^{+2} + 2PO_4^{-3}$	-33.06	recalculated from (Singer 1972)
Hydroxyapatite	$Ca_5(PO_4)_3OH(s) + 4H^+ = H_2O + 3HPO_4^{-2} + 5Ca^{+2}$	-3.421	(Parkhurst and Appelo 1999)
Symplesite	$Fe_3(AsO_4)_2(s) = 3Fe^{+2} + 2AsO_4^{-3}$	-33.25	This study
Manganous arsenate	$Mn_3(AsO_4)_2(s) = 3Mn^{+2} + 2AsO_4^{-3}$	-32.12	recalculated from (Sadiq 1997)
Ferrous hydroxide	$Fe(OH)_2(s) = Fe^{+2} + 2OH^-$	-15.1	(Stumm and Morgan 1996)

Saturation indices (SI's) for various solid phases were calculated for each sample in the NHS dataset as the log of the ratio of the Ion Activity Product to the equilibrium constant. A SI of zero represents equilibrium conditions, while negative and positive SI's represent conditions of under- and oversaturation, respectively. In order to graphically present the SI's for each mineral, the SI's are sorted and plotted against the percentage of the total sample having values greater than or equal to that SI value. The resulting curve is called a cumulative frequency distribution (CFD). CFDs of saturation indices (SI's) for the different waters with respect to the various minerals are plotted in Figure 2-5.

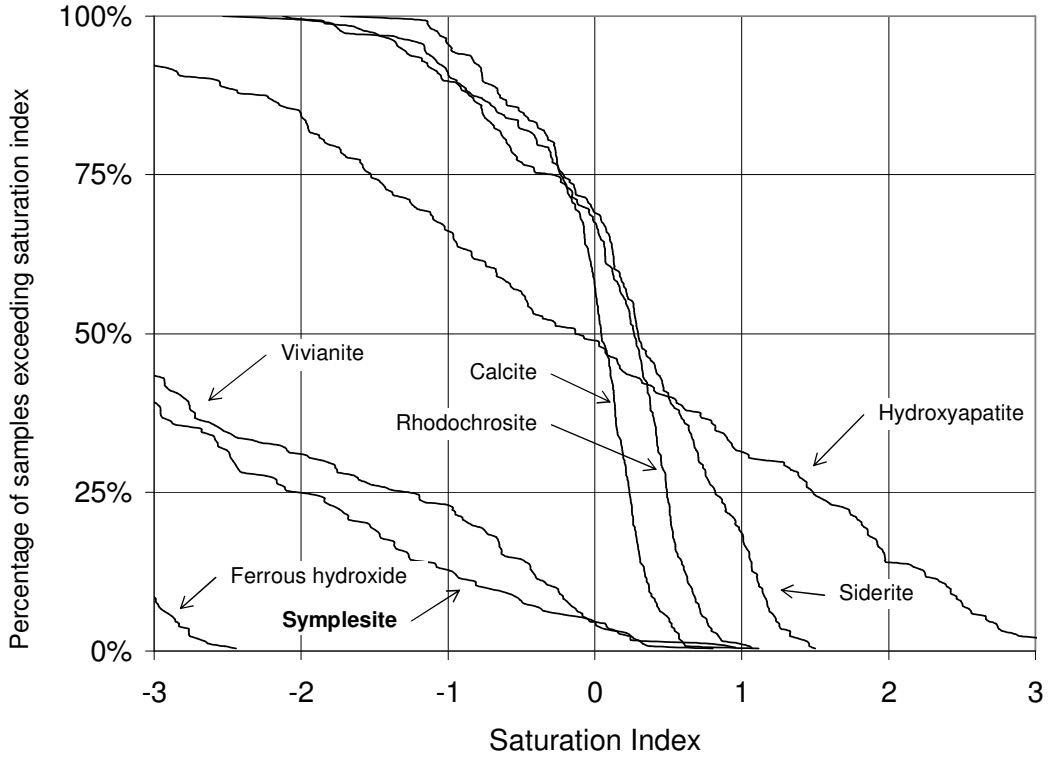

Figure 2-5: Cumulative frequency distributions of saturation indices for various minerals. Geochemical data from (DPHE/BGS/MML 2000).

Over half of the samples in the database (57%) were found to be oversaturated with respect to calcite, and approximately two thirds were oversaturated with respect to siderite and rhodochrosite. The steep slope of the CFDs for these three carbonate minerals just above the equilibrium solubility (SI = 0) is consistent with the presence of these minerals in the subsurface and the control they exert on the chemical composition of the respective waters. Precipitation of these carbonate minerals may account for the low concentrations of Fe(II) and Mn(II) in a number of these waters. In contrast, about half of the waters are oversaturated with respect to hydroxyapatite ($Ca_5(PO_4)_3OH$), but the CFD shows no change in slope above

the saturation point. This may reflect a kinetic limit on precipitation for this mineral. All of the waters are highly undersaturated (SI < -2) with respect to ferrous hydroxide and manganous arsenate (not shown).

About 4% of the samples were found to be oversaturated with respect to symplesite, and 5% with respect to vivianite. (If the Khoe et al. (1991) solubility constant is used, more than 90% of the samples are oversaturated with respect to symplesite). However, only about a third of the samples saturated with respect to symplesite were also saturated with respect to vivianite. The chemical composition of the samples oversaturated with respect to symplesite is summarized in Table 2-4. These samples are typical of circumneutral reduced groundwater in Bangladesh, where oxygen, nitrate, and sulfate have been reduced by microbial consumption of organic matter, resulting in high alkalinity and dissolved iron. Even under these conditions, significant amounts of dissolved arsenic can be found in the oxidized arsenate state.

Table 2-4: Geochemistry of Bangladesh groundwater samples oversaturated with respect to symplesite (n=12). Dissolved concentrations in mg/L.

	pH	*As(V)*	*As(V)/ As_{tot}*	*Fe*	*HCO_3*	*O_2*	*NH_4-N*	*NO_3-N*	*SO_4*	*Ionic Strength*
Minimum	6.86	0.204	35%	5.4	393	< 0.1	1.4	< 0.01	0.3	0.009
Median	7.15	0.271	63%	8.9	561	< 0.1	2.9	< 0.3	0.5	0.013
Maximum	7.23	0.713	91%	24.8	785	1.9	14.7	0.14	8.2	0.029

Ferrous phosphate phases have been identified in sediments from arsenic-contaminated aquifers in Bangladesh (Harvey, Swartz et al. 2002). Since the CFD for symplesite saturation is very similar to that of vivianite and the solubility constants are similar (see Table 2-3), it seems likely that ferrous arsenate phases may also exist in the same aquifers. Furthermore, since a solid solution is expected between vivianite and symplesite,

arsenate may be sequestered in ferrous phosphate phases even when the water is undersaturated with respect to symplesite.

If arsenate were present in phosphate phases, it should be released during acid dissolution of the solid phase. Several studies of sequential dissolution experiments have been conducted on sediments from arsenic-affected aquifers in Bangladesh, though acid-soluble arsenic is generally interpreted as being carbonate-bound. Most find little to moderate amounts of arsenic in the acid-soluble fraction (e.g. Harvey, Swartz et al. 2002; Akai, Izumi et al. 2004), suggesting that phosphate minerals would be a minor rather than a major sink for arsenic in these sediments.

2.4.2 Other environments

Apart from reduced groundwater, there are a number of extreme environments in which symplesite could be stable. For example, the high pH (9.8) and elevated concentration of As(V) (200 uM) in Mono lake (Oremland, Stolz et al. 2004) would limit dissolved Fe(II) to 8 μg/L. Symplesite has been identified in industrial waste sites where arsenic-rich smelter slag has been used as landfill (USEPA 1998). Finally, ion exchange resins are used to remove arsenate from drinking water. Resin regenerant is highly enriched in arsenate, and typically must be processed before disposal. Addition of ferrous salts to precipitate symplesite could present an attractive alternative to conventional co-precipitation and adsorption of arsenate using ferric or aluminum coagulants, which generates large volumes of waste sludge.

In arid alkaline groundwaters, arsenic is typically present as As(V). For example, drinking water in the US city of Fallon, Nevada is alkaline (pH 9.1) and contains from 70-120 μg/L As, predominantly as As(V) (Welch, Stollenwerk et al. 2003). Under these

conditions, modeling suggests that symplesite would limit As(V) concentration to under 10 μg/L upon addition of approximately 10-15 mg/L Fe(II). Ferrous iron would quickly react with the low levels of dissolved oxygen in these waters (~1 mg/L), producing small amounts of hydrous ferric oxide which would also remove As(V) through adsorption and co-precipitation. While conventional treatment would require pH reduction to favor adsorption of the arsenate anions onto hydrous ferric oxide, the high pH of these waters would actually improve As(V) removal through precipitation of ferrous arsenate.

2.5 CONCLUSIONS

A new experimentally-derived solubility constant has been calculated for the ferrous arsenate mineral symplesite. Geochemical modeling using the new constant suggests that some reduced groundwaters of Bangladesh are oversaturated with respect to symplesite. Precipitation of authigenic symplesite could be a significant sink for both As(V) and Fe(II) under these conditions. Geochemical modeling results confirm the work of others, indicating that Bangladesh groundwaters are frequently oversaturated with respect to siderite, vivianite and rhodochrosite and that these minerals could represent important sinks for Fe(II) and Mn(II). However, previous studies have not considered the possibility of precipitation of ferrous arsenate phases such as symplesite. Precipitation of ferrous arsenate could be an effective control measure to reduce arsenate levels in As(V)-rich alkaline waters used to produce drinking water, or in specialized applications such as management of ion exchange regenerant brines.

CHAPTER 3: REDOX REACTIONS IN THE FE–AS–O2 SYSTEM[3]

3.1 Introduction

Both arsenic and iron have two stable oxidation states in natural aquatic systems, with Fe(II) and As(III) being favored under the reducing conditions typical of groundwater and hypolimnetic water, and Fe(III) and As(V) dominating (at equilibrium) in the presence of oxygen. Reduction and oxidation reactions involving either or both of these elements can occur in natural waters, especially in groundwater. Where groundwater is used as a drinking water source, arsenic contamination may be a serious public health issue and iron frequently gives rise to aesthetic problems. These redox reactions can have important implications regarding the presence of arsenic and iron in water used for drinking water supply or irrigation.

The reactions of As(III) and Fe(II) with various oxidants have been extensively studied individually, but there has been relatively little work done on redox reactions involving both arsenic and iron species. This paper explores two of these reactions at circumneutral pH: the reduction of As(V) by Fe(II) under anoxic conditions, and the co-oxidation of As(III) during Fe(II) oxygenation. The impact of goethite, pH buffers, and radical scavengers on these reactions is also examined.

[3] This paper was published, in a slightly different form, in *Chemosphere* 69(4): 517-525, 2007.

3.1.1 Iron

The oxygenation of Fe(II) has been extensively studied, and kinetics have been found to be first-order with respect to iron and oxygen, and second-order with respect to hydroxide concentration (Stumm and Lee 1961),

$$-d[Fe(II)]/dt = k[Fe(II)][OH^-]^2 p_{O2} \quad \text{(Equation 3-1)}$$

where p_{O2} is the partial pressure of oxygen, and k is the rate constant in units of $min^{-1}atm^{-1}M^{-2}$. Davison and Seed (1983) reviewed the available literature and found reasonable agreement on the value of the rate constant k, and suggested a 'universal' rate constant of $10^{13.30}$ $min^{-1}atm^{-1}M^{-2}$.

The reaction of Fe(II) with oxygen can occur through both homogeneous and heterogeneous pathways. Although this reaction has been studied for decades, important questions about the molecular processes remain. The most commonly invoked mechanism, originally proposed by Weiss (1935) for homogeneous oxidation, involves dissolved oxygen being reduced to water through four single-electron transfers, passing respectively through the intermediary stages of superoxide, hydrogen peroxide, and hydroxyl radical.

$$Fe(II) + O_2 \rightarrow Fe(III) + \cdot O_2^- \quad \text{(Equation 3-2)}$$

$$Fe(II) + \cdot O_2^- + 2H^+ \rightarrow Fe(III) + H_2O_2 \quad \text{(Equation 3-3)}$$

$$Fe(II) + H_2O_2 + H^+ \rightarrow Fe(III) + \cdot OH + H_2O \quad \text{(Equation 3-4)}$$

$$Fe(II) + \cdot OH + H^+ \rightarrow Fe(III) + H_2O \quad \text{(Equation 3-5)}$$

Equation 3-4 is the Fenton reaction, and can lead to chain reactions involving production of additional reactive oxygen species (Equations 3-6 and 3-7), and the regeneration of Fe(II) (Equation 3-8). The chain is terminated when ·OH reacts to produce non-radical species, as in Equation 3-5.

$$\cdot OH + H_2O_2 \rightarrow \cdot O_2^- + H^+ + H_2O \qquad \text{(Equation 3-6)}$$

$$\cdot O_2^- + \cdot O_2^- + 2H^+ \rightarrow H_2O_2 + O_2 \qquad \text{(Equation 3-7)}$$

$$Fe(III) + \cdot O_2^- \rightarrow Fe(II) + O_2 \qquad \text{(Equation 3-8)}$$

Equations 3-2 through 3-5 can be written with a variety of Fe(II) and Fe(III) species. Reaction energetics and kinetics will vary depending on pH and the presence of other solutes which determine Fe(II) speciation. $Fe(OH)_2$ has been proposed as the critical ferrous iron species (Millero 1985), but other possibilities exist. King (1998) has demonstrated that ferrous carbonate species dominate the oxidation of Fe(II) in waters containing more than 1 mM carbonate. Carbonate buffer has been used extensively in studies on Fe(II) oxidation (e.g. Stumm and Lee 1961; Tamura, Goto et al. 1976; Sung and Morgan 1980; Millero, Sotolongo et al. 1987; Hug and Leupin 2003), and it is plausible that ferrous carbonate complexes, rather than $Fe(OH)_2$, may have been rate-limiting in these studies.

Both the conventional four-step oxygenation of Fe(II) (Equations 3-2 through 3-5), and the Fenton system (Equations 3-4 through 3-8) indicate that Fe(II) is oxidized by hydrogen peroxide and hydroxyl radical. This is inconsistent with findings that Fe(II) oxidation at circumneutral pH is not significantly decreased in the presence of scavengers which quantitatively consume hydroxyl radical or hydrogen peroxide (e.g. Reinke, Rau et al.

1994). This implies that non-hydroxyl oxidant species are generated during Fe(II) oxidation. Hug and Leupin (2003) have proposed an alternate pathway in which an intermediate non-hydroxyl species – perhaps Fe(IV) – is the active oxidant at circumneutral pH.

The above discussion holds primarily for homogeneous oxidation. Oxidation of Fe(II) is known to be catalyzed by surfaces such as clays and metal oxides (Tamura, Goto et al. 1976), which bind Fe(II) and donate electron density to the central ferrous ion through both π and σ bonds, thereby stabilizing the ferric product of oxidation (Wehrli 1990).

A variety of adsorbed Fe(II) species may be formed, due to differences among surfaces as well as a diversity of adsorption sites for a given surface. Furthermore, adsorbed Fe(II) species may also undergo reactions with ligands in the bulk solution. Just as solution speciation is important for homogeneous oxidation, the speciation of adsorbed Fe(II) is likely to be important in heterogeneous redox reactions, but is still relatively poorly understood at present despite decades of study.

3.1.2 Arsenic and iron

As(III) is a moderately strong reductant in acid solution, and is oxidized to an intermediate As(IV) species which is rapidly oxidized to As(V) (Klaning, Bielski et al. 1989). Oxygen is a readily available oxidant in natural waters, and is thermodynamically favored to oxidize As(III) over a wide range of pH values. However this reaction is very slow, taking days to weeks (Cherry, Shaikh et al. 1979; Pierce and Moore 1982).

A number of redox reactions are theoretically possible between arsenic and iron at circumneutral pH values, where the dominant As(III) and Fe(II) species are H_3AsO_3 and Fe^{+2}, respectively. As(V) is present as both $H_2AsO_4^-$ and $HAsO_4^{-2}$, while Fe(III) is relatively

insoluble in the absence of strong ligands. Depending on the species, arsenic can either oxidize or reduce iron. For example[4]:

$$H_3As^{III}O_3 + 2\ Fe^{III}(OH)_{3(am)} + 3\ H^+ =$$

$$H_2As^{V}O_4^- + 2\ Fe^{+2} + 5\ H_2O \qquad \Delta G^\circ_w = \text{-7.8 kJ/mol (Equation 3-9)}$$

$$HAs^{V}O_4^{-2} + 2\ Fe^{II}(OH)_2 + H_2O =$$

$$H_3As^{III}O_3 + 2\ Fe^{III}(OH)_{3(am)} + 2\ H^+ \qquad \Delta G^\circ_w = \text{-150 kJ/mol (Equation 3-10)}$$

Relatively little work has been done on the As(V)-Fe(II) reaction. Fe(II) adsorbed to oxide surfaces is more reactive than dissolved Fe(II), and Charlet et al. (2002) showed that Fe(II) adsorbed to a clay surface was oxidized by As(V), producing a Fe(III) coating along surface defects. However at higher Fe(II) concentrations As(V) may precipitate, forming symplesite rather than undergoing electron transfer (Johnston and Singer 2007b).

Oxidation of As(III) by dissolved Fe(III) is thermodynamically favorable, but unlikely in natural waters due to the low solubility of Fe(III) above ~pH 3. Spectroscopic studies have shown that As(III) is not oxidized upon adsorption to goethite (Manning, Fendorf et al. 1998) or lepidocrocite (Farquhar, Charnock et al. 2002). Others have reported that As(III) adsorbed to goethite is slowly oxidized, but attribute this to the presence of oxygen or manganese oxides (Sun and Doner 1998).

As(III) is oxidized indirectly during oxidation of Fe(II) by H_2O_2 or O_2, presumably by scavenging of reactive intermediary species. This species could be the hydroxyl radical but, at near-neutral pH, addition of radical scavengers does not affect As(III) oxidation rates

[4] Free energies of formation are calculated for pH 7 and 1 μM Fe^{II}.

(Hug, Canonica et al. 2001). Hypervalent iron species (e.g. Fe(IV)) can oxidize As(III) (Lee, Um et al. 2003), and have been postulated as the actual oxidant of As(III) during oxidation of Fe(II) by oxygen or H_2O_2 at neutral pH (Hug and Leupin 2003).

3.2 Materials and methods

3.2.1 Chemicals

All chemicals were of Certified ACS grade or better, and were used without further purification. Phosphate and two of the biologic buffers proposed by Good (1966), MES (pK_a = 6.15) and HEPES (pK_a 7.55), were used for pH control.

3.2.2 Goethite

Goethite was chosen as the model catalytic iron oxide, and was synthesized by slowly adding 450 mL 1.0 M KOH to 50 mL of 1.0 M $Fe(NO_3)_3$ under a nitrogen atmosphere (Schwertmann and Cornell 2000). The resulting precipitate slurry was incubated at 25 °C for 14 days (Peak and Sparks 2002) and dialyzed to remove residual dissolved salts (Spectra-Por 7, 3500 MW cut-off) until the permeate conductivity was less than that of a 0.1 mM $NaNO_3$ solution. The precipitate was freeze-dried and confirmed to be goethite using X-ray powder diffractometry (Rigaku Multiflex) with a Cu-Kα radiation source (λ = 1.5418 Å). The specific surface area measured by 5-point N_2 BET adsorption was 65 m^2/g (NOVA Quantachrome 1200). Particle size was measured (Brightwell DPA4100), with the majority of particles identified to be in the 2-3 micron range or smaller.

3.2.3 Reduction of As(V) by Fe(II)

All experiments were conducted inside a glove box (2% hydrogen atmosphere, Coy Laboratory Products Inc.). De-ionized water, which had been de-aerated by boiling under a nitrogen atmosphere outside the glove box for 30 minutes, was used for dilutions, and HNO_3 and KOH were used for pH adjustment. All stock solutions were prepared inside the glove box.

50 mM As(V) stock solutions were prepared by dissolving $NaH_2AsO_4 \cdot 7H_2O$ in 100 mM NaOH, then adjusting pH to ~ 7. Stock solutions of 5 mM Fe(II) were prepared by dissolving $Fe(NH_4)_2(SO_4)_2$ in 1 mM HNO_3 which had been de-aerated by boiling outside the glove box, and adjusting pH to ~ 5. A 4000 mg/L goethite suspension and 200 mM $NaNO_3$ and 200 mM HEPES buffer (pH 7) stock solutions were prepared in de-ionized water.

Stocks were mixed to prepare a suspension of 640 mg/L goethite, 16 mM $NaNO_3$, and 8 mM HEPES. Following pH adjustment to the desired level, 9 mL aliquots were transferred to reaction vessels (15 mL centrifuge tubes, Falcon) and equilibrated overnight on an end-over-end shaker. Variable amounts of Fe(II) stock were then added, along with de-aerated water for a total volume of 14 mL, and equilibrated on the shaker for 2 hours to allow for Fe(II) adsorption. Two series of reactors were prepared, the first containing variable concentrations of Fe(II) (0 – 200 µM) at pH 7.00, and the second containing 200 µM Fe(II) with variable pH (6.50 – 8.00). All reactors were prepared in duplicate, including Fe(II)-free, As(V)-free, and goethite-free controls.

After Fe(II) equilibration, 1000 µL of the suspension was withdrawn to allow measurement of residual dissolved Fe(II). The experiment was then initiated by spiking reactors with 400 µL of the As(V) stock solution and replacing them on the shaker. The final

composition was 400 mg/L goethite, 10 mM $NaNO_3$, 5 mM HEPES, 1500 µM As(V). This amount of goethite is equivalent to approximately 560 µM adsorption sites, based on adsorption isotherm experiments (see Chapter 4).

After 30 minutes, and then every two hours for eight hours, a 2-mL sample was withdrawn from the reactors and filtered through a syringe filter (0.2 µm nylon, Fisher). Ferrozine was added to a portion of the filtrate for measurement of Fe(II), while another portion was filtered through an anion exchange resin column and acidified for measurement of As(III).

3.2.4 Co-oxidation of As(III) and Fe(II) by O_2

200 mM $NaNO_3$ and 200 mM pH buffer (phosphate, MES, or HEPES) solutions were prepared in de-ionized water. 50 mM As(III) stock solutions were prepared by dissolving As_2O_3 in 10 mM NaOH, and adjusting the pH to ~7 with HNO_3. Fe(II) stock solutions were freshly prepared by dissolving $Fe(NH_4)_2(SO_4)_2$ in 1 mM HNO_3.

A solution of 10 mM $NaNO_3$, pH buffer (1-10 mM phosphate, MES, or HEPES), and 1 mM As(III) was stirred and sparged with compressed air (pO_2 = 0.21 atm) for at least 30 minutes in a water-jacketed beaker at 25 °C. In some experiments, 14 mM propanol was added as a radical scavenger (Hug and Leupin 2003).

To initiate the reaction, Fe(II) was spiked into the solution to the desired level, ranging from 10 to 100 µM. Samples were collected for Fe(II) and As(III) measurement as in the glovebox experiments. As(V) was subsequently eluted from the anion exchange cartridge. pH was monitored throughout the reaction, and did not vary by more than 0.01 units. Most experiments ran for 60 minutes, with samples collected every five minutes.

Glassware was thoroughly washed with concentrated HCl after each experiment to remove any Fe(III) residues.

3.2.5 Speciation and measurement of dissolved arsenic and iron

Arsenic was measured using Zeeman graphite furnace atomic absorption spectrophotometry (Perkin-Elmer 5100PC). An EDL lamp was used (λ = 193.7 nm) and all samples were spiked with Pd/Mg matrix modifier according to the Perkin-Elmer manual.

Arsenic (III) was separated from total arsenic by solid phase extraction onto an anion exchange resin column (Supelco, Sigma-Aldrich) which adsorbs anionic As(V) species (Ficklin 1983). Samples with pH > 7 were acidified prior to filtration to convert all As(III) to the uncharged H_3AsO_3 form in order to prevent any retention on the columns. As(V) was analyzed directly with GF-AAS following elution from the column using a mixture of 240 mM HNO_3 and 18 mM H_2SO_4. This speciation method requires that the ionic strength of solutions be low, so in most cases, 10 mM $NaNO_3$ was used to fix ionic strength.

Fe(II) was measured using a modified Ferrozine method (Stookey 1970; Gibbs 1976). Stock solutions of 1.0 mM Ferrozine were prepared in 500 mM ammonium acetate at pH 7.0. Variable amounts of stock were added to samples depending on Fe(II) concentration, but in all cases the final pH was above 4. The absorbance at 562 nm was measured at least an hour after Ferrozine addition, to allow full color development.

For both arsenic and iron analysis, a 5-point calibration curve was used, with r^2 of 0.999 or greater. Calibration standards were prepared by dilution from 1000 µg/mL ICP standards (Fisher) in a matrix similar to the samples being analyzed, and in 240 mM HNO_3/18 mM H_2SO_4 for As(V) analysis. Quality control standards, prepared from separate stocks than calibration standards, were analyzed before and after every batch of 6-10

samples, and sample concentrations were adjusted accordingly by linear interpolation. If the standard deviated from the expected value by more than 5% the instrument was recalibrated and samples were re-analyzed.

In experiments involving goethite, samples were filtered prior to analysis through a 0.2 micron polyvinyl fluoride (PVDF, Supelco) or nylon (Fisher) syringe filter prior to analysis.

3.3 Results and discussion

3.3.1 Reduction of As(V) by Fe(II)

In the absence of goethite, 1500 μM As(V) and 200 μM Fe(II) produced no measurable As(III) within 8 hours at pH 6, 7, or 7.5. At pH 8, traces of As(III) were noted, but there was significant loss of Fe(II) through precipitation of symplesite ($Fe_3(AsO_4)_2 \bullet 8H_2O$) (Johnston and Singer 2007b).

In the reactors containing goethite, As(V) was present greatly in excess to surface adsorption sites, minimizing the likelihood that any As(III) produced would be lost to adsorption. Small but measurable amounts of dissolved As(III) were produced, and production rates increased with pH and initial Fe(II) concentration (Figure 3-1).

Because of the low production of As(III) observed (< 1 μM), the concentration of As(V) and Fe(II) can be considered constant over time in any given reactor, leading to zero-order production of As(III):

$$d[As(III)]/dt = k_{obs} \qquad \text{(Equation 3-11)}$$

Linear regression lines shown in Figure 3-1 all have significantly positive slopes, with 95% confidence, except for the lowest initial Fe(II) concentration (33 μM). The slopes of the regression lines give rate constants k_{obs} for the reaction, in units of moles As(III) produced per second.

As(III) production was not observed in any control reactors. The production of As(III) only in the reactors containing both goethite and Fe(II) suggests that an adsorbed Fe(II) species is the active reductant. While it is likely that a wide variety of different adsorbed Fe(II) species exist, these are collectively denoted as $Fe(II)_{ads}$ and the concentration of $Fe(II)_{ads}$ is estimated as the difference between the initial Fe(II) concentration and dissolved Fe(II) after the initial equilibration with goethite. Figure 3-2 shows that, as expected, $Fe(II)_{ads}$ increased with increasing pH and with increasing initial Fe(II) concentration. Replicate analyses of Fe(II) in duplicate reactors were within 15% in all cases, and usually within 5%.

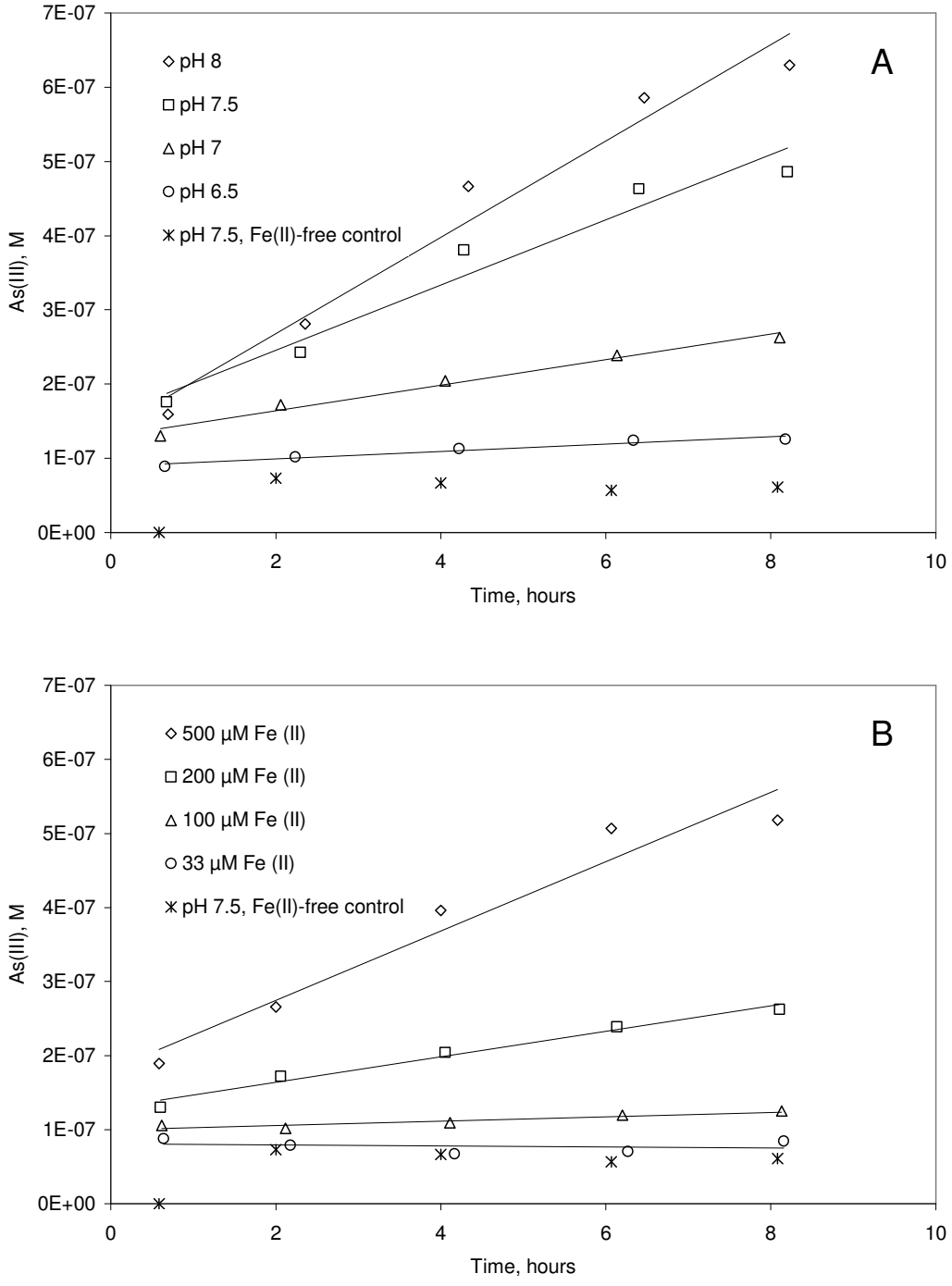

Figure 3-1: As(III) production in goethite suspension. Conditions: 400 mg/L goethite, 1500 µM As(V), 10 mM $NaNO_3$, 5 mM HEPES. A: effect of pH at 200 µM Fe(II). B: effect of Fe(II) at pH 7.0.

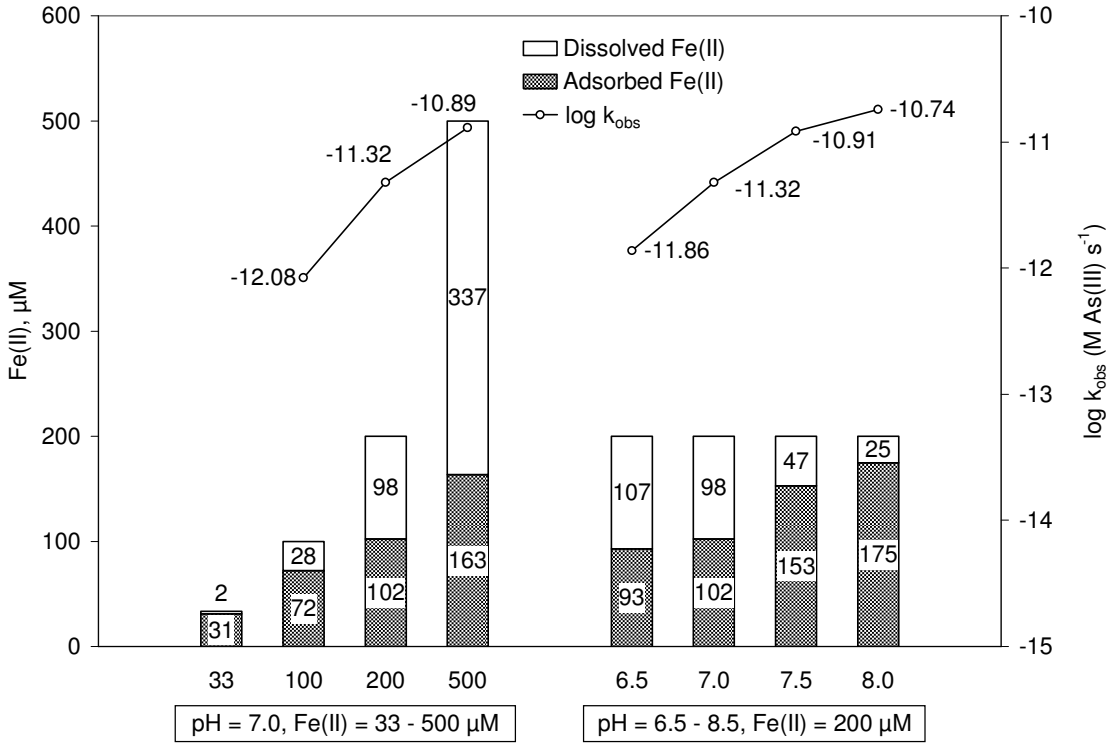

Figure 3-2: Comparison of extent of Fe(II) adsorption and observed rate constant for As(III) production.

The calculated rate constants shown in Figure 3-2 demonstrate a strong linear relation with $Fe(II)_{ads}$ in both the variable Fe(II) and variable pH series of experiments (see Figure 3-3), indicating that the reaction is first-order with respect to $Fe(II)_{ads}$. Assuming that the reaction is first-order with respect to As(V) (Equation 3-12), and that [As(V)] remains constant throughout the reaction, the intrinsic rate constant can be calculated by dividing the slope of the regression line in Figure 3-3 by the As(V) concentration. This calculation gives an intrinsic rate constant of $k = 10^{-3.96}\ M^{-1}\ s^{-1}$ (95% CI: $10^{-4.10}$ - $10^{-3.86}$).

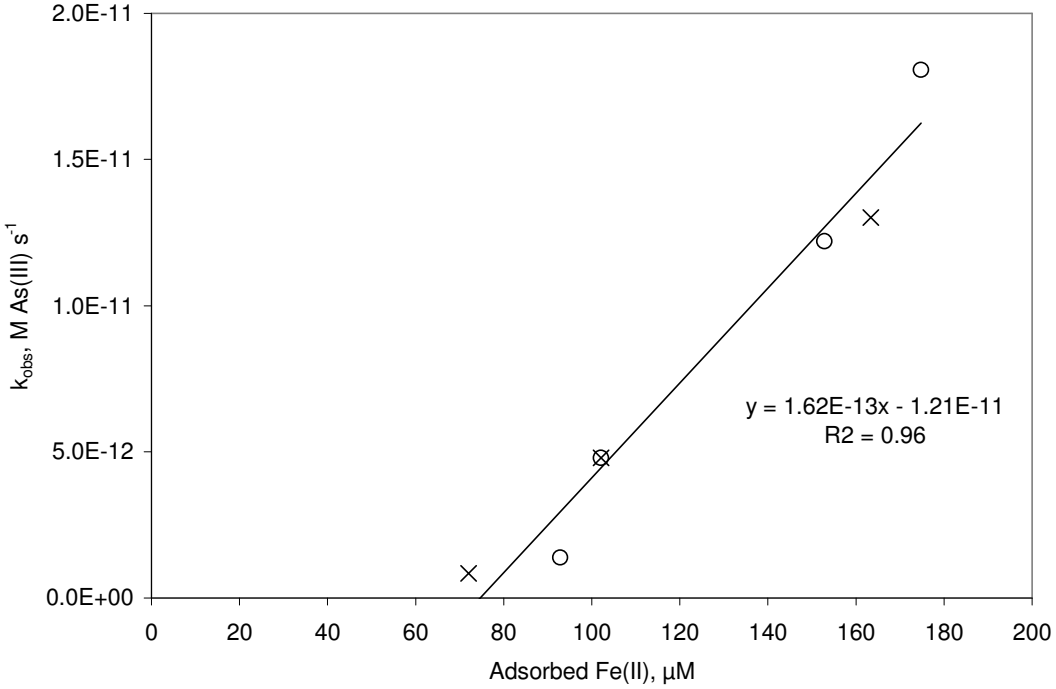

Figure 3-3: Impact of sorbed Fe(II) on observed rate constant for As(III) production. Crosses denote pH 7.0, total Fe(II) 33-500 µM; circles denote pH 6.5-8.65, total Fe(II) 200 µM.

$$d[As(III)]/dt = k[Fe(II)_{ads}][As(V)] \qquad \text{(Equation 3-12)}$$

This is very slow compared to rates reported for other reactions involving $Fe(II)_{ads}$. For example, the reduction of the uranyl cation ($U(VI)O_2^{+2}$) by Fe(II) adsorbed to hematite has a rate constant of 399 $M^{-1}s^{-1}$ (Liger, Charlet et al. 1999).

The substantial intercept in Figure 3-3 is unexpected, and can be interpreted to indicate that a threshold of $Fe(II)_{ads}$ is required for reduction of As(V) to take place. This could be caused by differing reactivities of different adsorbed Fe(II) species as a function of loading.

3.3.2 Co-oxidation of As(III) and Fe(II) by O_2

Before investigating production of As(V) during oxygenation of Fe(II), preliminary experiments were conducted to confirm previous reports that As(III) is stable in solutions containing oxygen (p_{O2} = 0.21 atm) for at least several hours, both in the presence and absence of goethite. Next, a series of preparatory experiments were conducted with Fe(II) oxidation in the absence of As(III) using MES (pH 6.75) and HEPES (pH 7, 7.25) buffers, but the experiments showed oxidation kinetics much slower than expected based on model predictions using Equation 3-1 with the rate constant of Davison and Seed (1983) (Figure 3-4a). No dependence on buffer concentration was seen (data not shown). The experimental data also show a marked curvature which is not consistent with first-order kinetics. The curvature could be explained by precipitation of Fe(III) and autocatalysis, but this is unlikely given the low Fe(II) levels. In all cases, pH varied by less than 0.03 pH units through the duration of the experiment.

A series of experiments were then made using phosphate buffer. The results showed first-order kinetics and a marked correlation between Fe(II) oxidation kinetics and buffer concentration (Figure 3-4b), which were again inconsistent with model predictions using the rate constant of Davison and Seed (1983). Note that experiments were made in duplicate, but samples were not collected at exactly the same time intervals so duplicates are shown with dotted lines rather than error bars.

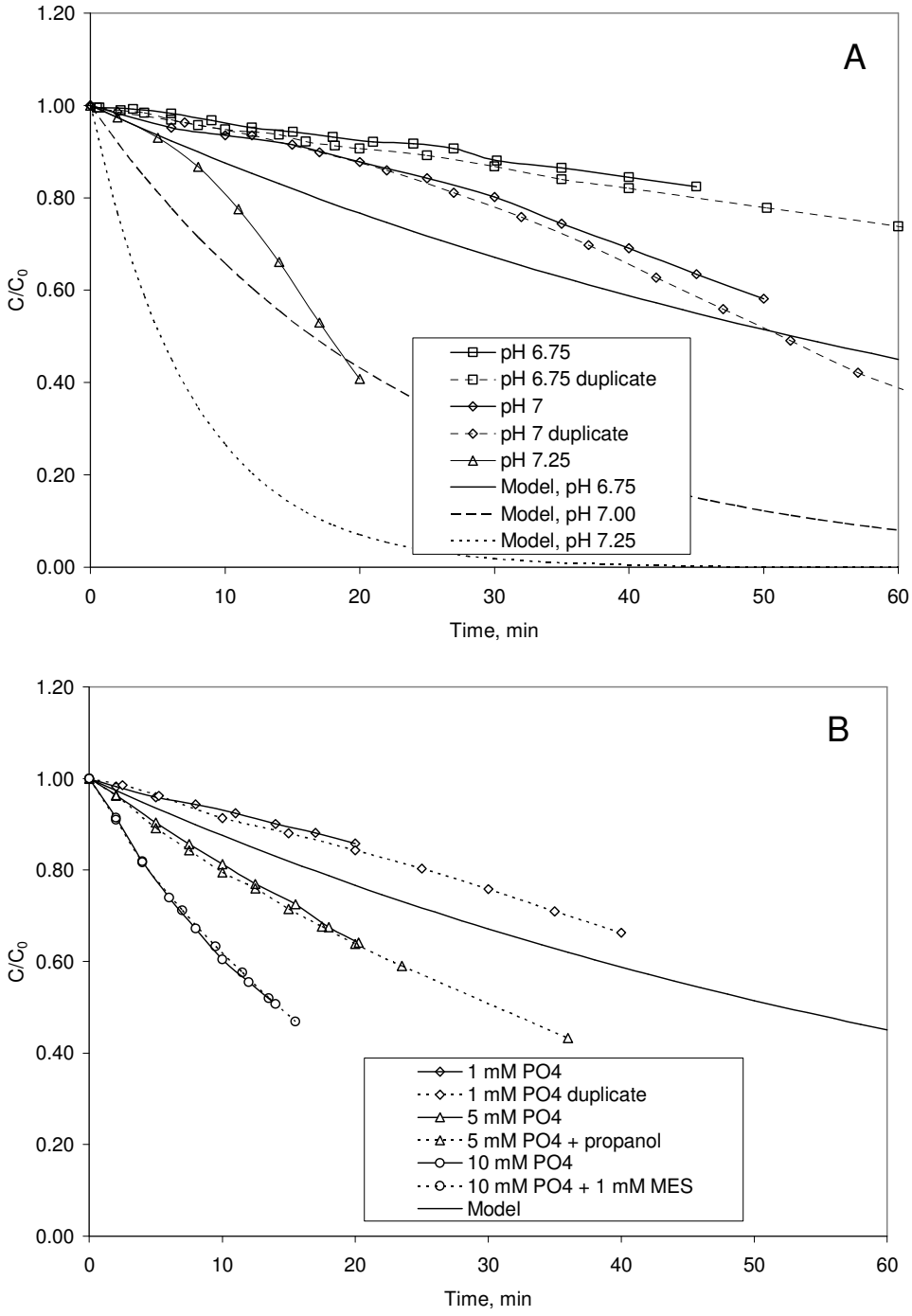

Figure 3-4: Effect of buffering agents on iron oxidation kinetics. Conditions: 25 μM Fe(II), 10 mM $NaNO_3$, 25 °C. Dashed lines indicate duplicate experiments. A: 5 mM MES (pH 6.75) or HEPES (pH 7.00, 7.25). B: 1-10 mM phosphate buffer (pH 6.75).

The enhancement of Fe(II) oxidation by phosphate has been noted previously (Cher and Davidson 1955) and is likely due to the formation of relatively labile dissolved ferrous phosphate complexes. The oxygen atoms of the phosphate molecule donate electron density to the iron atom, stabilizing the ferric state. Reinke et al. (1994) noted that Fe(II) oxidation in the presence of phosphate led to reactive intermediary species which increased with increasing phosphate concentration. Experiments with scavengers indicated that these species were neither superoxide nor hydroxyl radical. Likewise, in our experiments, addition of the hydroxyl radical scavenger 2-propanol had no effect on Fe(II) oxidation in 5 mM phosphate. Furthermore, 1 mM MES did not change Fe(II) oxidation in 10 mM phosphate (Figure 3-4b).

The slow Fe(II) oxidation kinetics in our experiments involving MES or HEPES buffers (Figure 3-4a) can be interpreted as indicating the absence of a labile ferrous ligand species. It is also possible that MES and HEPES actively depress Fe(II) oxidation, either by forming unreactive solution species or by scavenging reactive intermediaries. The first seems unlikely: while HEPES has been shown to form weak complexes with Cu(II), and thus might be expected to form similar complexes with Fe(II), MES has proven inert to metal complexation, because of its molecular structure (Yu, Kandegedara et al. 1997; Mash, Chin et al. 2003). The second possibility is more plausible, but we still consider it is not likely to be the main cause of the slow Fe(II) oxidation rates observed. Grady et al. (1988) investigated radical formation in several of the Good's buffers and found that the hydroxyl radical reacts readily with HEPES, but not with MES, to produce organic radicals. The authors consider that the piperazine ring of HEPES and related buffers is able to form a nitroxide radical, while the morpholine ring of MES is not. Furthermore, in our experiments,

MES had no impact on the oxidation of Fe(II) in 10 mM phosphate (Figure 3-4b), which seems to rule out a major radical scavenging effect.

After dealing with the issue of kinetics in various buffer systems, a series of Fe(II) oxygenation experiments were conducted in the presence of 1 mM As(III) using MES and phosphate buffers at pH 6.75 and HEPES at pH 7. Fe(II) varied from 25 to 100 µM. As(V) was rapidly produced under these conditions (Figure 3-5), and the presence of As(III) markedly slowed Fe(II) oxidation kinetics in all cases (Figure 3-6).

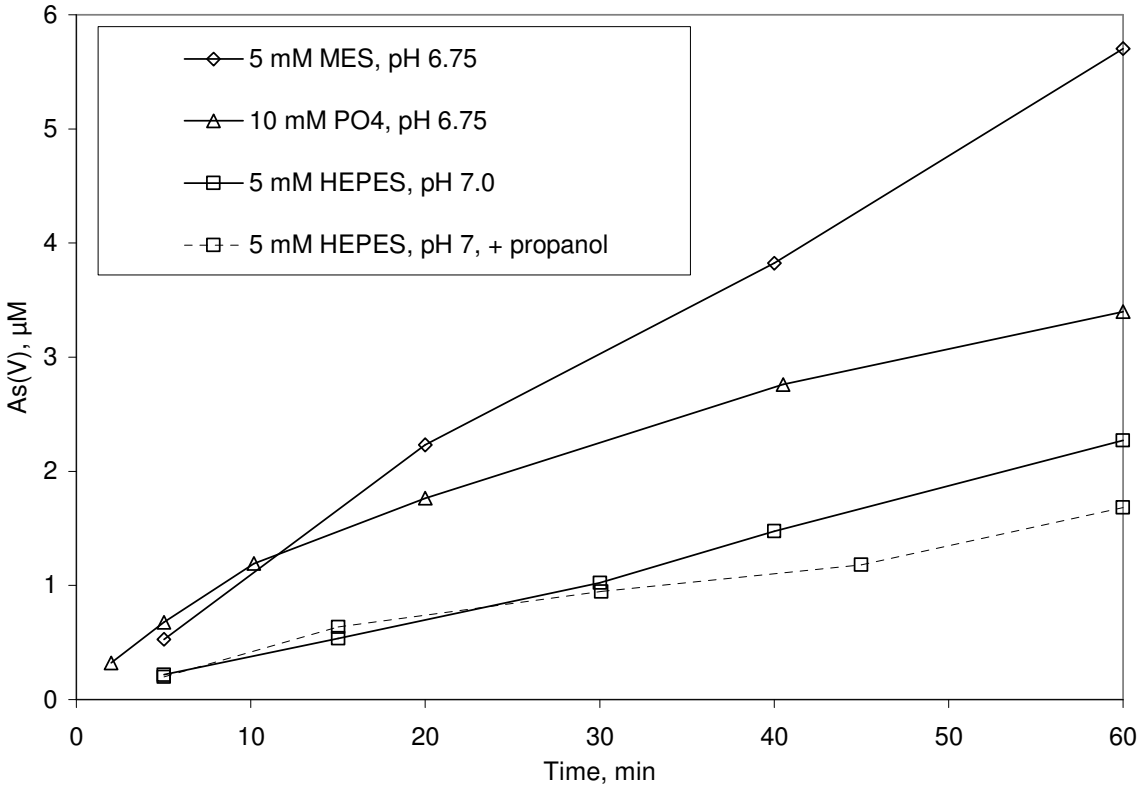

Figure 3-5: As(V) production resulting from co-oxidation of As(III) with Fe(II) in the presence of various buffering agents.

In the presence of 1 mM As(III) and 5 mM MES (pH 6.75), Fe(II) had a half-life of 332 minutes, compared to the prediction of 52 minutes using the rate constant of Davison and Seed (1983). In the MES and HEPES systems relatively little Fe(II) was oxidized, and As(V)

production remained relatively constant over time. Propanol had a slight inhibitory effect on As(V) production in the HEPES system. In the presence of 10 mM phosphate, Fe(II) was rapidly oxidized (half-life 34 minutes) and As(V) production slowed.

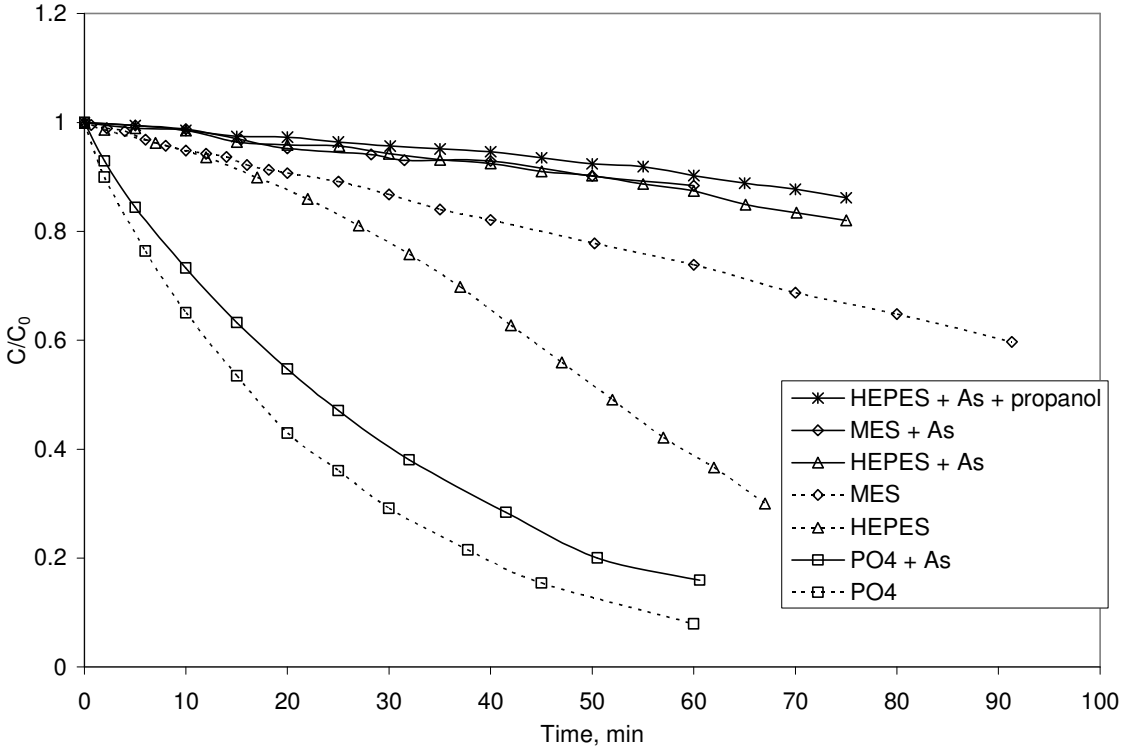

Figure 3-6: Effect of As(III) on the kinetics of Fe(II) oxidation. Buffers are 5 mM HEPES (pH 7.00), 5 mM MES (pH 6.75), and 10 mM PO_4 (pH 6.75). Solid lines are in the presence of 1 mM As(III), dashed lines are without As.

Both the decrease in Fe(II) oxidation rates and the production of As(V) show that As(III) is able to compete with Fe(II) for the transient oxidative species that are produced during the oxygenation of Fe(II). The ratio of As(V) produced to Fe(II) oxidized when As(III) is present in excess gives an indication of the relative efficiency of As(III) at capturing these reactive oxidative species. Figure 3-7 shows that this ratio is highest in the MES experiments, where approximately one mole of As(V) is produced per mole of Fe(II)

oxidized. With HEPES buffer, the ratio is approximately 0.7, and is unaffected by the presence of 14 mM propanol, though the propanol did slow Fe(II) oxidation slightly (Figure 3-6). The ratio is much lower in the phosphate system (pH 6.75) with 0.2 moles As(V) produced per mole of Fe(II) oxidized.

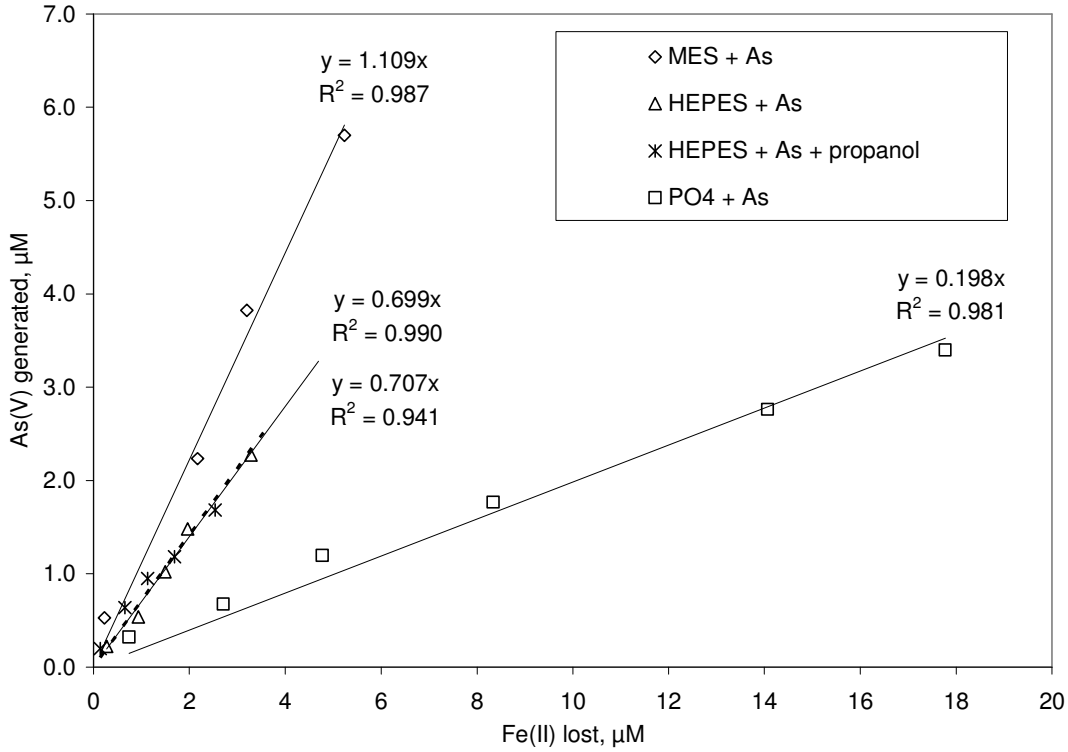

Figure 3-7: Comparison of As(V) yield per mole Fe(II) oxidized. Regression lines are forced through the origin. Buffers are 5 mM HEPES (pH 7), 5 mM MES (pH 6.75), and 10 mM PO_4 (pH 6.75). Fe(II) ranged from 25 to 100 µM.

These findings are consistent with the following mechanism. In the MES and HEPES systems, Fe(II) complexed with a ligand – possibly hydroxide or carbonate – reacts with molecular oxygen producing superoxide. Superoxide reacts with As(III), producing hydrogen peroxide and As(IV), which rapidly reacts with molecular oxygen producing more superoxide.

$$Fe(II)\text{-}L + O_2 = Fe(III) + \bullet O_2^- \quad \text{(Equation 3-13)}$$

$$As(III) + \bullet O_2^- = As(IV) + H_2O_2 \quad \text{(Equation 3-14)}$$

$$As(IV) + O_2 = As(V) + \bullet O_2^- \quad \text{(Equation 3-15)}$$

Equations 3-14 and 3-15 form a chain reaction that is broken when superoxide reacts with other species such as Fe(II), Fe(III), or HEPES. The hydrogen peroxide produced in Equation 3-14 goes on to oxidize Fe(II), producing Fe(IV) at neutral pH, which in turn reacts with either Fe(II) or As(III) (Equations 3-16 through 3-18, after Hug and Leupin, 2003). As these reactions progress, reactive species become more important and Fe(II) oxidation increases, causing the auto-catalytic curvature seen in Figures 3-4a and 3-6.

$$H_2O_2 + Fe(II) = Fe(IV) \quad \text{(Equation 3-16)}$$

$$Fe(IV) + Fe(II) = 2Fe(III) \quad \text{(Equation 3-17)}$$

$$Fe(IV) + As(III) = Fe(III) + As(IV) \quad \text{(Equation 3-18)}$$

In the phosphate system, the chemistry is similar except that the first step is a two-electron transfer, bypassing superoxide entirely (Equation 3-19):

$$Fe(II)\text{-}PO_4 + O_2 = Fe(IV) + H_2O_2 \quad \text{(Equation 3-19)}$$

Equation 3-19 proceeds more quickly than Equation 3-13 in our experiments because of the lack of labile ferrous complexes in the MES and HEPES systems. The presence of phosphate may make Equations 3-16 and 3-17 more rapid as well.

3.4 Summary and conclusions

Direct homogenous reduction of As(V) by Fe(II) is thermodynamically possible but is kinetically limited. In the presence of goethite, the reaction is catalyzed to some degree, but the kinetics are relatively slow. Higher pH accelerates reaction kinetics because of the increase in sorbed Fe(II) that accompanies the increase in pH. However, higher pH also favors precipitation of symplesite. While adsorbed Fe(II) might be expected to reduce As(V) in some circumstances (e.g. groundwater) this reaction would proceed slowly.

Co-oxidation of As(III) was observed during oxygenation of Fe(II), but the relative extent of As(V) production and Fe(II) consumption was highly dependent on buffer type and concentration. As(III) oxidation was more prevalent in the MES and HEPES buffer systems compared to phosphate. The oxidant reacting with As(III) was not hydroxyl radical, but could have been Fe(IV) species. In the MES and HEPES systems, superoxide may also contribute to the oxidation of As(III).

The kinetics of oxygenation of Fe(II) are highly dependent on the presence of complexing ligands that form labile species that accelerate oxidation. When the biologic buffers MES and HEPES are used, oxidation of Fe(II) is very slow at neutral pH. Phosphate buffer catalyzes Fe(II) oxidation, presumably through the formation of labile ferrous phosphate species. Earlier studies of Fe(II) oxidation commonly used carbonate buffers, which also form complexes with Fe(II) and may have impacted oxidation kinetics.

The reducing conditions that lead to high levels of naturally occurring arsenic in groundwater also frequently result in elevated Fe(II) levels. When oxygen is introduced to these waters, for example after abstraction from aquifers, Fe(II) speciation will determine Fe(II) oxidation kinetics. While it might be expected that As(III) would be co-oxidized during oxygenation of Fe(II) in these systems, the competing ferrous complexes with carbonate, phosphate, and organic species that may be present in these waters are likely to scavenge a significant proportion of radical intermediates, thereby inhibiting the oxidation of As(III) and leading to the persistence of As(III) in oxygenated waters.

CHAPTER 4: COMPETITIVE ADSORPTION OF AS(III), AS(V), AND FE(II) ONTO GOETHITE

4.1 Introduction

Naturally occurring contamination of groundwater with arsenic has been documented at regional scales in Bangladesh, India, and China, as well as in a host of other countries at a more local scale (Smedley and Kinniburgh 2002). One of the main mechanisms for arsenic mobilization at regional scales is the reductive dissolution of ferric oxide phases, which have a strong affinity for both As(III) and As(V). The resulting groundwater chemistry is highly reducing, with high levels of dissolved iron and arsenic and low levels of oxidants, such as dissolved oxygen and nitrate. Arsenic in such settings is present predominantly (typically 66-97%) as As(III) (Bhattacharya, Jacks et al. 2002). Reductive dissolution of iron(III) can mobilize arsenic from aquifer sediments (Matisoff, Khourey et al. 1982), but does not necessarily result in the reduction of As(V) (Cummings, Caccavo et al. 1999), For example, in some Bangladesh groundwaters having high levels of Fe(II), As(V) is present at concentrations significantly higher than As(III), which is inconsistent with thermodynamic expectations (Johnston and Singer 2007b).

Mobility of arsenic and iron in the aquifer, as well as removal of these species after abstraction, is highly dependent on adsorption processes. Adsorption of As(III) and As(V) species onto ferric oxides, including goethite, which are ubiquitous in oxidized natural aquifers, has been well studied and it is accepted that ferric oxides have a strong affinity for

both species (Pierce and Moore 1982; Wilkie and Hering 1996; Manning and Goldberg 1997; Raven, Jain et al. 1998; Sun and Doner 1998; Jain, Raven et al. 1999; Goldberg and Johnston 2001; Manning, Fendorf et al. 2002; Dixit and Hering 2003).

Adsorption of Fe(II) onto iron oxides including goethite has been the subject of numerous investigations (Nano and Strathmann 2006 and references therein) which sometimes yield conflicting results. Some researchers report full recovery of adsorbed Fe(II) following mild acid extraction (Dixit and Hering 2006), while others find hysteretic desorption which is hypothesized to result from Fe(II) incorporation into the bulk oxide (Coughlin and Stone 1995; Jeon, Dempsey et al. 2001; Jeon, Dempsey et al. 2003).

Adsorption of one ionic species may impact adsorption of another species in two ways: by directly competing for the same surface sites, and by altering the electrical charge of the surface. In addition, dissolved complexes may form which have different affinities for the surface. Inner-sphere adsorption can change the surface charge, depending on the nature of the surface species. The presence of other anions (e.g. phosphate, bicarbonate, silicate) is known to negatively impact As(III) and As(V) adsorption onto ferric oxide surfaces (e.g. Manning and Goldberg 1996; Su and Puls 2001; Meng, Korfiatis et al. 2002), but few studies have examined competition between As(III) and As(V) on goethite (Jain and Loeppert 2000; Goldberg 2002). Appelo et al. have postulated that carbonate could effectively compete with arsenate on iron oxide surfaces, and described this competitive effect with surface complexation models (Appelo, Van der Weiden et al. 2002). The model predictions, however, are at odds with several laboratory studies showing little to no competitive effect, even at high carbonate levels (Radu, Subacz et al. 2005; Stollenwerk, Breit et al. 2007)

Fe(II) and anions such as As(III) or As(V) may, in principle, bind at the same surface hydroxyl sites. Generally speaking, anion adsorption makes the surface charge more negative while cation adsorption makes it more positive. Thus, adsorption of charged species should make adsorption of oppositely charged species more favorable from an electrostatic standpoint. At high loadings, however, cations and anions may compete for the limited number of surface sites. Several studies have demonstrated a cooperative effect between arsenate, arsenite, or phosphate with divalent metals, e.g. Cd^{2+} (Juang and Chung 2004; Wang and Xing 2004; Liang, Xu et al. 2007) and Cu^{2+} (Khaodhiar, Azizian et al. 2000; Lin, Kao et al. 2004), and Appelo et al. (2002) have predicted that Fe(II) adsorption will increase arsenate adsorption. However, Fe(II) adsorption has been shown to be significantly reduced in the presence of moderate levels of carbonate (Vikesland and Valentine 2002). Dixit and Hering (2006) have examined co-adsorption of Fe(II) and As(III) , as discussed below.

Adsorption can be described using surface complexation models which capture both the intrinsic affinity of a solute for a surface and the electrostatic component of adsorption. Different models address the electrostatic component in different ways, and equilibrium constants derived for one model are not easily transferable to other models. The most commonly used models are the diffuse double layer (DDL), constant capacitance, and triple layer models (Davis and Kent 1990; Dzombak and Morel 1990) .

Using the constant capacitance model, Goldberg (2002) modeled adsorption of As(III) and As(V) on hydrous ferric oxide (HFO) and found no evidence of competition between As(III) and As(V). Arsenic loadings, however, were intentionally well below the total site concentration (approximately 3% of the available surface sites, at 0.1 $\mu mol/m^2$), in order to model arsenic levels representative of drainage and well waters in the study area.

Working at higher loadings of arsenic onto HFO, Jain and Loeppert (2000) examined competitive effects between As(III) and As(V) adsorption onto HFO and found that arsenate adsorption had a greater inhibitory effect on arsenite adsorption than vice versa. No attempts were made to model the competitive findings.

Manning and Goldberg (1996), however, did find competition between As(V) and P or Mo adsorption onto goethite when the total adsorbate load was 2.4 $\mu mol/m^2$, approximately 64% of the available surface sites. Attempts to describe the competitive effects using the constant capacitance model were able to match the observed data qualitatively but not quantitatively. Monodentate and bidentate models were used, with the monodentate model providing the best match to experimental data. Likewise, Wilkie and Hering (1996) found that a DDL surface complexation model could only qualitatively capture the effect of sulfate and calcium on adsorption of As(III) and As(V) on HFO.

Dixit and Hering (2006) studied adsorption of Fe(II) onto goethite and derived new surface complexation constants using a site density of 2.0 sites/nm^2. Using the DDL model, they were able to reproduce adsorption of Fe(II) and As(III) in single-sorbate experiments, but not binary-sorbate systems. The model predicted a mutually negative effect of co-adsorption under the experimental conditions, since both sorbates were well in excess of available sites. However, the experimental data showed that, from pH 6.0 to 7.5, addition of up to 1000 µM As(III) (5.1 $\mu mol/m^2$) had no impact on adsorption of up to 1500 µM Fe(II) (7.7 $\mu mol/m^2$). Likewise, addition of up to 1500 µM Fe(II) had no impact on adsorption of 500 µM As(III). 2.8 $\mu mol/m^2$ Fe(II) and 2.2 $\mu mol/m^2$ As(III) were adsorbed without any observed competitive effects, implying a surface capacity of at least 5 $\mu mol/m^2$, 50% higher than the modeled maximum capacity of 3.3 $\mu mol/m^2$ (2.0 sites/nm^2). The authors noted that

if a higher site density were used, the model could reproduce the observed lack of competitive adsorption. At 1000 μM As(III) and at pH 7 or greater, both As and Fe sorption density increased dramatically. The authors suggested that this due to surface precipitation or formation of ternary complexes.

Hiemstra et al. (2007) applied the CD-MUSIC model to the Dixit and Hering data and were unable to replicate all the observed single-sorbate results without using two separate sets of binding constants for the two goethites used by Dixit and Hering. Matching the binary sorbate results was possible when different binding constants for the two goethites were used, and a reaction was introduced to model formation of a monodentate ternary complex. While the model fit was satisfactory, it came at the cost of a large number of adjustable constants.

This paper describes a series of experiments in which As(III), As(V), and Fe(II) were adsorbed onto goethite, either in single-sorbate or binary-sorbate systems. Adsorbate concentrations were chosen to be within the range found in natural waters and adjusted so that, with a fixed goethite concentration, the maximum loading was slightly in excess of the concentration of surface sites. Adsorption isotherms and envelopes were generated from experimental data and modeled using the PHREEQC geochemical software (Parkhurst and Appelo 1999).

4.2 Experimental section

4.2.1 Chemicals

All chemicals were of Certified ACS grade or better, and were used without further purification. 50 mM As(V) stock solutions were prepared from NaH_2AsO_4-$7H_2O$ (Sigma), while liquid 50 mM As(III) stock solutions were purchased directly (Fisher). Fe(II) stock

solutions were freshly prepared by dissolving $Fe(NH_4)_2(SO_4)_2$ in 1 mM HNO_3. Three of the Good et al. (1966) biologic buffers [MES (pKa 6.15), HEPES (pKa 7.55), and CHES (pKa 9.3)] were used to buffer pH. HNO_3 and KOH were used for pH adjustment.

4.2.2 Goethite synthesis

Goethite was chosen as the model iron oxide, and was synthesized by slowly adding 450 mL 1.0 M KOH to 50 mL of 1.0 M $Fe(NO_3)_3$ under a nitrogen atmosphere (Schwertmann and Cornell 2000). The resulting slurry was incubated at 25 °C for 14 days (Peak and Sparks 2002) and dialyzed to remove residual dissolved salts (Spectra-Por 7, 3500 MW cut-off) until the permeate conductivity was less than that of a 0.1 mM $NaNO_3$ solution. The precipitate was freeze-dried and confirmed to be goethite, with no significant crystalline impurities, using X-ray powder diffractometry (Rigaku Multiflex). The specific surface area measured by 5-point N_2 BET adsorption was 65 m^2/g (NOVA Quantachrome 1200).

All adsorption experiments were made with a 0.2 g/L (13 m^2/L) goethite concentration. Goethite additions were made from concentrated suspensions as these gave better reproducibility than direct addition of small volumes of dried goethite.

4.2.3 Adsorption kinetics

In order to choose an appropriate equilibration period for arsenic adsorption, kinetic experiments were conducted using disposable 10 mL syringes (BD) as reactors: precise volumes of a concentrated slurry suspension, buffer and diluent were added using a 6-port injection valve with Teflon sample loops, filling the syringe without headspace. A small magnetic stir bar was placed in the syringe to aid with mixing. Experiments were initiated by injecting As(III) or As(V) stock solution into the reactor. Initial reactor conditions were 30

μM As in a 0.2 g/L goethite suspension, with a background electrolyte of 0.1 M $NaNO_3$ and pH fixed at 7.0 with 0.02 M HEPES. Duplicate reactors were prepared for As(III) and As(V), as well as one goethite-free control for each. After loading, the reactors were capped and placed on an end-over-end shaker.

At set intervals, a small volume of the suspension (~500 μL) was withdrawn and filtered through a 0.2 micron polyvinylidene fluoride (Supelco) or nylon (Fisher) syringe filter. Samples were then diluted 10:1 with 24 mM HNO_3 for total arsenic analysis, or with deionized water for As speciation. Samples were collected frequently over the first hours and days, with less frequent sampling continuing for 30 days.

4.2.4 Adsorption isotherms

Arsenic adsorption experiments were conducted under ambient atmospheric conditions. 15 mL disposable centrifuge tubes (Falcon) were used as reactors, which were equilibrated on an end-over-end shaker for 24 hours. After equilibration, samples were filtered as previously described. Adsorption of As(III) and As(V) were measured at pH 8.0 and 4.5, using 0.2 g/L goethite in 0.1 M $NaNO_3$ background electrolyte and 0.02 M HEPES or MES buffer, respectively.

Fe(II) adsorption experiments were done in a glove box (2% hydrogen/98% nitrogen atmosphere, Coy Laboratory Products, Inc.) using 10 mL brown glass crimp-top vials as reactors. Goethite and ionic strength conditions were the same as in the arsenic experiments, while pH was fixed at 8.36 (HEPES) which geochemical calculations indicated was below saturation of $Fe(OH)_2(s)$ at the highest Fe(II) loading (500 μM, or 38.5 $\mu mol/m^2$). Vials were equilibrated on an end-over-end shaker for 4 hours, as Fe(II) adsorption is reported to be rapid (Vikesland and Valentine 2002)

4.2.5 Adsorption edges and envelopes

Adsorption edges for Fe(II) and adsorption envelopes for As(III) and As(V) were developed for single-ion systems. Two sets of binary experiments examined the co-adsorption of As(III) along with As(V) or Fe(II). As in the kinetic experiments, experiments involving only arsenic were conducted under ambient atmospheric conditions, while experiments involving Fe(II) were done in the glove box. The same types of reactors were used as in the kinetic experiments.

In the single-ion experiments, experimental conditions were 0.2 g/L goethite, 0.1 M $NaNO_3$, and 0.02 M pH buffer (acetate from pH 3-5.5, MES from pH 5.5-6.5, HEPES from pH 6.5-8.5, and CHES from pH 8.5-10). Variable amounts of acid or base were added to adjust pH to the desired level, and adsorbate (50 µM As(III), 50 µM As(V), or 300 µM Fe(II), equivalent to 3.85 µmol/m^2 As and 23 µmol/m^2 Fe(II)) was added. Equilibration time was fixed at 24 hours for arsenic and 1 hour for Fe(II). After equilibration, the final pH was recorded and samples were collected and filtered for arsenic and Fe(II) analysis.

Binary experiments were also performed under the same experimental conditions, except for a lower ionic strength (0.01 M $NaNO_3$) and pH buffer concentration (0.005 M) to facilitate arsenic speciation analysis. (The anion exchange cartridges retaining As(V) would be rapidly saturated by excess nitrate under the original conditions.)

The As(III)/As(V) experiments were initiated by spiking goethite suspensions with 100 µM As using equimolar As(III)/As(V) stock solutions. Duplicates were run for all reactors; goethite-free controls were also prepared. Samples were equilibrated on an end-over-end shaker for 24 hours. Approximately 5 mL of the suspension was filtered through 0.2 micron syringe filters: one aliquot was diluted in 10 mM HNO_3 for measurement of total

arsenic, while another aliquot was passed through the anion exchange cartridge before dilution and analysis of As(III). As(V) was calculated as the difference between total arsenic and As(III).

A second set of experiments was made in a glove box to investigate the effect of As(III) on adsorption of Fe(II) and vice versa. Reactors (brown glass vials) were prepared and equilibrated with either 300 µM Fe(II) for four hours or 50 µM As(III) for 24 hours. An aliquot of the suspension was then removed and spiked with the second adsorbate and equilibrated for an additional 4 or 24 hours (for Fe(II) and As(III), respectively). Goethite-free blanks were prepared in 10 mM nitric acid and at pH 8.0. After equilibration with one or both adsorbates, samples were collected, filtered through a 0.2 µM polyvinylidene fluoride filter, and diluted in 10 mM HNO_3 for subsequent Fe(II) and As analysis outside the glove box. Note that this experimental approach yielded both single-ion and binary adsorption edges for both As(III) and Fe(II), in addition to the single-ion edges collected in previous experiments.

4.2.6 Speciation and measurement of dissolved arsenic and iron

Arsenic was measured using graphite furnace atomic absorption spectrophotometry (Perkin-Elmer 5100PC) with an EDL lamp and Pd/Mg matrix modifier. Arsenic (III) was separated from total arsenic by solid-phase extraction onto an anion exchange resin column (Supelco, Sigma-Aldrich) which adsorbs anionic As(V) species (Ficklin 1983). As(V) was calculated as the difference between total arsenic and As(III).

Fe(II) was measured using a modified Ferrozine method (Stookey 1970; Gibbs 1976). Stock solutions of 1.0 mM Ferrozine were prepared in 500 mM ammonium acetate at pH 7.0. Variable amounts of the Ferrozine stock solution were added to samples, depending on the

Fe(II) concentration, but in all cases the final pH was above 4. Absorbance at 562 nm was measured at least an hour after Ferrozine addition to allow full color development.

In experiments involving goethite, samples were filtered through a 0.2 micron polyvinylidene fluoride (Supelco) or nylon (Fisher) syringe filter prior to analysis.

For both arsenic and iron analysis, a 5-point calibration curve was used, with r^2 of 0.999 or greater. Calibration standards were prepared by dilution of 1000 µg/mL ICP stock solutions (Fisher) in 24 mM HNO_3. Quality control standards, prepared from separate stock solutions, were analyzed before and after every batch of 6-10 samples, and analytical results were adjusted accordingly by linear interpolation. If the standard deviated from the expected value by more than 5%, the instrument was re-calibrated and samples were re-analyzed.

4.2.7 Geochemical modeling

PHREEQC version 2.13 was used for all geochemical modeling (Parkhurst and Appelo 1999). The model simulates adsorption using a double diffuse layer, and calculates activity coefficients using the Davies equation. Equilibrium constants and other parameters used in the model are summarized in Table 4-1. While cation adsorption onto HFO generally requires two types of surface sites (strong and weak, Dzombak and Morel 1990), only one site is recommended for modeling surface complexation at the goethite surface (Mathur and Dzombak 2006).

Table 4-1: PHREEQC model parameters

Reaction	*Log K*	*Source*
	Solution reactions	
Ferrous iron		
$Fe^{+2} + OH^- \leftrightarrow FeOH^+$	4.5	(Morel and Hering 1993)
$Fe^{+2} + 2OH^- \leftrightarrow Fe(OH)_{2,\,aq}$	7.4	(Morel and Hering 1993)
$Fe^{+2} + SO_4^{-2} \leftrightarrow FeSO_4$	2.25	(Parkhurst and Appelo 1999)
$Fe^{+2} + HSO_4^- \leftrightarrow FeHSO_4^+$	1.08	(Parkhurst and Appelo 1999)
Arsenite		
$H_3AsO_3 \leftrightarrow H_2AsO_3^- + H^+$	-9.228	(Ball and Nordstrom 1991)
$H_3AsO_3 \leftrightarrow HAsO_3^{-2} + 2H^+$	-21.33	(Ball and Nordstrom 1991)
$H_3AsO_3 \leftrightarrow AsO_3^{-3} + 3H^+$	-34.74	(Ball and Nordstrom 1991)
Arsenate		
$H_3AsO_4 \leftrightarrow H_2AsO_4^- + H^+$	-2.24	(Ball and Nordstrom 1991)
$H_3AsO_4 \leftrightarrow HAsO_4^{-2} + 2H^+$	-9.00	(Ball and Nordstrom 1991)
$H_3AsO_4 \leftrightarrow AsO_4^{-3} + 3H^+$	-20.60	(Ball and Nordstrom 1991)
	Surface reactions	
Goethite surface charging		
$>SOH + H^+ \leftrightarrow >SOH_2^+$	7.47	(Dixit and Hering 2003)
$>SOH \leftrightarrow >SO^- + H^+$	-9.51	(Dixit and Hering 2003)
Ferrous iron adsorption		
$>SOH + Fe^{+2} \leftrightarrow >SOFe^+ + H^+$	-0.54	(Dixit and Hering 2006)
$>SOH + Fe^{+2} + H_2O \leftrightarrow >SOFeOH + 2H^+$	-10.89	(Dixit and Hering 2006)
Arsenite adsorption		
$>SOH + H_3AsO_3 \leftrightarrow >SH_2AsO_3 + H_2O$	5.19	(Dixit and Hering 2003)
$>SOH + H_2AsO_3^- \leftrightarrow >SHAsO_3^- + H_2O$	6.88	(Dixit and Hering 2003)
Arsenate adsorption		
$>SOH + H_3AsO_4 \leftrightarrow >SH_2AsO_4 + H_2O$	10.40	(Dixit and Hering 2003)
$>SOH + H_2AsO_4^- \leftrightarrow >SHAsO_4^- + H_2O$	8.46	(Dixit and Hering 2003)
$>SOH + HAsO_4^{-2} \leftrightarrow >SAsO_4^{-2} + H_2O$	8.62	(Dixit and Hering 2003)

4.3 Results and discussion

4.3.1 Adsorption kinetics

Adsorption of both As(III) and As(V) was initially rapid, but continued for at least 30 days (Figure 4-1). The slower phase of adsorption can be interpreted as diffusion of As into the bulk of the goethite through microfissures and pores (Luengo, Brigante et al. 2007).

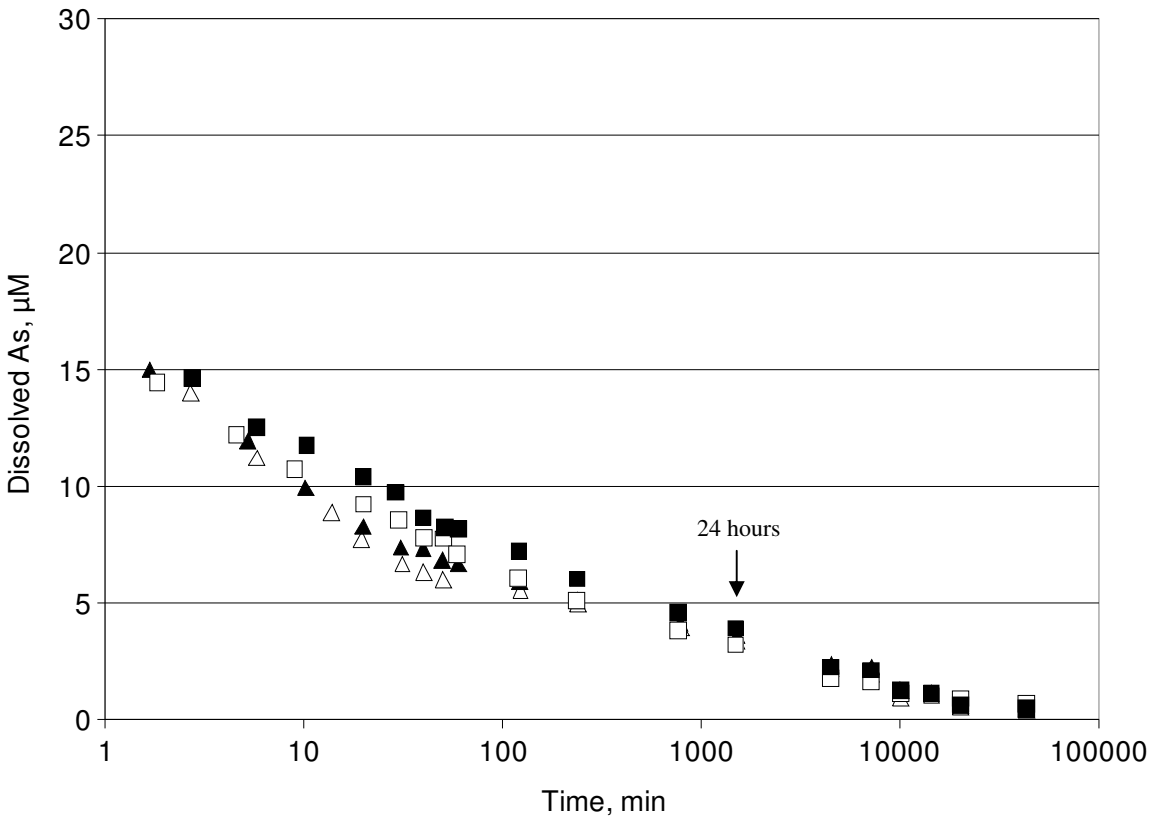

Figure 4-1: Adsorption kinetics for 30 µM As(III) (triangles) and As(V) (squares) onto goethite. Hollow and filled symbols are duplicates. Conditions: 0.2 g/L goethite, 0.1 M $NaNO_3$, 0.02 M HEPES buffer (pH 7.0).

Approximately half of the initial 30 µM arsenic was adsorbed within 2 minutes, and approximately 90% of the ultimate amount which would be adsorbed over 30 days had been adsorbed within the first 24 hours. Total arsenic in the control reactors was constant over the course of the experiment. As(V) was not detected at significant levels in either the adsorption or control reactors containing As(III) for up to 30 days. However, in both reactors initially containing goethite and As(V), As(III) was detected on day 3 and, by day 7, As(III) constituted more than half of the total dissolved arsenic. A similar but slower trend was seen in the goethite-free control reactor. Because no As(III) was detected in the As(V) reactors before day 3, and because 90% of the As adsorption occurred within the first 24 hours, a 24-

hour equilibration period was chosen for subsequent adsorption experiments to preclude any unwanted reduction of As(V).

4.3.2 Adsorption isotherms

Sorption of As(III) and As(V) conformed well to the Langmuir model (Figure 4-2), and resulted in a maximum adsorption density of 209 µmol As(III) and 185 µmol As(V) per gram of goethite. Given the measured surface area for goethite of 65 m^2/g, the isotherms yield a density of 1.94 sites/nm^2 for As(III) and 1.72 sites/nm^2 for As(V) (3.2 and 2.8 µmol/m^2, respectively). The site density for As(III) is in excellent agreement with the value of 2.0 reported by Dixit and Hering (2003) for both As(III) and As(V). These experiments found a slightly lower capacity for As(V) than that reported by Dixit and Hering, possibly because pH was fixed at 4.5 rather than the pH of 4.0 used in their study.

Sorption of Fe(II) also conformed well to the Langmuir model (Figure 4-2), but the goethite surface exhibited a very high capacity for Fe(II) of 1380 µmol/g (21.2 µmol/m^2), more than 6 times higher than its capacity for As. This gives a site density of 12.75 sites/nm^2. The apparent higher capacity of the goethite surface for Fe(II) than for As is interesting and warrants further discussion.

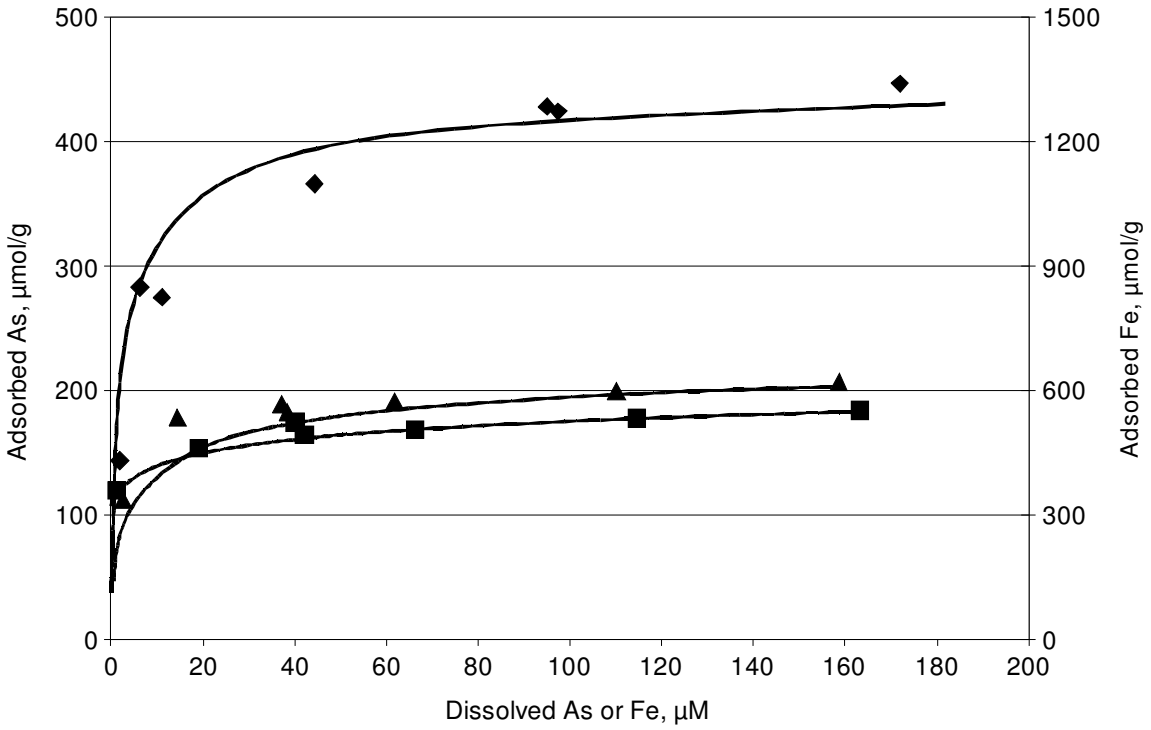

Figure 4-2: Adsorption isotherms for As(III) (triangles), As(V) (squares), and Fe(II) (diamonds). Lines are PHREEQC model predictions. Conditions: 0.2 g/L goethite, 0.1 M $NaNO_3$, 0.02 M HEPES (pH 8.0) for As(III), 0.02 M MES (pH 4.5) for As(V), 0.02 M HEPES (pH 8.63) for Fe(II).

There are at least four possible explanations for the observed loss of Fe(II) from solution: a higher site density for Fe(II), oxidation or precipitation of Fe(II), and interfacial electron transfer. The difference in observed capacities for As and Fe(II) could be explained if some surface sites can adsorb Fe(II) but not As. This is plausible because Fe(II) is structurally similar to Fe(III) atoms in the goethite matrix. Surface hydroxyl site density on the goethite surface has been calculated using crystallographic analysis, isotopic exchange, and acid-base titrations, yielding measurements ranging from 1.7 to 18 sites/nm^2 (Mathur and Dzombak 2006). Hiemstra et al. (1996) have identified four different surface species which differ in the number of Fe atoms to which the surface O is coordinated. They calculate a total site density of 15 sites/nm^2, of which only singly coordinated species (3 sites/nm^2) are

considered reactive to protonation, deprotonation, and adsorption of anions (Geelhoed, Hiemstra et al. 1997).

Most surface complexation modeling is done with site densities ranging from 1-2.5 sites/nm^2 (Liger, Charlet et al. 1999; Amonette, Workman et al. 2000; Dixit and Hering 2006), though earlier models used higher densities of about 7.0 sites/nm^2 (Hayes and Leckie 1986; Coughlin and Stone 1995). The density of sites accessible to Fe(II) has been estimated at 1.6 to 2.9 sites/nm^2 from isotherms made near pH 7.0 (Coughlin and Stone 1995; Amonette, Workman et al. 2000; Mettler 2002). This is similar to the generic density of 2.3 sites/nm^2 recommended for all minerals (Davis and Kent 1990). However, the maximum adsorption capacity is strongly pH-dependent: Mettler (2002) found a maximum capacity of 10.2 sites/nm^2 at pH 8, compared to 2.9 sites/nm^2 for the same goethite at pH 7. Vikesland and Valentine (2002) could model adsorption of Fe(II) below pH 7 and in the absence of carbonate using standard site densities, but needed to invoke a much higher site density of 13 sites/nm^2, citing the precedent of Davies and Morgan (1989), in order to match Fe(II) adsorption at higher pH and in the presence of carbonate. This higher density was equally good at matching Fe(II) adsorption in the absence of carbonate, and is in good agreement with our findings from a higher-pH isotherm. Our isotherm is not consistent with that of Dixit and Hering (2006), conducted at pH 7.5, which found a maximum capacity of 1.8 sites/nm^2.

Another possible explanation for the apparent higher adsorption capacity of Fe(II) in our experimental system could have been due to loss of Fe(II) through oxidation, rather than adsorption. While oxygen was strictly excluded in our experiments, the nitrate used to control ionic strength is thermodynamically capable of oxidizing Fe(II). This seems unlikely

as goethite-free blanks showed only minor Fe(II) loss at pH 8. Furthermore, other researchers working in nitrate-containing solutions have not reported any oxidation of Fe(II), while others have found a high capacity of goethite for Fe(II) while using chloride (Mettler 2002) and perchlorate (Vikesland and Valentine 2002) electrolytes.

A third explanation for the apparent higher charge density for Fe(II) might be surface precipitation. Although conditions were selected to keep the system undersaturated with respect to $Fe(OH)_2$ in bulk solution, surface precipitation might occur. However, the shape of the isotherm (Figure 4-2) is inconsistent with precipitation, which would be marked by a sudden increase in 'lost' Fe(II) at concentrations above saturation, while maintaining a nearly constant dissolved Fe(II) level. Given the smooth decrease in dissolved Fe(II) seen in our experiments, this explanation seems unlikely.

Finally, recent work has shown that adsorbed Fe(II) is re-worked into the interior of the goethite matrix through an electron transfer process (Coughlin and Stone 1995; Jeon, Dempsey et al. 2001; Jeon, Dempsey et al. 2003):

$$>Fe^{III}OH + Fe^{II} \rightarrow >Fe^{III}OFe^{II}OH \rightarrow >Fe^{II}OFe^{III}OH \qquad \text{(Equation 4-1)}$$

This reaction regenerates reactive ferric surface sites, greatly increasing the "apparent" adsorptive capacity of the surface. Spectroscopic evidence for such an electron transfer reaction, occurring after one or more days of Fe(II) adsorption, has been shown recently (Williams and Scherer 2004; Silvester, Charlet et al. 2005). It is not clear if such a reaction might have taken place on the time scale of our adsorption experiments.

In an attempt to determine which of these mechanisms contributed to the observed loss of significant amounts of Fe(II) from solution, surface complexation modeling was used to explore the first possibility, i.e. that goethite has a much higher adsorption capacity for Fe(II) than for other specifically adsorbing species. A system with two types of sites was modeled: one group accessible to protons, anions, and Fe(II), and another group inert to all species except for Fe(II). (Attempts to make this second type of site accessible to protons as well as Fe(II) led to poor fits for arsenic adsorption.) Site concentrations were set at 2 sites/nm^2 (43 μM) for universally accessible sites and 10.75 (12.75 – 2) sites/nm^2 (232 μM) for Fe(II)-only sites. This approach was able to match the single-sorbate data well, as shown in Figure 4-2.

4.3.3 Competitive adsorption of As(III) and As(V)

In single-ion experiments, As(III) showed a broad adsorption envelope, with maximum adsorption of 35 μM occurring at pH 8.5-9.0, close to the pK_a of 9.2 for arsenious acid (Figure 4-3A). In contrast, As(V) adsorption increased as pH decreased, again showing a maximum adsorption of approximately 35 μM As(V) at pH 3-3.5 (Figure 4-3B). Both envelopes are in agreement with expectations based on pH and As speciation, and are similar to those reported by others (e.g. Dixit and Hering 2003). Duplicates were in good agreement, and the concentration and speciation of As(III) and As(V) in the goethite-free controls were within 5% of 50 μM.

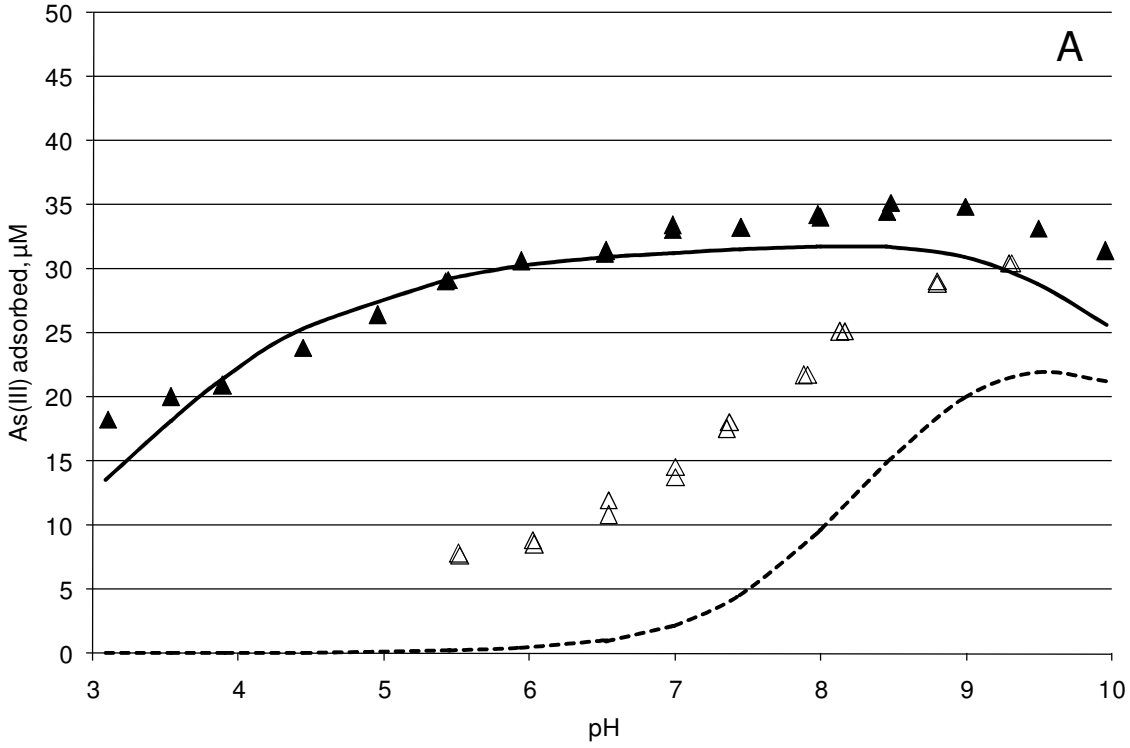
A
As(III) adsorbed, µM
pH
0
5
10
15
20
25
30
35
40
45
50
3
4
5
6
7
8
9
10

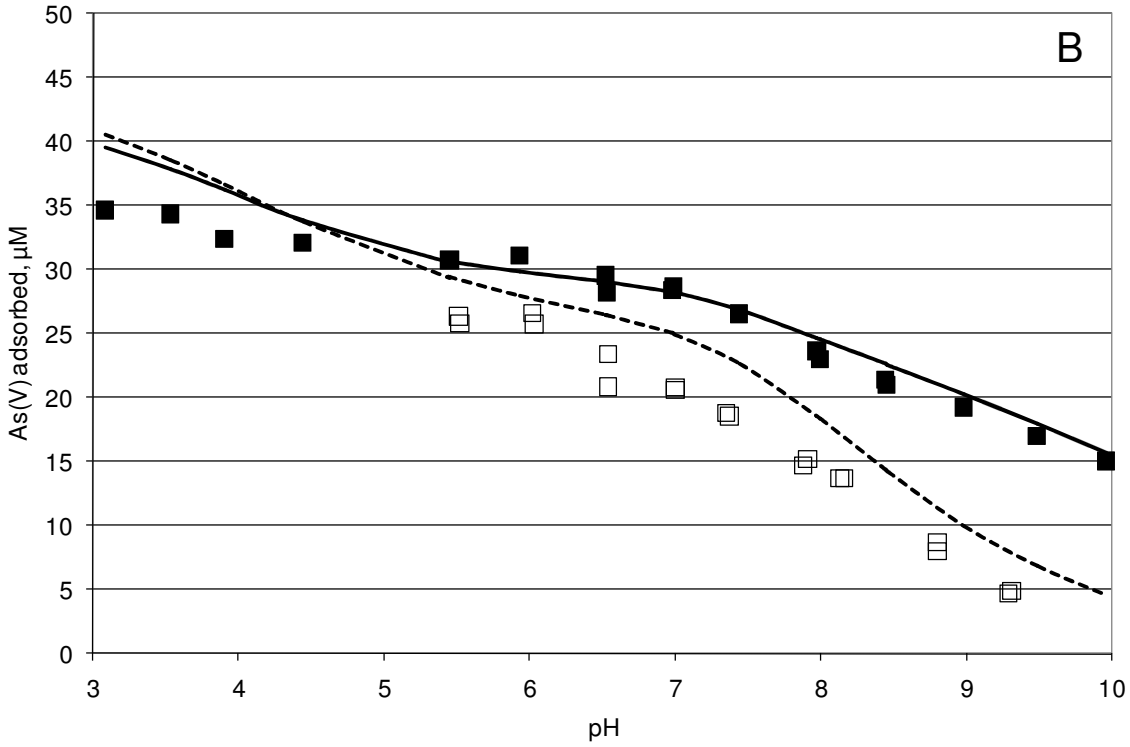
B
As(V) adsorbed, µM
pH
0
5
10
15
20
25
30
35
40
45
50
3
4
5
6
7
8
9
10

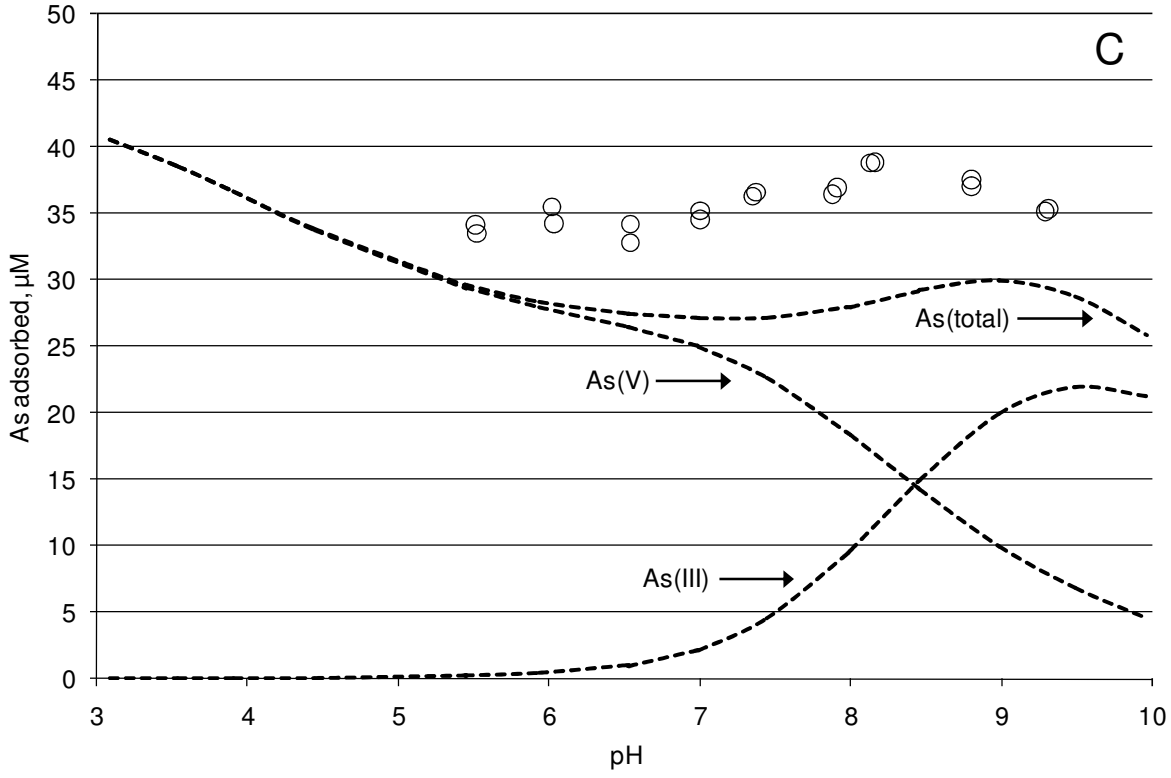

Figure 4-3: Adsorption of (A) As(III), (B) As(V), and (C) As(total) in single-sorbate and binary-sorbate systems. Triangles and squares represent As(III) and As(V), respectively. Filled and hollow symbols are respectively single-ion and binary experiments. Hollow circles indicate total arsenic (As(III) + As(V)) adsorption in binary experiments. Solid and dotted lines indicate model predictions for single and binary systems, respectively.

In the binary experiments, an inhibitory effect was seen for each As species on adsorption of the other (Figure 4-3, panels A and B). The effect of As(V) on the adsorption of As(III) was more pronounced, especially at lower pH, than the effect of As(III) on As(V) adsorption. In the single-ion systems, the goethite surface at pH 6 adsorbed approximately 31 µM As(III) or As(V). In the binary experiment at the same pH, total adsorbed arsenic was slightly higher (34 µM), but As(III) accounted for only 25% of the total. In contrast, above approximately pH 7.5, As(III) species dominated adsorption in the binary experiments.

Figure 4-3 (panels A and B) shows that PHREEQC was able to capture the general shape of the adsorption envelopes in the single solute systems, but somewhat under-predicted As(III) adsorption below pH 3.5 and above pH 7. The As(V) model predictions matched the data more closely, but over-predicted the extent of adsorption below pH 5 and slightly under-predicted adsorption above pH 9. Lumsdon and Evans (1994) have noted that the diffuse double layer model over-predicts charge on the goethite surface at low pH, which could explain the over-prediction for As(V) adsorption.

In the binary systems, PHREEQC correctly predicts the shift in adsorbed arsenic speciation, with adsorption of As(III) being seriously diminished in the presence of equimolar concentrations of As(V). However, the model under-predicts As(III) adsorption by 5-10 µM at all pH values, and predicts a pH of equal adsorption at 8.5 (Figure 4-3C), whereas the data show the pH of equal adsorption occurring at approximately pH 7.5. The model predicts that total adsorption at pH 6-9 would be *less* in the binary experiments compared to the single-ion As(III) experiments, because it considers As(V) adsorption to strongly suppress As(III) adsorption. However, the experimental data show the opposite, which suggests that some sites – approximately 15 µM or 30% of the arsenic-active sites – are more selective for As(III) than for As(V). This would match the observation of Jain and Loeppert (2000) that some sites on the ferrihydrite surface had a much higher affinity for As(III) than for phosphate, which is a chemical analogue of As(V).

4.3.4 Competitive adsorption of As(III) and Fe(II)

In the absence of As(III), 0.2 g/L goethite was equilibrated with 300 µM Fe(II), slightly above the calculated maximum adsorption capacity of 275 µM. The adsorption edge (Figure 4-4A, solid symbols) shows adsorption increasing with increasing pH until pH 8,

with 50% adsorption at pH 7.4. (Experiments could not be conducted at higher pH due to concerns about $Fe(OH)_2(s)$ precipitation.) Because of our assumption of a high site density, the surface loading (23 $\mu mol/m^2$) in our experiment is much higher than in most adsorption studies, which are typically in the range of 2-5 $\mu mol/m^2$ (Liger, Charlet et al. 1999; Gao and Mucci 2001; Mettler 2002). Our adsorption edge is comparable to that of Dixit and Hering (Dixit and Hering 2006), but is shifted to higher pH values compared to those of others (Coughlin and Stone 1995; Liger, Charlet et al. 1999; Vikesland and Valentine 2002). Some Fe(II) adsorption was observed at low pH in our experiments, which could be explained by strong sites which would dominate an adsorption edge at low surface loadings (e.g. 0.2 $\mu mol/m^2$ in (Coughlin and Stone 1995)). Vikesland and Valentine noted that the Fe(II) adsorption edge shifted substantially to the right in the presence of as little as 2 mM carbonate, even at high Fe(II) loadings (17 $\mu mol/m^2$). No special measures were taken in these dissertation experiments to exclude carbonate from goethite during preparation or subsequent experiments, so carbonate contamination of the goethite surface is possible.

When the goethite was pre-equilibrated with 50 µM As(III) and subsequently reacted with 300 µM Fe(II), the experimental data showed the Fe(II) curve shifting to the right (Figure 4-4A, hollow symbols). The extent of the shift increased with increasing pH. While little competitive effect was seen at low pH, pre-equilibration with As(III) decreased Fe(II) adsorption by nearly 50% between pH 6.5 and 8.

The single-ion adsorption curve for As(III) (Figure 4-4B) is similar to that shown in Figure 4-3A, derived from a separate experiment. When the goethite was pre-equilibrated with 300 µM Fe(II), As(III) adsorption was reduced by approximately 5 µM, with little apparent dependence on pH. These findings are at odds with the results of Dixit and Hering

(2006), which showed little competitive effect between As(III) and Fe(II). One explanation for this could be that our surface loading of Fe(II) (23 μmol/m^2) was approximately three times higher than the highest loading in their experiments. However, this explanation is not entirely satisfactory because, at the highest loadings, Dixit and Hering found Fe(II) and As(III) to increase maximum coverage, not reduce coverage.

While PHREEQC was able to match the single-ion adsorption edges for Fe(II) and As(III) reasonably well, it failed to match the observed behavior of either element in the binary experiments (Figure 4-4, dotted lines). The model predicts that pre-equilibration with 50 μM As(III) will increase Fe(II) adsorption below pH 7.3 due to electrostatic effects (the goethite surface charge becomes more negative as As(III) is adsorbed), and decrease Fe(II) adsorption at higher pH (as As(III) competes increasingly for surface sites) (see Figure 4-4A). Instead, the data show the adsorption edge shifting uniformly to the right. Vikesland and Valentine (2002) also found that adsorption of Fe(II) onto goethite was decreased in the presence of another anion (carbonate), but were also unable to successfully model this effect.

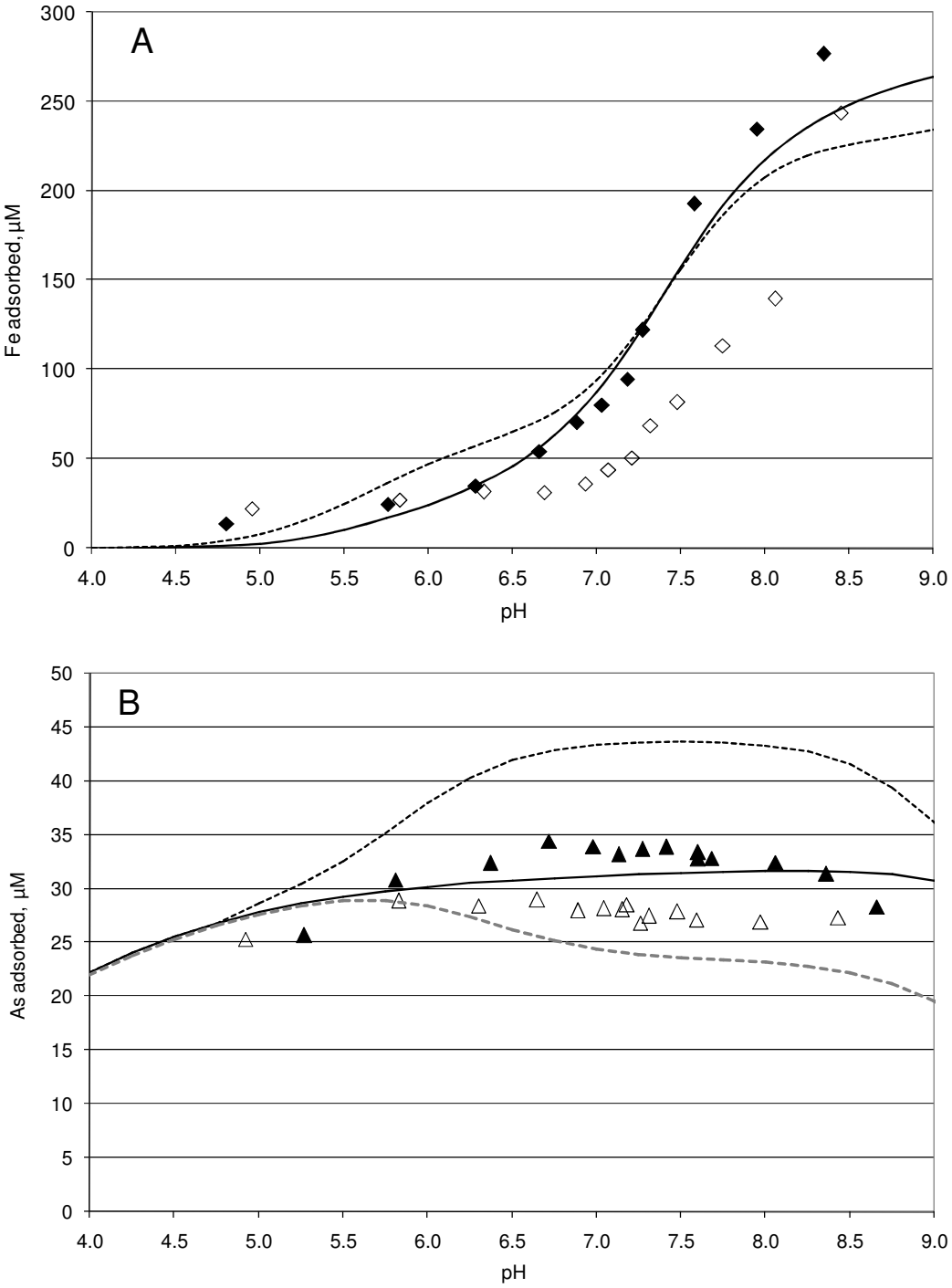

Figure 4-4: Adsorption of (A) Fe(II) and (B) As(III) in single-ion and binary systems. Experimental conditions: 0.01 M $NaNO_3$; 0.005 M pH buffer, 50 µM As(III) and/or 300 µM Fe(II). Filled and hollow symbols are single-ion and binary experiments, respectively.

The model fares even worse in describing As(III) adsorption in the binary system. It predicts that preloading of Fe(II) will significantly increase As(III) adsorption from pH 5 to 9 (Figure 4-4B, top dotted line) due to the increase in surface charge resulting from the $>SOFe^{+}$ species at the Fe(II)-only sites. In fact, a modest decrease in As(III) adsorption is seen at all pH values. A second set of geochemical model runs was made allowing only the surface species >SOFeOH to form at the Fe(II)-specific sites (lower dotted line), which does not alter surface charge. In effect, the model simulates a "sink" for Fe(II) removal from solution without impacting the surface sites where As(III) adsorbs. This qualitatively captures the observed competitive effect of Fe(II) on As(III) adsorption, but is hard to justify at a molecular level.

It is more likely that the relatively large decrease in dissolved Fe(II) observed in our experiments is due to some other mechanism besides adsorption. Precipitation or oxidation could be responsible for the Fe(II) loss, but these explanations are unlikely, as discussed above. The most likely explanation remaining is that interfacial electron transfer has occurred in our experiments, translocating Fe(II) into the bulk of the oxide while regenerating adsorptive Fe(III) sites at the surface. This phenomenon has been shown to occur at circumneutral pH (Williams and Scherer 2004; Silvester, Charlet et al. 2005), and is favored at higher pH (Hiemstra and van Riemsdijk 2007).

CHAPTER 5: IN SITU REMOVAL OF FE(II) AND AS(III): COLUMN STUDIES

5.1 Introduction

Globally, naturally occurring arsenic contamination of groundwater is a major public health concern, affecting more than 140 million people in at least 70 countries (Ravenscroft 2008). Several different geochemical conditions can lead to elevated levels of dissolved arsenic in groundwater, but the most pervasive one is reductive dissolution of iron and manganese oxides, which are strong adsorbents for arsenic. These oxides typically occur as coatings on aquifer sediments deposited under alluvial conditions. Young alluvial sediments also contain high levels of organic matter, which is consumed by bacteria after deposition. After oxidants such as dissolved oxygen and nitrate are exhausted, manganese and iron oxides can serve as electron receptors in the microbiologically mediated oxidation of organic matter (Nickson, McArthur et al. 2000). This dissimilatory reduction leads to high levels of dissolved Mn(II) and Fe(II), along with the release of arsenic and other ions previously adsorbed to the oxide surfaces. Such waters are often supersaturated with respect to Mn(II) and Fe(II) minerals such as rhodochrosite and siderite (Johnston and Singer 2007b), and arsenic may be incorporated into or adsorbed onto ferrous minerals such as vivianite, symplesite (Johnston and Singer 2007b), or pyrite (Bostick and Fendorf 2003).

Conventional processes for arsenic removal from contaminated groundwater involve 'pump-and-treat' approaches, using coagulation, adsorption, ion exchange, or membrane separation to remove arsenic. In many cases, an oxidation step is required to convert As(III) to As(V). These processes all generate substantial arsenic-rich waste streams, involve significant inputs of chemicals, and require fairly sophisticated operators and infrastructure.

An alternate to pump-and-treat processes is *in situ* arsenic removal. Although *in situ* iron removal has been practiced for decades, mostly in Europe (Grombach 1985; Jechlinger, Kasper et al. 1985; Braester and Martinell 1988b; Braester and Martinell 1988a; Maogong 1988), the mechanisms of iron removal are not well understood, and have only recently been examined rigorously. Likewise, the potential applicability of this technology for arsenic control has not been extensively investigated.

In situ iron treatment consists of the introduction of a volume of oxygen-rich water into an aquifer through an injection well. The oxygen oxidizes reduced iron to ferric oxides and hydroxides that are relatively insoluble. The injectate is usually allowed to react for some time (a few hours to a day) before extracting groundwater from the aquifer. Iron-free water can then be withdrawn from the aquifer for extended periods before dissolved iron breaks through. At that point, the process is repeated. The injection well can also be used for extraction (a "push-pull" configuration), or a series of satellite injection wells can surround a central extraction well [e.g. the Vyredox™ system (Braester and Martinell 1988b; Braester and Martinell 1988a; Maogong 1988)]. The efficiency of the process, defined as the volume ratio of groundwater abstracted to oxidized water injected, ranges from about 3 to 12 (Appelo, Drijver et al. 1999), and typically increases with time.

Since Fe(III) is created during the injection and reaction phases of the cycle, adsorption of Fe(II) onto ferric oxide surfaces during the abstraction phase of the cycle is clearly one important mechanism at work. The mechanism of Fe(II) oxidation during injection is somewhat controversial. Some attribute the oxidation to biological processes (Grombach 1985; Rott and Friedle 2000), while others consider heterogeneous oxidation at the ferric oxide surface (Mettler 2002) or homogeneous oxidation (Appelo, Drijver et al. 1999) to be the key mechanisms. Work by Mettler and colleagues (Mettler, Abdelmoula et al. 2001; Mettler 2002) suggests that at slightly elevated pH (characteristic of a calcareous aquifer), abiotic oxidation rates are so fast that biotic oxidation of Fe(II) is insignificant. The rapid kinetics of ferrous iron oxygenation above pH 7, catalyzed by oxide surfaces, allow Fe(II) to be oxidized even in the presence of competing reductants such as Mn(II) or natural organic material (Mettler 2002).

The fresh ferric oxide surfaces emplaced as coatings on sediment surfaces as a result of the introduction of oxygen should be effective adsorbents for many dissolved species besides Fe(II). Mettler, Abdelmoula et al. (2001) have demonstrated that goethite is the main product of ferrous iron oxidation during *in situ* iron removal, and it is well known that goethite has a high affinity for many dissolved species (Mathur and Dzombak 2006) including As(III), As(V), and Fe(II) (Dixit and Hering 2003; Dixit and Hering 2006). Rott and co-workers have demonstrated that *in situ* treatment can remove arsenic as well as iron (Rott and Friedle 2000; Rott, Meyer et al. 2002). *In situ* iron and arsenic removal processes are complicated, involving oxidation, adsorption, and possibly ion exchange and/or precipitation reactions. Efficiency of *in situ* removal is affected by many factors including pH, concentration and speciation of Fe and As, presence of other solutes, and heterogeneity

of surface sites. Surface complexation modeling, coupled with transport modeling, can be employed to simulate these processes.

One-dimensional solute transport of an adsorbing solute can be described with the advection-dispersion equation:

$$\frac{\partial C}{\partial t} = D\frac{\partial^2 C}{\partial x^2} - v\frac{\partial C}{\partial x} - \frac{\partial q}{\partial t} \qquad \text{(Equation 5-1)}$$

where C is the solute concentration [ML^{-3}], D is the hydrodynamic dispersion coefficient [L^2T^{-1}], v is velocity [LT^{-1}], and q is the amount of solute adsorbed, expressed in terms of mass per volume of pore fluid [ML^{-3}]. The adsorption component of this equation can be converted into a dimensionless retardation factor R:

$$R\frac{\partial C}{\partial t} = D\frac{\partial^2 C}{\partial x^2} - v\frac{\partial C}{\partial x} \qquad \text{(Equation 5-2)}$$

When the Péclet number (the ratio of advection to diffusion, in this case vL/D) is high (> 100), transport is dominated by advection. In this case, given a constant step input function increasing from zero to C_0 at time zero, the retardation factor will be approximately equal to the dimensionless mean breakthrough time of the solute, i.e. the time at which C/C_0 = 0.5. A non-reactive solute will break through after one pore volume (R = 1), while adsorbing solutes will be retarded and break through later (R > 1). Different adsorption models (e.g. linear, Freundlich, Langmuir) yield different formulations for R.

Using the geochemical reactive transport code PHREEQC (Parkhurst and Appelo 1999), Appelo (2003) was able to qualitatively match field data from a Dutch *in situ* treatment plant to the transport model. Iron and phosphate were significantly retarded after seven push-pull cycles, with retardation factors of approximately 4. Arsenic was less retarded ($R_{As} \approx 2$), while ammonia and manganese were almost unaffected.

In a push-pull *in situ* iron removal scheme, dissolved oxygen in the 'push' phase reacts with adsorbed iron (or manganese), leading to a retardation of the penetrating dissolved oxygen front. The approximate extent of retardation can be estimated by assuming that one mole of dissolved oxygen can oxidize up to four moles of adsorbed Fe(II), but in practice oxygen may react with other reductants, and some adsorbed iron will be removed through desorption and flushing before being reached by the (retarded) oxygen front.

In the 'pull' phase, dissolved iron and arsenic in the native groundwater being drawn through the emplaced ferric oxide zone created during the 'push' phase is adsorbed onto the fresh ferric oxide surfaces, causing a retardation in the Fe(II) and As fronts. With each successive push-pull cycle, fresh ferric oxide is deposited on sediment grains, and the retardation factor for iron increases. Because arsenic removal is controlled by the availability of ferric oxide surfaces, the arsenic retardation factor R_{As} should also increase with increasing numbers of cycles.

The goal of this research is to conduct laboratory investigations under controlled circumstances to simulate *in situ* removal of iron and arsenic and to assess the extent of retardation of these two elements. Goethite-coated sand was prepared as a surrogate for aquifer material and, in a series of packed column experiments alternating pulses of air-saturated solutions and anaerobic solutions of Fe(II) and/or As(III) were passed through the

column to simulate injection and abstraction phases of *in situ* treatment. Experiments continued for several cycles to allow ripening of the column as more ferric iron was generated on the sand. Experiments were made at three different pH values, and attempts were made to model the *in situ* treatment process with geochemical solute transport software in order to better understand the underlying processes.

5.2 Materials and methods

5.2.1 Chemicals

All chemicals were of Certified ACS grade or better, and were used without further purification. Standard 50 mM As(III) solutions (Fisher) were used to prepare stock solutions. Fe(II) stock solutions were freshly prepared by dissolving $Fe(NH_4)_2(SO_4)_2$ in 1 mM HNO_3. Ionic strength was fixed with 0.1 M $NaNO_3$, pH was buffered at 7.0, 7.5, or 8.0 with 0.02 M HEPES (pKa 7.55). HNO_3 and KOH were used for pH adjustment.

5.2.2 Goethite-coated sand

Goethite was synthesized from a $Fe(NO_3)_3$ solution, as described in Chapter 4. The specific surface area of the goethite, measured by 5-point N_2 BET adsorption, was 65 m^2/g (NOVA Quantachrome 1200). A concentrated slurry was prepared by equilibrating 100 g of goethite in 300 mL of 10 mM $NaNO_3$ at pH 2.5 on an end-over-end shaker for 24 hours. 500 g of silica sand (50-70 mesh) was then added to the slurry and placed on the shaker for another 24 hours (Schwertmann and Cornell 2000). The goethite-coated sand was then washed on a nylon sieve (63 μm) with 1 N $NaNO_3$ at pH 3, followed by washing with deionized water (DIW), before air-drying for 24 hours. Iron content of the sand was

determined by digesting ten separate samples of sand in concentrated HCl, diluting, and measuring dissolved Fe. The resulting coverage was 195 µg Fe/g goethite-coated sand (0.020 m^2/g), with a residual standard deviation among the ten samples of 7%.

5.2.3 Column packing and characterization

30 cm glass columns (Ace), with an internal diameter of 1.5 cm and identical nylon plug adapters at each end, were filled with DIW and packed with goethite-coated sand until full. Sand was lightly tamped down after each 1-2 cm. After filling, the columns were preconditioned by using a peristaltic pump (MasterFlex, Cole-Parmer) to continually cycle buffer solution containing 0.1 M $NaNO_3$ and 0.02 M HEPES buffer at the appropriate pH through the column overnight.

The pore volume of the column was measured by switching the column influent to a buffer solution saturated with air, recording the mean breakthrough time of dissolved oxygen (C/C_0 = 0.5), and multiplying this time by the flow rate. Both positive and negative breakthrough curves were developed for each newly packed column. Pore volumes were found to range from 23.2 to 24.4 mL, equivalent to porosities of 0.458 and 0.438. This is consistent with the observation that approximately 75 g (30 cm^3) of goethite-coated sand was needed to fully pack a column. On average, one column contained 270 micromoles (24 mg) of goethite, with a total BET surface area of 1.6 m^2.

5.2.4 Experimental design

Experiments were designed to simulate a ‘pull’ phase, in which groundwater is abstracted from an anoxic aquifer contaminated with arsenite and ferrous iron, followed by a ‘push’ phase of injection of oxygen-rich water into the aquifer. Experiments consisted of

several successive pull and push cycles, to permit measurement of any change in solute retardation over time as increasing amounts of ferric oxide are formed on the sand. Columns were mounted vertically and inverted after each phase, so that flow was always upwards. The influent reservoir during the 'pull' phases was continuously sparged with nitrogen gas to remove all traces of dissolved oxygen. Thick-walled narrow-bore tubing with low gas permeability (TYGON F-4040-A, L/S 13, Cole-Parmer) was used to minimize oxygen diffusion from the atmosphere between the reservoir and column. A separate influent reservoir used for 'push' phases was sparged with compressed air to maintain a dissolved oxygen level of approximately 267 μM at 26 °C.

Adsorption of Fe(II) during the 'pull' phase was expected to be rapid (Vikesland and Valentine 2002), but adsorption of As(III) is slower. In previously conducted batch experiments (see Chapter 4), about 80% of the total amount of As(III) found to be adsorbed over 30 days was adsorbed in the first 30 minutes. By fixing the empty bed contact time (EBCT) for the column at 30 minutes, it was possible to conduct a complete pull-push cycle within about five hours, allowing duplicate column runs to be conducted within one day. Preliminary experiments indicated that varying the EBCT from 10 to 30 minutes had little impact on breakthrough of arsenic or iron. Following the final push phase with dissolved oxygen, columns were stored until the following day, providing approximately 19 hours for oxidation and adsorption to occur. This simulated the practice of allowing an actual *in situ* injection to equilibrate for some period before beginning the abstraction phase.

In an actual *in situ* treatment application, the pull phase would be terminated when iron or arsenic reached some threshold value. However, in order to gain more information about contaminant transport dynamics, our experiments were designed to approach full

breakthrough; accordingly, in most cases, the pull phase lasted from 16-20 pore volumes. The goal of the push phase in our experiments was to assure the presence of dissolved oxygen throughout the reactive zone, for which a much shorter pulse of three pore volumes was used.

Before initiating the main phase of the experiment (alternating abstraction of solutions containing Fe(II) and As(III) with injection of oxygen-rich solution), it was necessary to first condition the columns with adsorbate to reach a steady state. When As(III) is first introduced to the column, the retardation factor R_{As} is expected to be relatively high because all of the adsorption sites on the virgin goethite are available. In subsequent 'pull' cycles during this conditioning activity, retardation should be lower because some of the adsorption sites are already filled with arsenic from previous cycles, and some arsenic remains in the pore liquid. This decrease in R_{As} during the initial cycles would tend to counteract any increase in R_{As} caused by emplacement of fresh ferric oxide surfaces, complicating the interpretation of experimental results. The same phenomenon is expected to occur for R_{Fe}. Geochemical modeling of the experimental setup (see below), confirmed by preliminary laboratory experiments, indicated that after two pull-push cycles, a steady state would be reached. Accordingly, in all cases, a series of 'conditioning' cycles were performed prior to the 'experimental' cycles. In this way, conditions were developed in the column similar to those in an anaerobic aquifer before introduction of oxygen to the system.

Three sets of column experiments were performed, at pH 7.0, 7.5, and 8.0. At each pH value, two sets of experiments were made with separate columns; at pH 8 the two experiments were identical while at the lower pH values one experiment was made with As(III) and Fe(II) while the other involved Fe(II) alone (see Table 5-1).

Table 5-1: Experimental conditions

Column	pH	Conditioning			Experimental		
		Cycles	Pull	Push	Cycles	Pull	Push
A	7.0	5	As	aerated	8	Fe + As	aerated
B	7.0	4	Fe	anoxic	6	Fe	aerated
C	7.5	3	As	aerated	17	Fe + As	aerated
D	7.5	4	Fe	anoxic	7	Fe	aerated
E	8.0	3	As	aerated	11	Fe + As	aerated
F	8.0	3	As	aerated	11	Fe + As	aerated

In each experiment, cycles of alternating 'pull' and 'push' pulses were passed through the column. Influent for the 'pull' pulses was a solution of 100 µM Fe(II) and/or 10 µM As(III), which are similar levels to those found in natural arsenic-contaminated groundwater (e.g. in Bangladesh, DPHE/BGS/MML 2000). Ionic strength and pH were buffered using 0.1 M $NaNO_3$ and 0.02 M HEPES buffer (as in batch adsorption experiments, see Chapter 4), and kept oxygen-free by continuous sparging with nitrogen. 'Push' influent consisted of the same buffer solution, sparged with laboratory air. In all cases, columns were wrapped in aluminum foil throughout the experiment to prevent interference by ultraviolet radiation.

Column effluent was collected in a fraction sampler at 6-minute intervals, each corresponding to approximately 0.5 pore volumes. Glass collection vials were partially pre-filled with 10 mM HNO_3 preservative to prevent post-column Fe(II) oxidation. Actual hydraulic loading rates were measured gravimetrically by weighing fraction collector vials before and after the push/pull pulse. It was observed that the pumping rate varied from approximately 1.5 to 2.0 mL/min, with intra-cycle variation (ratio of standard deviation to mean) of 2-5%. Inter-cycle variation was slightly greater at 9%, but can still be considered relatively constant.

5.2.5 Measurement of As and Fe

Arsenic was measured using graphite furnace atomic absorption spectrophotometry (AAS; Perkin-Elmer 5100PC) with an EDL lamp and Pd/Mg matrix modifier. Fe was measured using flame AAS and also with a modified Ferrozine method (Stookey 1970; Gibbs 1976) described elsewhere (Chapter 4). Calibration standards were prepared by dilution of 1000 µg/mL ICP stock solutions (Fisher) in 24 mM HNO_3. Quality control standards, prepared from separate stock solutions, were analyzed before and after every batch of 6-10 samples, and analytical results were adjusted accordingly by linear interpolation. If the standard deviated from the expected value by more than 5%, the instrument was re-calibrated and samples were re-analyzed.

5.2.6 Measurement of dissolved oxygen

Dissolved oxygen (DO) was recorded at the column effluent using a microprobe (YSI) and data acquisition system (DATAQ), collecting data every ten seconds (approximately every 0.07 pore volumes). Fresh microprobe membranes were used daily and the instrument was calibrated with buffer solutions saturated with air.

5.2.7 Geochemical modeling

PHREEQC version 2.14 was used for all geochemical modeling (Parkhurst and Appelo 1999). The model simulates adsorption using a double diffuse layer, and calculates activity coefficients using the Davies equation. Advective transport was simulated using Dirichlet and Cauchy boundary conditions at the influent and effluent ends of the column. Dispersivity was set at 0.25 mm, the mean sand grain diameter. The standard database was augmented with constants for arsenic speciation in solution (Ball and Nordstrom 1991),

adsorption of arsenite, arsenate, and ferrous iron onto goethite (Dixit and Hering 2006), and precipitation of ferrous arsenate (Johnston and Singer 2007b). Arsenite, arsenate and nitrate were decoupled from redox reactions, to prevent the model from predicting reactions which are thermodynamically favored but kinetically limited, such as oxidation of arsenite by oxygen or of ferrous iron by nitrate. But ferrous iron was allowed to reach redox equilibrium with oxygen, forming goethite as the oxidation product. Two approaches to modeling site density were used: a two-site model in which surface site density was fixed at 2.0 sites/nm^2 for universally accessible sites (i.e. accessible for arsenite, arsenate, and ferrous iron) and 10.75 sites/nm^2 available only for adsorption of ferrous iron (see Chapter 4 for details); and a one-site model using only 2.0 sites/nm^2 as universally accessible sites (Dixit and Hering 2006).

5.3 Results

A large number of breakthrough curves were produced through the course of the experiments; during 'pull' phases, Fe(II) and As(III) breakthrough curves were generated, as well as negative breakthrough curves for dissolved oxygen as it was displaced by the anoxic infilling solution. During 'push' phases, positive breakthrough curves for dissolved oxygen were generated and, in a few cases, flushing of Fe(II) and arsenic from the column was also recorded. Figure 5-1 shows a typical set of breakthrough curves, generated from the pull phase of cycle 7 of the pH 7 experiment involving both arsenic and iron.

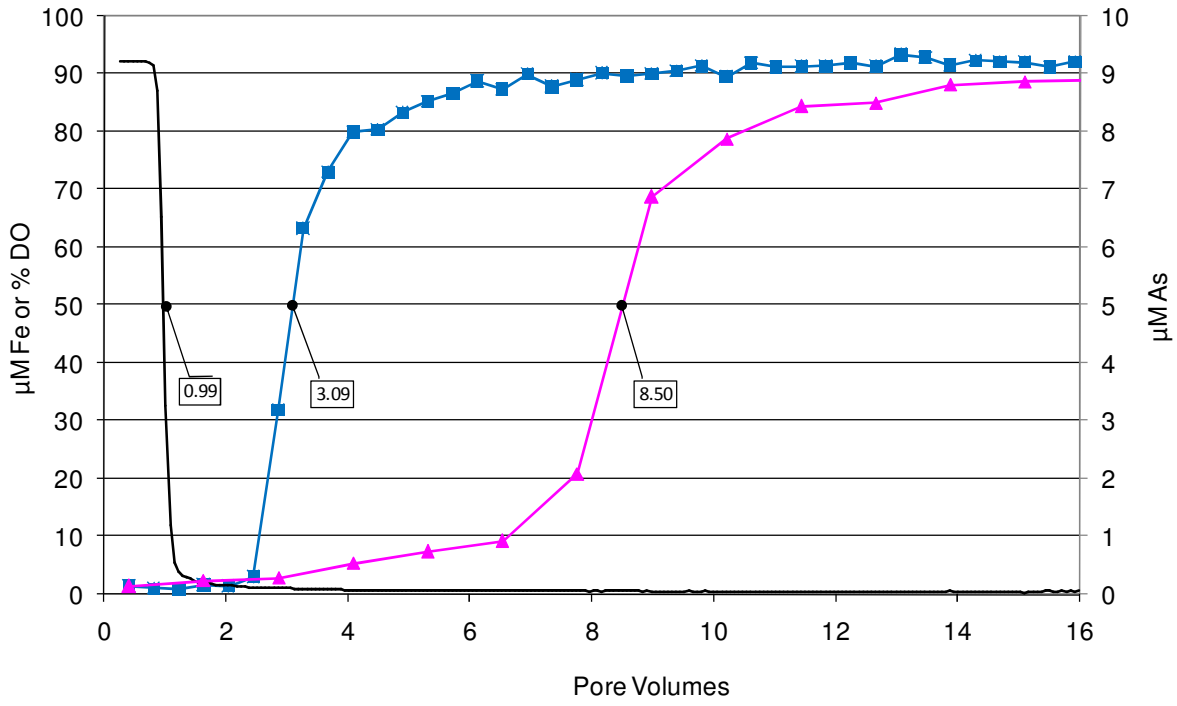

Figure 5-1: Breakthrough curves for dissolved oxygen (black line), ferrous iron (blue squares), and arsenic (pink triangles). Numbers in boxes indicate estimated retardation factors.

In order to represent the large number of breakthrough curves generated during these experiments in an efficient way, and to track any changes in retention during successive cycles, it is possible to estimate the retardation factor (*R*) for any solute as the mean breakthrough time, in units of dimensionless pore volume at which $C/C_0 = 0.5$. At the high Peclet numbers (>1000) in these experiments, diffusion is negligible and the mean breakthrough time will closely approximate the retardation factor (Shackelford 1994). This is shown in Figure 5-1 by the retardation factor of 0.99 (essentially 1 pore volume) for the flushing of dissolved oxygen out of the column by the anoxic influent solution containing Fe(II) and As(III), which are retarded by adsorption. Retardation factors are also used to

estimate the amount of solute retained in the column, though this estimation will be inaccurate if significant tailing occurs.

5.3.1 Iron

In the conditioning cycles, conducted with oxygen-free 'push' pulses, the retardation factor for Fe(II) (R_{Fe}) reached a steady-state value of ~3 at pH 7 and 7.5 (see Figure 5-2, cycles labeled -3 through 0). After introduction of oxygenated push cycles, R_{Fe} was consistent at a value of ~3 at pH 7, showing no change during successive cycles. Retardation was greater at pH 7.5, jumping from 3 to 5 in the first 'pull' after a 'push' of oxygenated water, and showing a slight tendency to increase during successive cycles. At pH 8, a marked and consistent increase in retardation was seen during successive cycles as the column 'ripened', eventually reaching $R_{Fe} > 11$. Duplicate columns showed reproducible results, both in terms of breakthrough curves and retardation factors. Arsenic-free experiments showed little difference from those containing arsenic.

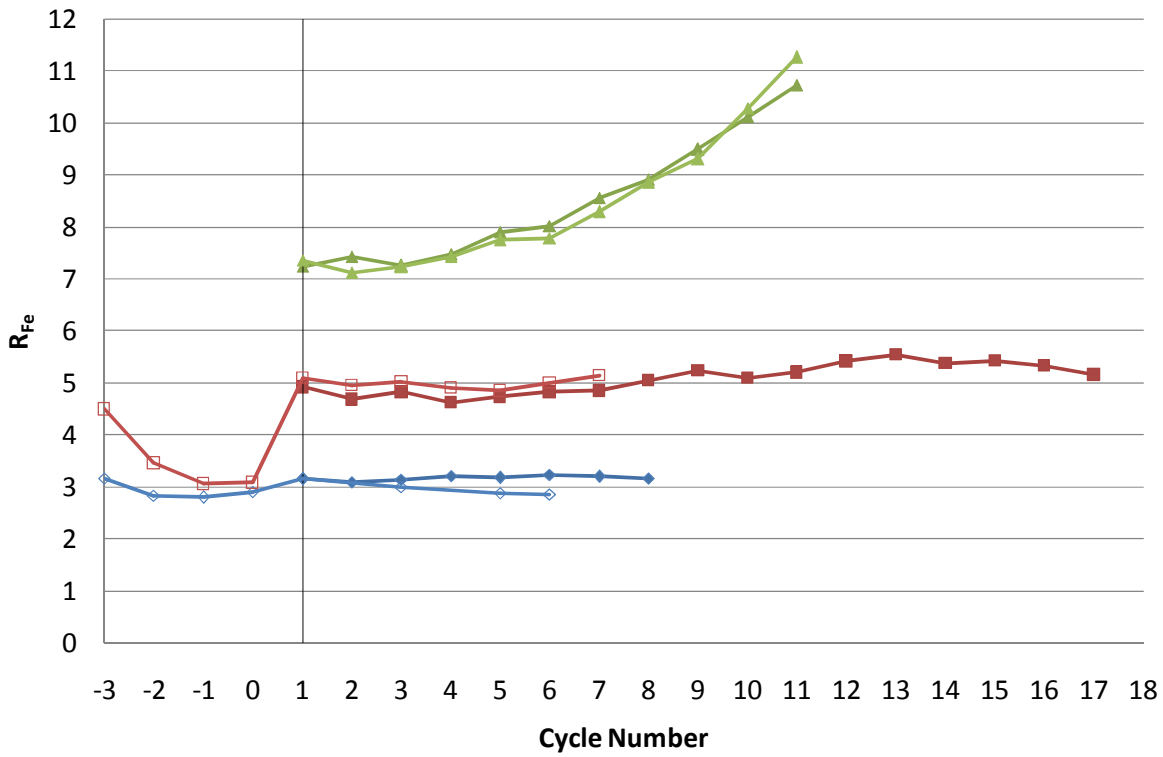

Figure 5-2: Retardation factors for Fe(II) at pH 7 (blue diamonds), 7.5 (red squares), and 8 (green diamonds). Arsenic-free experiments are shown with hollow symbols.

The amount of Fe(II) adsorbed on the column was calculated using the retardation factor and the known concentration of Fe(II) in the influent solution. At pH 8, approximately 15 µmoles of Fe(II) were retained on the column during the initial experimental cycles, rising to approximately 25 µmoles by the end of cycle eleven. Over the eleven cycles, a total of 199 µmoles of Fe(II) were adsorbed on the goethite-coated sand. If all of this Fe(II) were converted to iron oxide and retained on the sand, the iron content of the goethite-coated sand would be expected to increase from a baseline of 195 µg/g to 338 µg/g, on average. Acid digestion (in 5 M HCl) at the end of the experiments showed 304 and 308 µg/g Fe at the bottom of the two duplicate columns and 296 and 297 µg/g at the top. The increase in Fe content was thus about three quarters of the predicted value, and was fairly constant

throughout the column, as would be expected since both Fe(II) and dissolved oxygen achieved full breakthrough in each cycle.

5.3.2 Oxygen

In the absence of Fe(II), dissolved oxygen behaved consistently as a conservative tracer in both positive and negative breakthrough curves, with retardation factors (R_{O2}) averaging 1.0 (Figure 5-3). (In the interest of clarity, data from only one column per pH value are presented, but results from the other columns showed the same pattern.) In 'push' cycles following 'pull' cycles containing Fe(II), dissolved oxygen was consistently retarded, with the extent of retardation increasing with increasing pH. The amount of oxygen consumed in the column during 'push' phases increased from approximately 1.3 µmoles in the pH 7 experiments ($R_{O2} \sim 1.25$), to more than 5 µmoles by the end of the pH 8 experiment ($R_{O2} > 1.8$), which is consistent with the greater retention of Fe(II) on the columns at higher pH. In all experiments, the molar ratio of Fe(II) retained on the column to oxygen consumed in the subsequent push phase ranged from 3.3 to 4.8, with this ratio increasing with increasing pH. The observed ratio is consistent with the theoretical stoichiometric ratio of 4.0 for the oxidation of Fe(II) by oxygen.

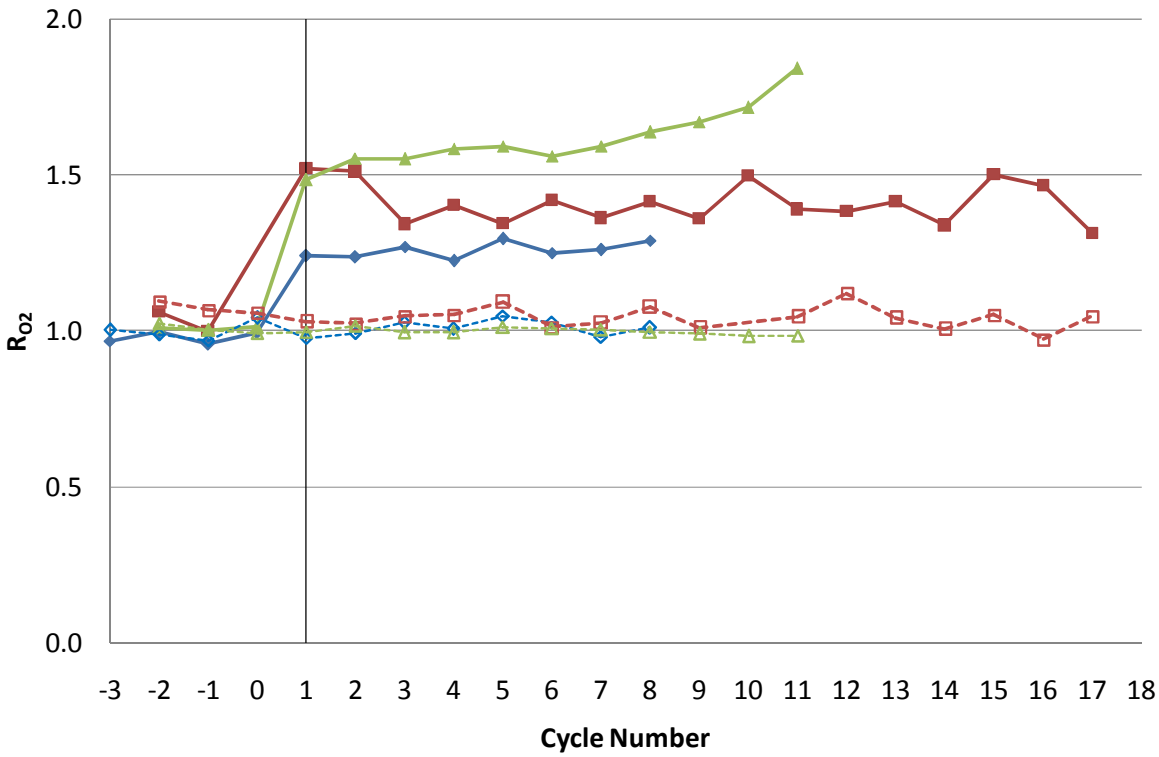

Figure 5-3: Retardation factors for dissolved oxygen at pH 7 (blue diamonds), 7.5 (red squares), and 8 (green triangles). Hollow and filled symbols are 'push' and 'pull' cycles, respectively. The dotted lines represent retardation factors from 'push' cycles.

5.3.3 Arsenic

Breakthrough of 10 uM As(III) was highly retarded in the first conditioning cycle at all pH values (R_{As} = 12-14), as arsenic was adsorbed to the virgin goethite (Figure 5-4). During the next several conditioning cycles R_{As} dropped to approximately 7-8 at all pH values, reaching a steady state after 2-3 cycles. In the first pull cycle containing both arsenic and iron, and before introduction of oxygen to the system, As(III) breakthrough was greatly retarded, with R_{As} comparable to or greater than that of the first conditioning cycle. Substantial tailing of arsenic was noted; even after 18 pore volumes C/C_0 was usually between 0.75 and 0.85. These effects were seen at all pH values, and duplicate columns at pH

8 showed good reproducibility. Whereas iron and dissolved oxygen showed fairly steady retardation factors with increasing cycle number at pH 7 and 7.5, R_{As} declined steadily with time. This suggests that even though Fe(II) is substantially retarded at pH 7 and 7.5 (R_{Fe} approximately 3 and 5, see Figure 5-2), the fresh ferric oxide produced in the column by oxygenation of adsorbed Fe(II) has a lower affinity for As(III) than the original goethite, or that many of the freshly generated surface sites are filled with As(III) still present in the column during the 'push' phase. At pH 8, however, R_{As} increased with time, tracking the observed increase in R_{Fe}.

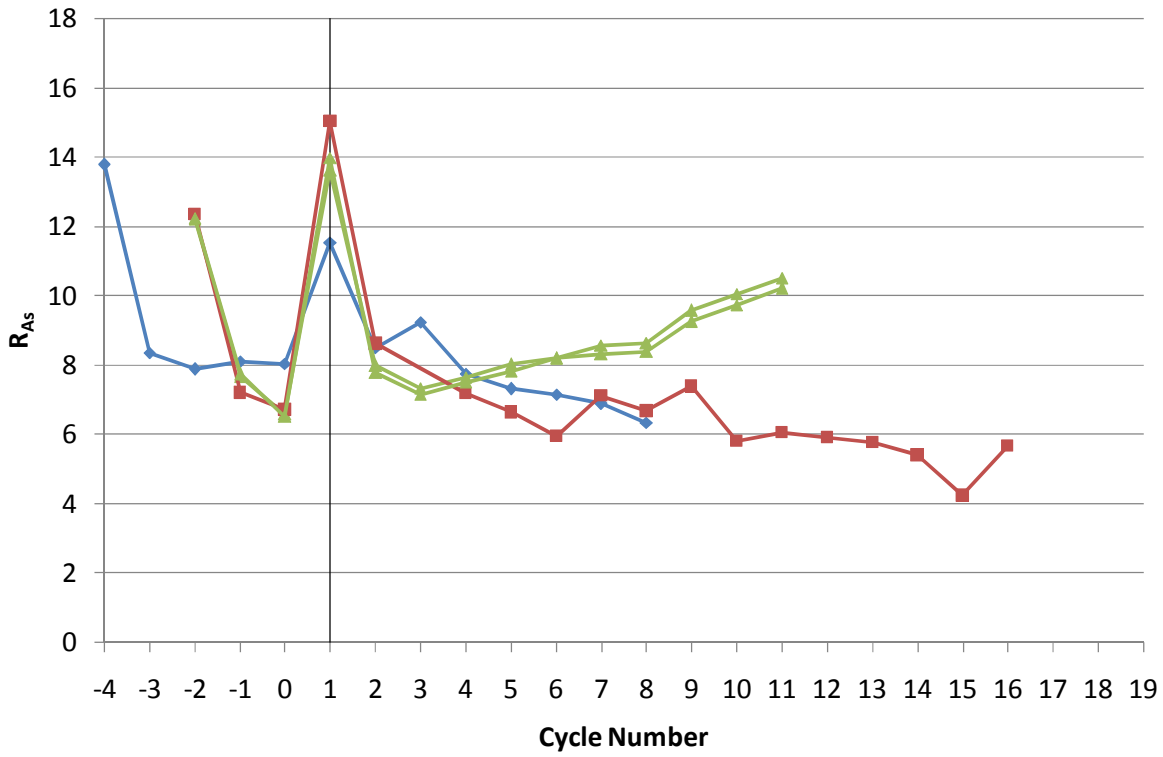

Figure 5-4: Retardation factors for As(III) at pH 7 (blue diamonds), 7.5 (red squares), and 8 (green diamonds).

5.3.4 Geochemical modeling

PHREEQC was used to model the experiments, using model parameters described above and in Chapter 4. It has previously been shown in batch experiments (see Chapter 4), the goethite used had a maximum capacity of approximately 2.0 sites/nm^2 for As(III), and a much larger capacity of 12.75 sites/nm^2 for Fe(II). This has been modeled by considering one type of site accessible to all species, with a density of 2.0 sites/nm^2, and a second type of site, accessible only to Fe(II), with a density of 10.75 sites/nm^2. In Chapter 4 it was shown that the two-site model does not fit multi-component adsorption well in batch experiments. For comparison, the column experiments have also been modeled using the conventional one-site model (Dixit and Hering 2006). Simulations from both models are shown in Figure 5-5. Only the multi-component model results are presented; similar trends hold for the Fe(II)-only modeling.

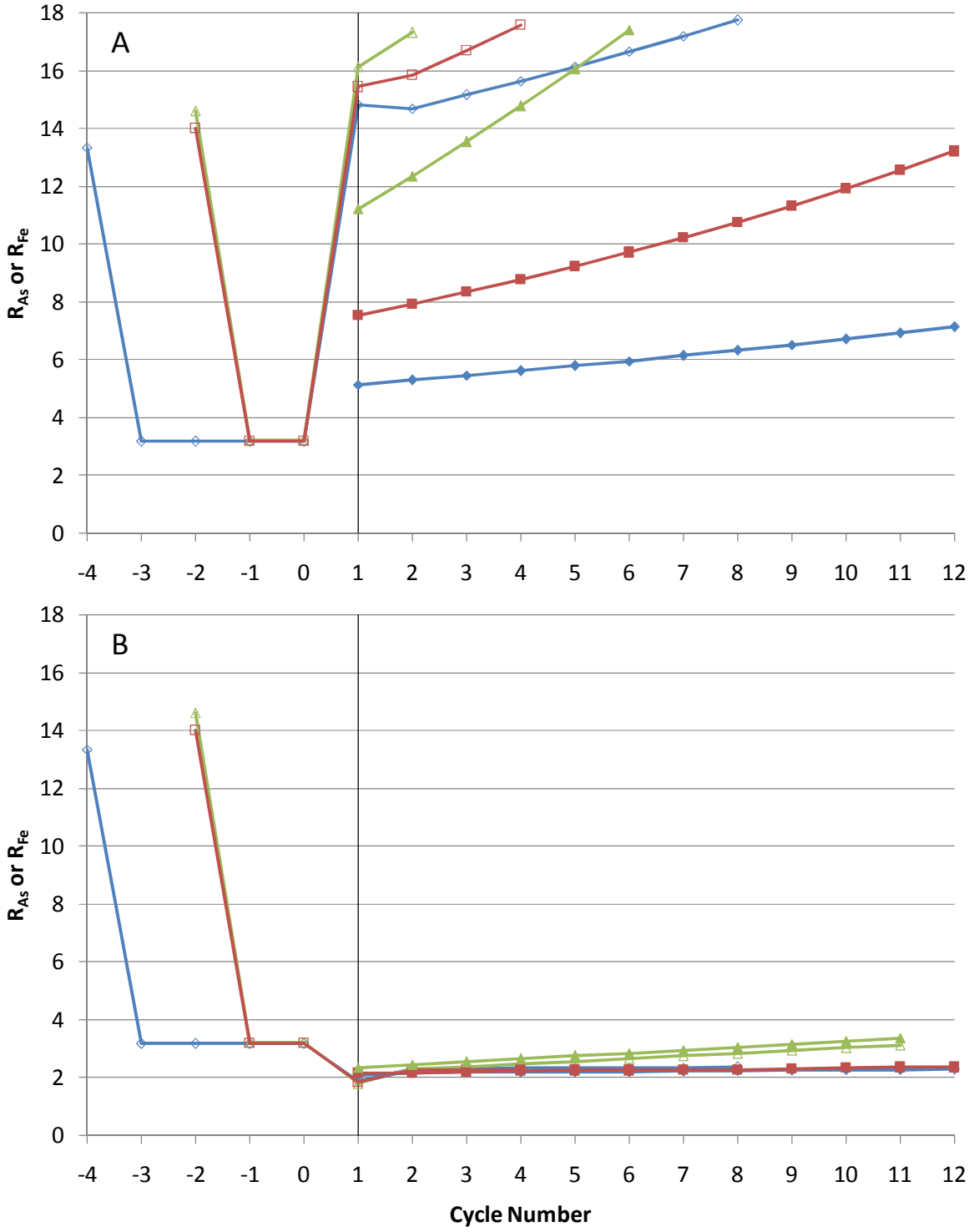

Figure 5-5: Modeled retardation factors for As(III) (hollow symbols) and Fe(II) (filled symbols) at pH 7 (blue diamonds), 7.5 (red squares), and 8 (green diamonds). Panels A and B are simulations using the two-site and one-site models, respectively.

The two-site model used in this research gives a qualitatively good prediction of R_{As} development in the conditioning cycles, and correctly predicts that upon the addition of Fe(II) to the first anoxic 'pull' solution following the Fe-free conditioning cycles, As(III) will be adsorbed to a much greater extent (compare Figures 5-4 and 5-5A). This large increase in R_{As} can be explained by the increase in surface charge caused by the $>OFe^{+}$ surface species, i.e. adsorbed Fe(II). For example, at the end of the final conditioning cycle at pH 7, in which As(III) was observed to break through after 8 pore volumes (Figure 5-4), the model indicates that As(III) has filled 53% of the universally accessible sites, and the surface has a potential Ψ of 21 mV. The next pull cycle included both As(III) and Fe(II), and As breakthrough was only seen after 15 pore volumes. At the end of this cycle the model indicates that Fe(II) has filled 34% of the Fe(II)-only sites with the $>OFe^{+}$ species, increasing the surface potential to 137 mV. This increase in surface potential favors anion adsorption, and the model predicts that As(III) has filled 98% of the universally accessible surface sites, which explains the increase in R_{As}.

However, the two-site model predicts that this enhanced retention of As(III) will continue in subsequent cycles, and will increase as more goethite is created through oxidation of Fe(II). In contrast, the experimental data consistently show a return to R_{As} levels similar to or lower than those of the conditioning cycles (compare Figure 4 and Figure 5-5A). Subsequently, R_{As} decreases over time at pH 7 and 7.5, while at pH 8.0 it slowly increases.

The two-site model also predicts greater retardation of Fe(II) than was observed (R_{Fe} about 1.5 to 2.0 times those observed), as well as a column ripening effect for both R_{As} and R_{Fe} even at pH 7.0, which was not seen.

If the two-site model over-predicts R_{As} and R_{Fe}, the one-site model seriously under-predicts them (compare Figures 5-4 and Figure 5-5B). Furthermore, the one-site model fails to predict the observed increase in R_{As} upon introduction of Fe(II) to the system, predicting instead a substantially earlier breakthrough because arsenic and iron compete for the same surface sites.

5.4 Discussion

5.4.1 Implications for *in situ* treatment

These experiments have successfully simulated an application of *in situ* removal of arsenic from groundwater using alternative phases of injection of oxygenated water and abstraction of anoxic water containing As(III) and Fe(II). As expected, retardation of both arsenic and Fe(II) is favored by higher pH, and a column ripening effect was seen at pH 8, with retardation increasing over successive cycles. At this pH, the amount of iron oxide in the column increased by more than 50% due to oxidation of adsorbed Fe(II). One approach to optimization of *in situ* arsenic treatment could be to increase the pH of the injection solution in an effort to improve adsorption and oxidation of Fe(II).

As seen in previous batch experiments, the goethite in the column had a higher capacity for Fe(II) than for As(III) at all pH values: although the molar concentration of Fe(II) was ten times that of As(III), the retardation factors for the two solutes were similar at pH 8, and only slightly greater for As(III) than for Fe(II) at lower pH values. An important consideration for actual *in situ* applications would be, which solute would break through first at the abstraction, arsenic or Fe(II). In these experiments Fe(II) was observed to break

through first in all cases; this would be preferable in an *in situ* application since it would allow greater emplacement of Fe(III) surface with each cycle.

At all pH values, approximately one mole of oxygen was consumed within the column for every four moles of Fe(II) retained on the column, which matches the theoretical stoichiometric ratio well. This implies that an effective strategy to improve in situ removal could be to saturate the injectate with pure oxygen instead of air. However, the column experiments and models presented in this paper have several important differences from actual *in situ* applications. Our experimental design allowed for complete breakthrough of Fe(II) in the pull phase, which meant that oxygen could react with adsorbed Fe(II) all along the length of the column in the subsequent push phase. This led to a nearly even distribution of Fe(III) in the column. In an actual *in situ* application, the pull phase would be terminated before Fe(II) in the abstracted water reached background aquifer levels. Thus, adsorbed Fe(II) levels would be lower in the vicinity of the well. Dissolved oxygen in subsequent cycles would therefore penetrate further into the aquifer, with most of the Fe(II) oxidation, and hence emplacement of new ferric oxide adsorption sites, occurring at some distance from the well and over a broad area. This effect will tend to minimize the risk of iron precipitates causing clogging in the vicinity of the well screen, and push the arsenic adsorption front further from the abstraction well. While saturating injectate with pure oxygen would allow penetrate to extend further into the aquifer, the retardation factors observed for dissolved oxygen were low, and reducing these retardation factors would probably have only a small effect on the distance of the active oxidation zone from the well screen.

The Fe content of our goethite-coated sand (0.02%) was not high; the Fe content in arsenic-contaminated sediments in Bangladesh ranges from 1-3% (Nickson, McArthur et al.

2000). Fe(III) represents from 20-80% of the total Fe content in these sediments (Horneman, Van Geen et al. 2004), but it is likely that iron oxides in natural settings are significantly less reactive with respect to adsorption than the pure goethite used in our studies. Still, the considerable attenuation noted in our studies, given a modest concentration of goethite, is encouraging and suggests that the Fe(III) levels seen in Bangladesh sediments are adequate to support an *in situ* treatment scheme.

These controlled experiments support the limited field data indicating that *in situ* arsenic removal could be an effective intervention for arsenic remediation in reducing groundwaters. The subject merits further field investigation.

5.4.2 Geochemical modeling and interpretation

The success of the two-site model in predicting the initial increase in R_{As} lends support to the hypothesis that Fe(II)-specific sites do indeed exist. It is not easy to explain why R_{As}, but not R_{Fe}, drops sharply following the first aerobic push, but this effect was consistently seen. A related anomalous observation was seen in the pH 7.5 As-free experiment, where R_{Fe} increased significantly after the first injection of oxygen-rich solution but not after subsequent aerated injections (Figure 5-2). Both observations indicate that the goethite surface reacts with Fe(II) in a different way following oxidation of adsorbed Fe(II).

The two-site model was also unable to produce a satisfactory fit to batch adsorption data in multi-component systems (see Chapter 4), and one plausible explanation is that in our experiments adsorbed Fe(II) transfers an electron to the goethite matrix. This electron shift, which has been shown by others after longer incubation periods (e.g. Silvester, Charlet et al. 2005) would have the effect of increasing the surface charge, thereby increasing the coulombic attraction for As(III) adsorption. It is possible that this interfacial electron transfer

occurs for virgin goethite but does not occur (at least to the same degree) in subsequent cycles, as the bulk goethite already contains substantial amounts of structural Fe(II). Further research is needed to understand the complex interactions at play during co-adsorption of As(III) and Fe(II) onto goethite.

CHAPTER 6: CONCLUSIONS AND RECOMMENDATIONS

This dissertation presents results from a series of experiments involving chemical interactions between iron and arsenic. Precipitation of ferrous arsenate, redox reactions between various Fe/As couples, and competitive adsorption were all explored in batch reactions, and described quantitatively using geochemical modeling. Implications of each of these processes on the fate and transport of arsenic in aquatic systems were also considered. Column experiments to simulate *in situ* removal of arsenic from groundwater are also presented and analyzed.

6.1 Conclusions

The geochemical processes controlling mobility of both arsenic and iron in groundwater are intimately related. Any attempts to remediate arsenic in groundwater must take iron chemistry into account, and indeed most arsenic removal systems are based on adsorption onto iron oxides. The chemical relationships between the two elements are complex and not always well understood. This dissertation has investigated some of the redox, precipitation, and adsorption reactions which can occur between various As and Fe species and may be important in *in situ* removal of iron and arsenic.

Experiments examining redox reactions between arsenic and iron have demonstrated that reduction of arsenate by ferrous iron does occur, but is kinetically slow. Ferrous iron is a more powerful reductant at high pH or in the presence of goethite, as oxygen-bearing ligands

donate electron density to the central Fe atom. While these experiments confirmed that the reduction of arsenate is faster under those conditions, the rates still remain slow compared to other environmentally significant redox reactions [e.g. the reduction of U(VI) by Fe(II)].

The same conditions which favor reduction of As(V) by Fe(II) – high pH and high concentrations of As(V) and Fe(II) – also favor precipitation of symplesite, a ferrous arsenate mineral. This precipitation reaction is likely to be more important than the redox reaction, and has implications both for natural systems (e.g. authigenic precipitation in aquifers) and engineering applications such as waste stabilization. A new solubility constant was calculated for symplesite (pK_{so} = 33.25), based on controlled laboratory precipitation experiments. Geochemical modeling suggests that some arsenic-impacted groundwaters in Bangladesh are super-saturated with respect to this mineral.

A series of oxidation experiments demonstrated that the kinetics of oxygenation of Fe(II) are highly influenced by the type and concentration of pH buffer. Oxidation kinetics are much faster in the presence of inorganic buffers (e.g. carbonate or phosphate) than when non-complexing organic buffers (e.g. HEPES or MES) are used. This can be explained by the formation of solute complexes, in which an oxyanion donates electron density to the Fe atom, stabilizing the ferric product of oxidation. Fe(II) oxidation experiments also showed little or no change in the presence of the hydroxyl radical scavenger propanol. These two findings call into question the classic formulation of Fe(II) oxygenation, and the long-accepted kinetic rate constants derived from experiments using carbonate buffer.

The oxidation of As(III) by dissolved oxygen in the presence of Fe(II) was also examined. While oxygen and ferric oxides are thermodynamically capable of oxidizing As(III), in practice these reactions are kinetically limited. However, it has been shown that

during the oxygenation of Fe(II), As(III) competes with Fe(II) for reactive oxidizing species. The fact that As(V) production is unaffected by the presence of hydroxyl radical scavengers points to the importance of other reactive oxidant species, possibly Fe(IV). The extent of As(III) oxidation is reduced in the presence of inorganic ligands, most likely because these ligands increase the reactivity of dissolved Fe(II), thus reducing the competitiveness of As(III) in scavenging oxidant species.

A series of competitive adsorption experiments using goethite have demonstrated competitive effects between As(III) and As(V), and between As(III) and Fe(II), when surface loadings approach or slightly exceed site density at the goethite surface. These effects are relatively minor. The experimental findings suggest that surface sites on goethite have variable affinities for these species, and that some sites are particularly selective for As(III). Batch experiments showed that much more Fe(II) was removed from solution than As(III) or As(V), after contacting the goethite surface. This could be explained by the existence of sites which can adsorb Fe(II) but not As. However, surface complexation modeling with this approach could not capture some of the aspects of multi-component adsorption, even qualitatively. An alternate explanation could be that upon adsorption Fe(II) transfers an electron into the bulk surface of the goethite, regenerating Fe(III) at the surface and allowing more adsorption to take place.

A series of column experiments were performed to simulate *in situ* removal of arsenic and iron, and demonstrated that an alternating push-pull configuration can lead to consistent retardation of both As and Fe. A 'ripening' effect, whereby the *in situ* process becomes increasingly efficient as more Fe(III) is emplaced on sediment surfaces, was observed at pH 8, where the process increased the amount of iron oxide in the column by more than 50%.

This increase was close to that predicted from calculations of the amount of Fe(II) retained on the column. The molar ratio of Fe(II) retained on the column to dissolved oxygen consumed on the column was close to four, the theoretical stoichiometric ratio for oxygenation of Fe(II).

Significant retardation of both Fe and As and a ripening effect were noted even though the iron oxide concentration in the columns was lower than in naturally arsenic-impacted aquifers such as Bangladesh, implying that *in situ* treatment in such settings is feasible. The strong pH effect noted suggests that pH adjustment to the injectate might lead to more effective removal of both Fe and As in field applications of *in situ* treatment.

6.2 Recommendations

The findings of this research advance the current knowledge regarding interactions between iron and arsenic in several important ways, and point to several recommendations for better understanding of the geochemical processes explored.

Although oxygenation of Fe(II) has been intensively studied for decades, fundamental questions remain about the species participating in the redox reaction, and the pathways followed. This work contributes to a growing body of evidence that hydroxyl radical and hydrogen peroxide are not the key oxidants at circumneutral pH. In particular, this work has shown that the kinetics of oxygenation of Fe(II) are highly dependent upon pH buffers which form dissolved complexes with Fe(II). By using organic rather than inorganic buffers, much slower kinetics were found than predicted using the conventionally accepted kinetic model. Further work should be done under conditions of strict exclusion of specifically binding ligands (especially carbonate) to determine reaction rates, as a function of pH, of the Fe^{+2}, $FeOH^{+}$, and $Fe(OH)_{2,(aq)}$ species. These could be followed by experiments with controlled

and varying amounts of carbonate, to elucidate the kinetic activity of different ferrous-carbonate complexes. Some work has been done on this by King and co-workers e.g. (King 1998; King and Farlow 2000) but their kinetic analyses remain predicated on the Haber-Weiss pathway which now seems incorrect. In recent years alternate pathways involving Fe(IV) instead of the hydroxyl radical have been proposed e.g. (Hug and Leupin 2003) – this is an area of active research which will surely yield important insights in coming years. The contribution of ligands such as carbonate must be considered in these investigations. Such ligands will affect kinetics both by complexation of Fe(II), and by scavenging of radical species (e.g. formation of carbonate radicals), which will complicate development of a unified model. Scientists conducting research involving oxidation of Fe(II) should be aware of the influence that pH buffers may have upon experimental results.

There is relatively little awareness in the environmental engineering literature about the ferrous arsenate mineral symplesite. Future research could use geochemical modeling to learn if natural waters impacted by As(V) and Fe(II) are super-saturated with respect to this mineral. Where models indicate super-saturation, mineralogical assays could be made to identify authigenic phases. Even in cases where waters are under-saturated with respect to symplesite itself, the possibility of significant incorporation of As(V) into ferrous phosphate solids should be investigated. In engineered applications, symplesite holds promise for management of As(V)-rich wastes resulting from arsenic removal through ion exchange; it would be illuminating to conduct research comparing the cost-effectiveness of symplesite precipitation to that of more conventional coagulation/adsorption processes. One research group (at University of Arizona) is experimenting with an arsenic sequestration technology which seems to immobilize As(V) wastes in symplesite crystals (Personal Communication,

D. Stone, 2008). Another area of research could be to explore the solubility of ferrous arsenite phases, evidence of which has been shown in recent work (Dixit and Hering 2006).

Competitive adsorption remains difficult to model. In the experiments conducted as part of this dissertation, an apparently much greater affinity of the goethite surface for Fe(II) than for As(III) or As(V) was found, which was hypothesized to be due to interfacial electron transfer. This is an area of active research, with many fundamental questions to address: if translocation occurred during these experiments, what are the kinetics of the reaction? what is the reactivity of Fe(II) within the bulk matrix? how are surface Fe(III) sites affected by the translocation? It is not clear why Fe(II) demonstrates unexpected behavior (high surface capacity, hysteretic desorption) in some experiments, while in others Fe(II) behaves more conservatively – these questions should be the focus of future experimental work. The adsorption experiments in this dissertation indicated that some surface sites seem to have a higher affinity for As(III) than for As(V) – this hypothesis could be further tested and quantified by a series of batch adsorption experiments using different As(III)/As(V) ratios, as an extension of the equimolar experiments made in this research.

The Diffuse Double Layer (DDL) model has shown only limited ability to describe multi-component adsorption. Although a number of equilibrium constants have been published describing adsorption at the goethite surface, reliable constants for As(III), As(V), and Fe(II) remain lacking. While these adsorption reactions were investigated in detail recently by Dixit and Hering (Dixit and Hering 2003; Dixit and Hering 2006), they used inappropriate equilibrium constants for protonation/deprotonation reactions of surface hydroxyl sites. Mathur and Dzombak (2006) have quantified adsorption of a large number of

anions and cations to the goethite surface using the DDL model; quantification of As(III), As(V), and Fe(II) binding constants using a similar approach would be a worthy endeavor.

The CD-MUSIC model (Hiemstra and Van Riemsdijk 1999) promises better description of metal oxide charging and adsorption constants, particularly for oxyanions which have electrostatically active moieties at some distance from the surface. However, the model requires more parameters and, given the relatively small number of studies which have characterized adsorption using this model, some of the parameters are poorly constrained. Increased use of sophisticated surface spectroscopy tools [e.g. X-ray absorption near edge spectroscopy (XANES), X-ray absorption fine structure spectroscopy (EXAFS, micro-EXAFS)] and *ab initio* models should lead to a greatly enhanced database of CD-MUSIC constants.

Column experiments have demonstrated the viability of *in situ* removal of iron and arsenic. The experiments conducted as a part of this dissertation were fairly limited, and did not investigate the impact of hydraulic parameters, oxidant concentrations, Fe/As ratios, or the presence of competing solutes on removal efficiency. Future laboratory work could explore these variables. In particular, carbonate, phosphate and dissolved organic compounds will likely affect the efficiency of the iron removal processes by altering Fe(II) speciation. These same constituents will compete, to varying degrees, for adsorption sites.

It has been demonstrated that As(III) is partially oxidized during the oxygenation of Fe(II). This process would most likely occur during *in situ* arsenic removal, since As(III) is the dominant arsenic species in reducing groundwater. Future work could examine changes in As speciation during *in situ* removal, which might have complicated implications for

process optimization, since arsenite and arsenate have different adsorption affinities for various oxide surfaces.

While much fundamental work could be done in the laboratory, there is a paucity of data from field investigations of *in situ* arsenic removal. Given the demonstrated effectiveness of *in situ* iron removal, and the frequent co-occurrence of arsenic with iron in groundwater, the time is ripe for conducting field work in an arsenic-impacted setting.

It is hoped and expected that this research into some of the geochemical processes which govern *in situ* arsenic removal can contribute to successful applications of *in situ* approaches for arsenic mitigation in the future.

APPENDIX A: X-RAY DIFFRACTION PATTERNS

An X-Ray Diffraction (XRD) pattern was collected for experimentally generated symplesite (see Chapter 2) and compared against a reference spectrum. The main peaks of the experimental sample matched those of the reference spectrum. Spectra are shown in terms of angle (2θ) as well as d-spacing (angstroms).

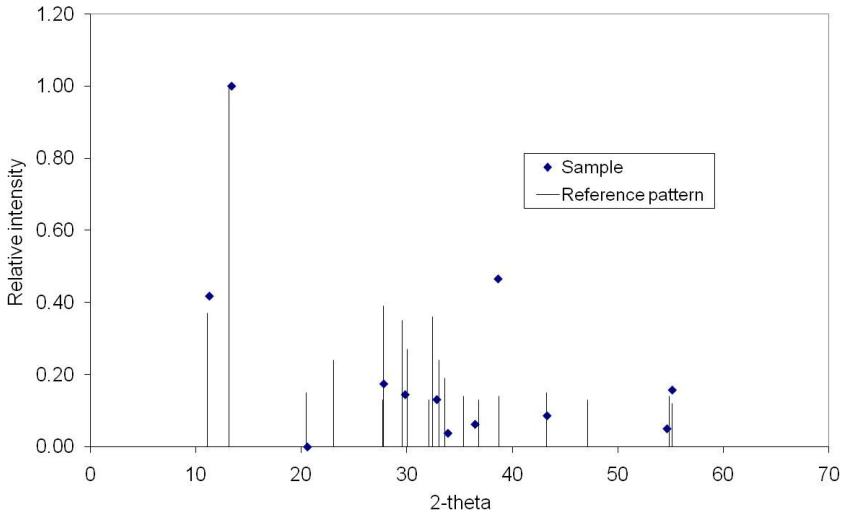

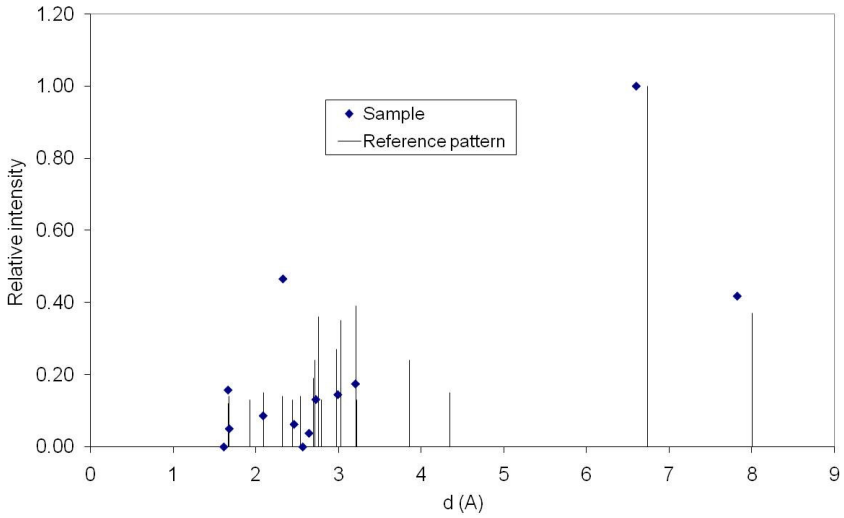

APPENDIX B: SUPPLEMENTARY INFORMATION

In Chapters 4 and 5, I used the following constants for goethite charging, citing the work of Dixit and Hering (2003):

$$>FeOH + H^+ \quad =>FeOH_2^+ \quad pK_{a1} = 7.47 \qquad \text{(Equation B-1)}$$

$$>FeO^- + H^+ \quad =>FeOH \quad pK_{a2} = 9.51 \qquad \text{(Equation B-2)}$$

Dixit and Hering drew these constants from a paper (Liger et al., 1999) in which the authors investigated adsorption of Fe(II) onto goethite. However, the Liger et al. paper used the Constant Capacitance (CC) model, while Dixit and Hering used the Diffuse Double Layer (DDL) model. It is invalid to use constants optimized in one model framework in a different framework. This calls into question the validity of the binding constants for As(III) and As(V) adsorption onto goethite, calculated in (Dixit and Hering, 2003), as well as the binding constant for Fe(II) onto goethite calculated in (Dixit and Hering, 2006).

I recognize that it would be best to re-optimize the As(III), As(V), and Fe(II) binding constants using goethite charging constants appropriate to the DDL model. However, I lack the time and ability to do this and instead have performed a sensitivity analysis to show that the variation in goethite charging constant has little impact under our experimental conditions.

Mathur and Dzombak (2006) have reviewed available data for goethite regarding surface charging and adsorption of anions and cations, and used these various datasets to optimize constants using the DDL model . They report somewhat different goethite charging

constants, with mean pK_{a1} = 6.93 +/- 0.07 and mean pK_{a2} = 9.65 +/- 0.05. Especially the first constant is substantially different from the value used by Dixit and Hering.

As a sensitivity test, I have run the model using the lower confidence interval value for pK_{a1} (6.86) and the higher confidence interval value for pK_{a2} (9.70), keeping the other binding constant unchanged.

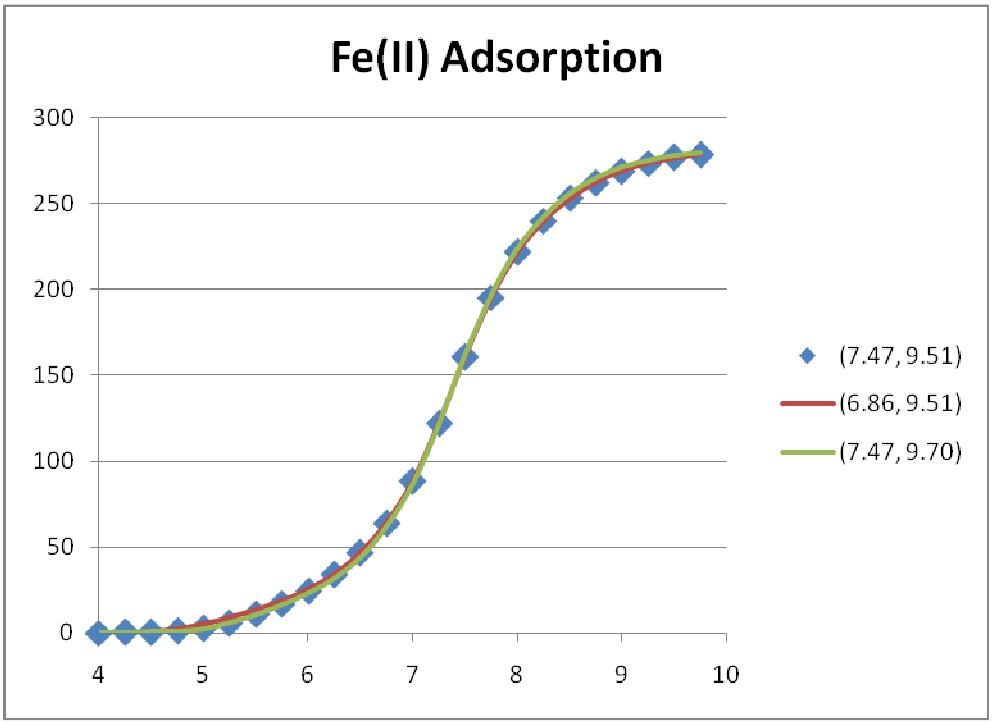

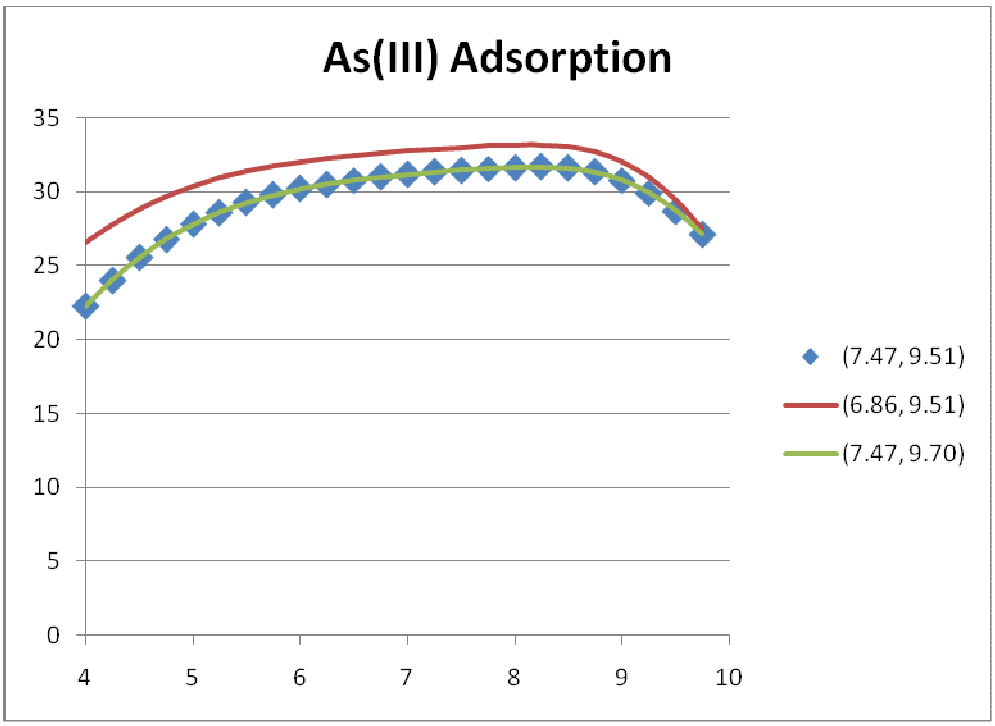

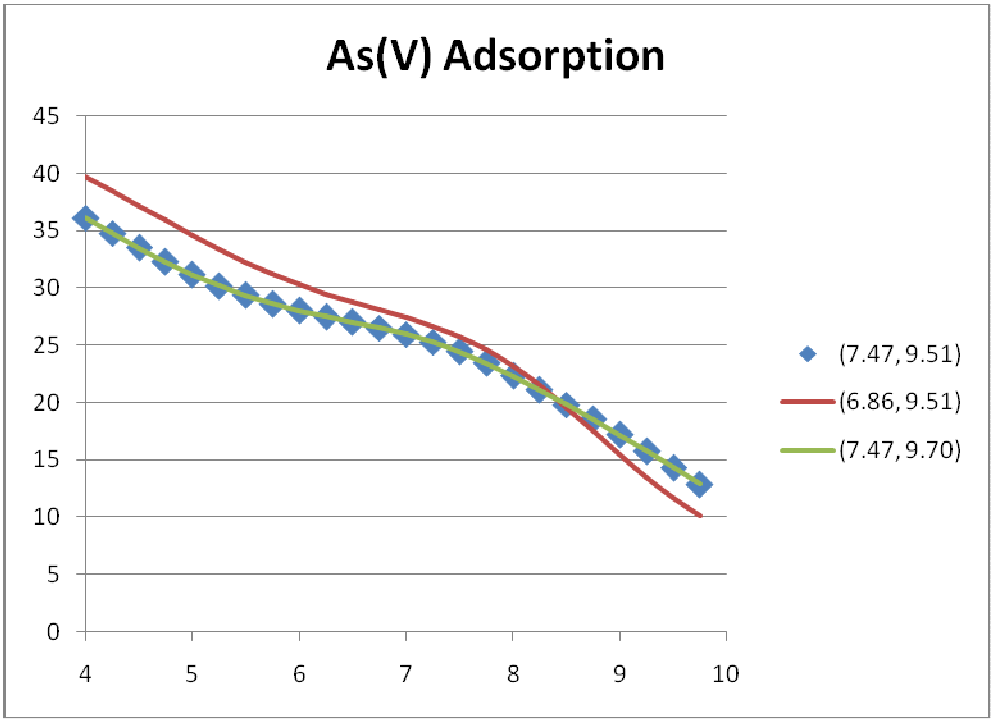

For adsorption of Fe(II), the impact of the different charging constants is negligible.

For As(III) and As(V), the use of the lower pK_{a1} leads to a model prediction of greater adsorption, due to a greater positive charge on the surface. The use of a slightly higher pK_{a2} had nearly no effect on the model.

The combination of the lower pK_{a1} and the arsenite bonding constants of Dixit and Hering leads to a prediction of greater adsorption of As(III) than when all of the Dixit and Hering parameters are used. The Dixit and Hering constants led to a slight underprediction of As(III) adsorption compared to our data, so it is possible that using the lower goethite charging constant a better data fit could be made. However, if the arsenite bonding constants were re-optimized using the lower pK_{a1} constant for goethite, much of this difference would be negated: presumably, the As(III) constants would be slightly different, leading to a similar overall prediction of adsorption. The same can be said of the As(V) surface complexation constants, though since the magnitude of adsorption varies more with pH, there could be larger differences between model predictions using the current and the re-optimized constants.

For the modeling work described in this dissertation, it would be best to re-optimize the arsenic and iron surface complexation constants, using more appropriate goethite charging constants. However, under the experimental conditions described, the impact of using a mix of appropriate (goethite charging) and incorrectly optimized [Fe(II), As(III), As(V)] constants is minor. I expect that using a fully consistent set of surface complexation modeling constants would yield model predictions very much similar to those generated using all of the Dixit and Hering constants.

REFERENCES

Aggett, J. and G. A. Obrien (1985). "Detailed Model for the Mobility of Arsenic in Lacustrine Sediments Based on Measurements in Lake Ohakuri." Environmental Science and Technology **19**(3): 231-238.

Ahmed, K. M., P. Bhattacharya, et al. (2004). "Arsenic enrichment in groundwater of the alluvial aquifers in Bangladesh: an overview." Applied Geochemistry **19**(2): 181-200.

Akai, J., K. Izumi, et al. (2004). "Mineralogical and geomicrobiological investigations on groundwater arsenic enrichment in Bangladesh." Applied Geochemistry **19**(2): 215-230.

Allison, J. D., D. S. Brown, et al. (1991). MINTEQA2/PRODEFA2, a geochemical assessment model for environmental systems. Athens, GA, USEPA Environmental Research Laboratory.

Amonette, J. E., D. J. Workman, et al. (2000). "Dechlorination of carbon tetrachloride by Fe(II) associated with goethite." Environmental Science and Technology **34**(21): 4606-4613.

Appelo, C. A. J. and W. W. J. M. de Vet (2003). Modeling in situ Iron Removal from Groundwater with Trace Elements such as As. Arsenic in Groundwater: Geochemistry and Occurrence. A. H. Welch and K. G. Stollenwerk. Boston, Kluwer Academic Publishers**:** 381-401.

Appelo, C. A. J., B. Drijver, et al. (1999). "Modeling in situ iron removal from ground water." Ground Water **37**(6): 811-817.

Appelo, C. A. J., M. J. J. Van der Weiden, et al. (2002). "Surface complexation of ferrous iron and carbonate on ferrihydrite and the mobilization of arsenic." Environmental Science and Technology **36**(14): 3096-3103.

Atkinson, R., A. Posner, et al. (1967). "Adsorption of potential-determining ions at the ferric oxide-aqueous electrolyte interface." Journal of Physical Chemistry **71**: 550.

Aurillo, A. C., R. P. Mason, et al. (1994). "Speciation and Fate of Arsenic in 3 Lakes of the Aberjona Watershed." Environmental Science and Technology **28**(4): 577-585.

Ball, J. W. and D. K. Nordstrom (1991). WATEQ4F—User's manual with revised thermodynamic data base and test cases for calculating speciation of major, trace and redox elements in natural waters, U.S. Geological Survey**:** 185.

Bhattacharya, P., G. Jacks, et al. (2002). "Arsenic in groundwater of the Bengal Delta plain aquifers in Bangladesh." Bulletin of Environmental Contamination and Toxicology **69**(4): 538-545.

Bissen, M., M. M. Vieillard-Baron, et al. (2001). "TiO_2-catalyzed photooxidation of arsenite to arsenate in aqueous samples." Chemosphere **44**(4): 751-757.

Bostick, B. C. and S. Fendorf (2003). "Arsenite sorption on troilite (FeS) and pyrite (FeS2)." Geochimica Et Cosmochimica Acta **67**(5): 909-921.

Bothe, J. and P. Brown (1999a). "Arsenic immobilization by calcium arsenate formation." Environmental Science and Technology **33**(21): 3806-3811.

Bothe, J. V. and P. W. Brown (1999b). "The stabilities of calcium arsenates at 23 +/- 1 degrees C." Journal of Hazardous Materials **69**(2): 197-207.

Braester, C. and R. Martinell (1988a). "Modeling of Flow and Transport Processes in Vyredox and Nitredox Subsurface Treatment Plants." Water Science and Technology **20**(3): 165-172.

Braester, C. and R. Martinell (1988b). "The Vyredox and Nitredox Methods of *in situ* Treatment of Groundwater." Water Science and Technology **20**(3): 149-163.

Breit, G. N., H. A. Lowers, et al. (2005). "Redistribution of arsenic and iron in shallow sediments of Bangladesh." Seminar Proceedings: Behaviour of arsenic in aquifers, soilds and plants: implications for management.

Charlet, L., D. Bosbach, et al. (2002). "Natural attenuation of TCE, As, Hg linked to the heterogeneous oxidation of Fe(II): an AFM study." Chemical Geology **190**(1-4): 303-319.

Chen, H.-W., M. M. Frey, et al. (1999). "Arsenic treatment considerations." Journal of the American Water Works Association **91**(3): 74-85.

Cher, M. and N. Davidson (1955). "The kinetics of the oxygenation of ferrous iron in phosphoric acid solution." Journal of the American Chemical Society **77**: 793-798.

Cherry, J. A., A. U. Shaikh, et al. (1979). "Arsenic species as an indicator of redox conditions in groundwater." Journal of Hydrology **43**: 373-392.

Cotton, F. A. and G. Wilkinson (1988). Advanced Inorganic Chemistry. New York, Wiley.

Coughlin, B. R. and A. T. Stone (1995). "Nonreversible adsorption of divalent metal-ions (Mn-II, Co-II Ni-II Cu-II and Pb-II) onto goethite - effects of acidification, Fe-II addition, and picolinic acid addition." Environmental Science and Technology **29**(9): 2445-2455.

CRC (2005). "CRC Handbook of Chemistry and Physics, 85th Ed."

Cummings, D. E., F. Caccavo, Jr, et al. (1999). "Arsenic mobilization by the dissimilatory Fe(III)-reducing bacterium Shewanella alga BrY." Environmental Science and Technology **33**(5): 723-729.

Davies, S. H. R. and J. J. Morgan (1989). "Manganese (II) oxidation kinetics on metal oxide surfaces." Journal of Colloid and Interface Science **129**(1): 63-77.

Davis, J. A. and D. B. Kent (1990). Surface complexation modeling in aqueous geochemistry. Reviews in Mineralogy: mineral-water interface geochemistry. M. F. Hochella and A. F. White. Washington, DC, Mineralogical Society of America. **23:** 177-260.

Davison, W. and G. Seed (1983). "The kinetics of the oxidation of ferrous iron in synthetic and natural waters." Geochimica et Cosmochimica Acta **47**: 67-79.

Dixit, S. and J. G. Hering (2003). "Comparison of arsenic(V) and arsenic(III) sorption onto iron oxide minerals: Implications for arsenic mobility." Environmental Science and Technology **37**(18): 4182-4189.

Dixit, S. and J. G. Hering (2006). "Sorption of Fe(II) and As(III) on goethite in single- and dual-sorbate systems." Chemical Geology **228**(1-3): 6-15.

Dove, P. M. and J. D. Rimstidt (1985). "The solubility and stability of scorodite, $FeAsO_4$-$2H_20$." American Mineralogist **70**: 838-844.

DPHE/BGS/MML. (2000). "Groundwater Studies for Arsenic Contamination in Bangladesh. Phase 2: *National Hydrochemical Survey*." Retrieved May, 2000, from http://www.bgs.ac.uk/arsenic/Bangladesh.

Dzombak, D. A. and M. M. Morel (1990). Surface complexation modeling. New York, Wiley & Sons.

Eary, L. E., J. A. Schramke, et al. (1990). Rates of inorganic oxidation reactions involving dissolved oxygen. Chemical modeling of aqueous systems II, American Chemical Society. Washington, DC, United States. 1990.

Edwards, M. (1994). "Chemistry of arsenic removal during coagulation and Fe-Mn oxidation." Journal of American Water Works Association **86**(9): 64-78.

Emett, M. T. and G. H. Khoe (2001). "Photochemical oxidation of arsenic by oxygen and iron in acidic solutions." Water Research **35**(3): 649-656.

Essington, M. E. (1988). "Division S-2 - Soil Chemistry - Solubility of Barium Arsenate." Soil Science Society of America Journal **52**(6): 1566-1570.

Farquhar, M. L., J. M. Charnock, et al. (2002). "Mechanisms of arsenic uptake from aqueous solution by interaction with goethite, lepidocrocite, mackinawite, and pyrite: An X-ray absorption spectroscopy study." Environmental Science and Technology **36**(8): 1757-1762.

Fendorf, S., M. J. Eick, et al. (1997). "Arsenate and chromate retention mechanisms on goethite .1. Surface structure." Environmental Science and Technology **31**(2): 315-320.

Fendorf, S. E. and G. C. Li (1996). "Kinetics of chromate reduction by ferrous iron." Environmental Science and Technology **30**(5): 1614-1617.

Ficklin, W. H. (1983). "Separation of As(III) and As(V) in groundwaters by ion-exchange." Talanta **30**(5): 371.

Frey, M. M., D. M. Owen, et al. (1998). "Cost to utilities of a lower MCL for arsenic." Journal of the American Water Works Association **90**(3): 89-102.

Frost, R. L., W. Martens, et al. (2003). "Raman spectroscopic study of the vivianite arsenate minerals." Journal of Raman Spectroscopy **34**(10): 751-759.

Gao, Y. and A. Mucci (2001). "Acid base reactions, phosphate and arsenate complexation, and their competitive adsorption at the surface of goethite in 0.7 M NaCl solution." Geochimica Et Cosmochimica Acta **65**(14): 2361-2378.

Geelhoed, J. S., T. Hiemstra, et al. (1997). "Phosphate and sulfate adsorption on goethite: Single anion and competitive adsorption." Geochimica Et Cosmochimica Acta **61**(12): 2389-2396.

Gibbs, C. R. (1976). "Characterization and application of Ferrozine iron reagent as a ferrous iron indicator." Analytical Chemistry **48**(8): 1197-1201.

Goldberg, S. (2002). "Competitive adsorption of arsenate and arsenite on oxides and clay minerals." Soil Science Society of America Journal **66**(2): 413-421.

Goldberg, S. and C. T. Johnston (2001). "Mechanisms of arsenic adsorption on amorphous oxides evaluated using macroscopic measurements, vibrational spectroscopy, and surface complexation modeling." Journal of Colloid and Interface Science **234**(1): 204-216.

Gonzalez, V. L. E. and A. J. Monhemius (1998). The mineraology of arsenates relating to arsenic impurity control. Arsenic Metallurgy, Fundamentals and Applications. R. G. Reddy, H. L. Hendrix and P. B. Queneau. Warrendale, PA, Metallurgical Society**:** 405-454.

Good, N. E., G. D. Winget, et al. (1966). "Hydrogen ion buffers for biological research." Biochemistry **5**(2): 467-&.

Grady, J. K., N. D. Chasteen, et al. (1988). "Radicals from Goods Buffers." Analytical Biochemistry **173**(1): 111-115.

Grombach, P. (1985). "Groundwater treatment *in situ* in the aquifer." Water Supply **3**(1): 13-18.

Harvey, C. F., C. H. Swartz, et al. (2002). "Arsenic mobility and groundwater extraction in Bangladesh." Science **298**(5598): 1602-1606.

Hayes, K. F. and J. O. Leckie (1986). "Mechanism of Lead-Ion Adsorption at the Goethite-Water Interface." Acs Symposium Series **323**: 114-141.

Hering, J. G., P. Y. Chen, et al. (1996). "Arsenic removal by ferric chloride." Journal American Water Works Association **88**(4): 155-167.

Hess, R. E. and R. W. Blanchar (1976). "Arsenic stability in contaminated soils." Soil Science Society America Journal **40**: 847-852.

Hiemstra, T. and W. H. Van Riemsdijk (1999). "Surface structural ion adsorption modeling of competitive binding of oxyanions by metal (hydr)oxides." Journal of Colloid and Interface Science **210**(1): 182-193.

Hiemstra, T. and W. H. van Riemsdijk (2007). "Adsorption and surface oxidation of Fe(II) on metal (hydr)oxides." Geochimica Et Cosmochimica Acta **71**(24): 5913-5933.

Hiemstra, T., P. Venema, et al. (1996). "Intrinsic proton affinity of reactive surface groups of metal (hydr)oxides: The bond valence principle." Journal of Colloid and Interface Science **184**(2): 680-692.

Horneman, A., A. Van Geen, et al. (2004). "Decoupling of As and Fe release to Bangladesh groundwater under reducing conditions. Part 1: Evidence from sediment profiles." Geochimica Et Cosmochimica Acta **68**(17): 3459-3473.

Hug, S. J., L. Canonica, et al. (2001). "Solar oxidation and removal of arsenic at circumneutral pH in iron containing waters." Environmental Science and Technology **35**(10): 2114-2121.

Hug, S. J. and O. Leupin (2003). "Iron-catalyzed oxidation of arsenic(III) by oxygen and by hydrogen peroxide: pH-dependent formation of oxidants in the Fenton reaction." Environmental Science and Technology **37**(12): 2734-2742.

Jain, A. and R. H. Loeppert (2000). "Effect of competing anions on the adsorption of arsenate and arsenite by ferrihydrite." Journal of Environmental Quality **29**(5): 1422-1430.

Jain, A., K. Raven, et al. (1999). "Arsenite and arsenate adsorption on ferrihydrite: Surface charge reduction and net OH- release stoichiometry." Environmental Science and Technology **33**(8): 1179-1184.

Jechlinger, G., W. Kasper, et al. (1985). "The removal of iron and manganese in groundwaters through aeration of the underground." Water Supply **3**(1): 19-25.

Jeon, B. H., B. A. Dempsey, et al. (2003). "Kinetics and mechanisms for reactions of Fe(II) with iron(III) oxides." Environmental Science and Technology **37**(15): 3309-3315.

Jeon, B. H., B. A. Dempsey, et al. (2001). "Reactions of ferrous iron with hematite." Colloids and Surfaces A: Physicochemical and Engineering Aspects **191**(1-2): 41-55.

Johnston, R. and P. C. Singer (2007a). "Redox reactions in the Fe–As–O_2 system." Chemosphere **69**(4): 517-525.

Johnston, R. B. and P. C. Singer (2007b). "Solubility of symplesite (ferrous arsenate): implications for reduced groundwaters and other geochemical environments." Soil Science Society of America Journal **71**(1): 101-107.

Juang, R. S. and J. Y. Chung (2004). "Equilibrium sorption of heavy metals and phosphate from single- and binary-sorbate solutions on goethite." Journal of Colloid and Interface Science **275**(1): 53-60.

Katsoyiannis, I., A. Zouboulis, et al. (2002). "As(III) removal from groundwaters using fixed-bed upflow bioreactors." Chemosphere **47**(3): 325-332.

Khaodhiar, S., M. Azizian, et al. (2000). "Copper, chromium, and arsenic adsorption and equilibrium modeling in an iron-oxide-coated sand, background electrolyte system." Water Air and Soil Pollution **119**(1-4): 105-120.

Khoe, G. H., J. C. Huang, et al. (1991). Precipitation chemistry of the aqueous ferrous-arsenate system. EPD Congress 1991.

King, D. W. (1998). "Role of carbonate speciation on the oxidation rate of Fe(II) in aquatic systems." Environmental Science and Technology **32**(19): 2997-3003.

King, D. W. and R. Farlow (2000). "Role of carbonate speciation on the oxidation of Fe(II) by H2O2." Marine Chemistry **70**(1-3): 201-209.

Klaning, U. K., B. H. J. Bielski, et al. (1989). "Arsenic(IV) - a Pulse-Radiolysis Study." Inorganic Chemistry **28**(14): 2717-2724.

Klausen, J., S. P. Trober, et al. (1995). "Reduction of Substituted Nitrobenzenes by Fe(II) in Aqueous Mineral Suspensions." Environmental Science and Technology **29**(9): 2396-2404.

Lazaridis, N. K., D. N. Bakoyannakis, et al. (2005). "Chromium(VI) sorptive removal from aqueous solutions by nanocrystalline akaganeite." Chemosphere **58**(1): 65-73.

Lee, Y., I. H. Um, et al. (2003). "Arsenic(III) oxidation by iron(VI) (ferrate) and subsequent removal of arsenic(V) by iron(III) coagulation." Environmental Science and Technology **37**(24): 5750-5756.

Lenhart, J. J. and B. D. Honeyman (1999). "Uranium(VI) sorption to hematite in the presence of humic acid." Geochimica Et Cosmochimica Acta **63**(19-20): 2891-2901.

Liang, J., R. K. Xu, et al. (2007). "Effect of arsenate on adsorption of Cd(II) by two variable charge soils." Chemosphere **67**(10): 1949-1955.

Liger, E., L. Charlet, et al. (1999). "Surface catalysis of uranium(VI) reduction by iron(II)." Geochimica Et Cosmochimica Acta **63**(19-20): 2939-2955.

Lin, S. H., H. C. Kao, et al. (2004). "An EXAFS study of the structures of copper and phosphate sorbed onto goethite." Colloids and Surfaces A: Physicochemical and Engineering Aspects **234**(1-3): 71-75.

Lovley, D. R. (1991). "Dissimilatory Fe(III) and Mn(IV) Reduction." Microbiological Reviews **55**(2): 259-287.

Luengo, C., M. Brigante, et al. (2007). "Adsorption kinetics of phosphate and arsenate on goethite. A comparative study." Journal of Colloid and Interface Science **311**(2): 354-360.

Lumsdon, D. G. and L. J. Evans (1994). "Surface complexation model parameters for goethite (α-FeOOH)." Journal of Colloid and Interface Science **164**(1): 119-125.

Luther III, G. W. (1990). The frontier-molecular-orbital theory approach in geochemical processes. Aquatic chemical kinetics: reaction rates of processes in natural waters. W. Stumm. New York, Wiley**:** 172-198.

Manning, B. and S. Goldberg (1996). "Modelling competitive adsorption of arsenate with phosphate and molybdate on oxide minerals." Soil Science Society of America Journal **60**: 121-13.

Manning, B. A., S. E. Fendorf, et al. (2002). "Arsenic(III) oxidation and arsenic(V) adsorption reactions on synthetic birnessite." Environmental Science and Technology **36**(5): 976-981.

Manning, B. A., S. E. Fendorf, et al. (1998). "Surface structures and stability of arsenic(III) on goethite: Spectroscopic evidence for inner-sphere complexes." Environmental Science and Technology **32**(16): 2383-2388.

Manning, B. A. and S. Goldberg (1997). "Arsenic(III) and arsenic(V) absorption on three California soils." Soil Science **162**(12): 886-895.

Maogong, F. (1988). "The Applications of Vyredox Method Regarding Iron Removal from Ground-Water in China." Ground Water **26**(5): 647-648.

Martin, T. A. and J. H. Kempton (2000). "In situ stabilization of metal-contaminated ground water by hydrous ferric oxide: An experimental and modeling investigation." Environmental Science and Technology **34**(15): 3229-3234.

Mash, H. E., Y. P. Chin, et al. (2003). "Complexation of Copper by Zwitterionic Aminosulfonic (Good) Buffers." Analytical Chemistry **75**(3): 671-677.

Mathur, S. S. and D. A. Dzombak (2006). Surface complexation modeling: Goethite. Surface complexation modeling. J. Lützenkirchen. Amsterdam, Elsevier**:** 443-468.

Matisoff, G., C. J. Khourey, et al. (1982). "The nature and source of arsenic in northeastern Ohio groundwater." Ground Water **20**: 446-456.

Matthess, G. (1981). "In situ treatment of arsenic contaminated groundwater." Science of the Total Environment **21**(99): 99-104.

Meng, X. G., G. P. Korfiatis, et al. (2002). "Combined effects of anions on arsenic removal by iron hydroxides." Toxicology Letters **133**(1): 103-111.

Mettler, S. (2002). In situ removal from ground water: Fe(II) oxygenation, and precipitation products in a calcareous aquifer. Water Resources and Drinking Water. Zurich, Swiss Federal Institute for Environmental Science and Technology**:** 122.

Mettler, S., M. Abdelmoula, et al. (2001). "Characterization of iron and manganese precipitates from an in situ groundwater treatment plant." Ground Water **39**(6): 921-930.

Millero, F. J. (1985). "The Effect of Ionic Interactions on the Oxidation of Metals in Natural-Waters." Geochimica Et Cosmochimica Acta **49**(2): 547-553.

Millero, F. J., S. Sotolongo, et al. (1987). "The Oxidation-Kinetics of Fe(II) in Seawater." Geochimica Et Cosmochimica Acta **51**(4): 793-801.

Morel, F. and J. G. Hering (1993). Principles and applications of aquatic chemistry. New York, Wiley.

Mori, H. and T. Ito (1950). "The structure of vivianite and symplesite." Acta Crystallographica **3**: 1-6.

Mouchet, P. (1992). "From conventional to biological removal of iron and manganese in France." Journal American Water Works Association **84**(4): 158-166.

Nano, G. V. and T. J. Strathmann (2006). "Ferrous iron sorption by hydrous metal oxides." Journal of Colloid and Interface Science **297**(2): 443-454.

Nickson, R., J. McArthur, et al. (1998). "Arsenic poisoning of Bangladesh groundwater [letter]." Nature **395**(6700): 338.

Nickson, R., J. McArthur, et al. (2000). "Mechanism of arsenic release to groundwater, Bangladesh and West Bengal." Applied Geochemistry **15**(4): 403-413.

O'Reilly, S. E., D. G. Strawn, et al. (2001). "Residence time effects on arsenate adsorption/desorption mechanisms on goethite." Soil Science Society of America Journal **65**(1): 67-77.

Oremland, R. S., J. F. Stolz, et al. (2004). "The microbial arsenic cycle in Mono Lake, California." FEMS Microbiology Ecology **48**: 15-27.

Papassiopi, N., K. Vaxevanidou, et al. (2003). "Investigating the Use of Iron Reducing Bacteria for the Removal of Arsenic from Contaminated Soils." Water, Air, & Soil Pollution: Focus **3**(3): 81 - 90.

Parkhurst, D. L. and C. A. J. Appelo (1999). User's guide to PHREEQC (version 2): a computer program for speciation, batch-reaction, one dimensional transport, and inverse geochemical calculations. Denver, CO, U.S. Geological Survey**:** xiv, 312.

Parkhurst, D. L., K. L. Kipp, et al. (2008). PHAST: a program for simulating ground-water flow, solute transport, and multicomponent geochemical reactions (version 1.5.1). U.S. Geological Survey Techniques and Methods 6–A8. Denver, CO, U.S. Geological Survey**:** 151.

Peacock, C. L. and D. M. Sherman (2004). "Copper(II) sorption onto goethite, hematite and lepidocrocite: A surface complexation model based on *ab initio* molecular geometries and EXAFS spectroscopy." Geochimica Et Cosmochimica Acta **68**(12): 2623-2637.

Peak, D. and D. L. Sparks (2002). "Mechanisms of selenate adsorption on iron oxides and hydroxides." Environmental Science and Technology **36**(7): 1460-1466.

Pecher, K., S. B. Haderlein, et al. (2002). "Reduction of polyhalogenated methanes by surface-bound Fe(II) in aqueous suspensions of iron oxides." Environmental Science and Technology **36**(8): 1734-1741.

Pettine, M., L. D'Ottone, et al. (1998). "The reduction of chromium (VI) by iron (II) in aqueous solutions." Geochimica Et Cosmochimica Acta **62**(9): 1509-1519.

Pierce, M. L. and C. B. Moore (1982). "Adsorption of arsenite and arsenate on amorphous iron hydroxide." Water Resources **16**: 1247-1253.

Radu, T., J. L. Subacz, et al. (2005). "Effects of dissolved carbonate on arsenic adsorption and mobility." Environmental Science and Technology **39**(20): 7875-7882.

Raven, K. P., A. Jain, et al. (1998). "Arsenite and arsenate adsorption on ferrihydrite: Kinetics, equilibrium, and adsorption envelopes." Environmental Science and Technology **32**(3): 344-349.

Ravenscroft, P. (2008). Predicting the global extent of arsenic pollution of groundwater and its potential impact on human health. New York, UNICEF.

Reinke, L., J. Rau, et al. (1994). "Characteristics of an oxidant formed during Fe(II) oxidation." Free radical biology and medicine **16**(4): 485-492.

Roberts, L. C., S. J. Hug, et al. (2004). "Arsenic removal with iron(II) and iron(III) waters with high silicate and phosphate concentrations." Environmental Science and Technology **38**(1): 307-315.

Roberts, W. L., T. J. Campbell, et al., Eds. (1990). Encyclopedia of minerals. New York, Chapman & Hall.

Rochette, E. A., G. C. Li, et al. (1998). "Stability of arsenate minerals in soil under biotically generated reducing conditions." Soil Science Society America Journal **62**: 1530-1537.

Rott, U. and M. Friedle (2000). "Eco-friendly and cost-efficient removal of arsenic, iron and manganese by means of subterranean ground-water treatment." Water Supply **18**(1): 632-635.

Rott, U., C. Meyer, et al. (2002). "Residue-free removal of arsenic, iron, manganese and ammonia from groundwater." Water Supply **2**(1): 17-24.

Sadiq, M. (1997). "Arsenic chemistry in soils: An overview of thermodynamic predictions and field observations." Water Air and Soil Pollution **93**(1-4): 117-136.

Sarkar, A. R. and O. T. Rahman (2001). In situ removal of arsenic - experiences of DPHE-Danida pilot project. Dhaka, Bangladesh, Danida SPS for Water Supply and Sanitation.

Schindler, P. W. and W. Stumm (1987). The Surface Chemistry of Oxides, Hydroxides and Oxide Minerals. Aquatic surface chemistry: chemical processes at the particle-water interface. W. Stumm. New York, Wiley**:** pp. 83-110.

Schreiber, M., J. Simo, et al. (2000). "Stratigraphic and geochemical controls on naturally occurring arsenic in groundwater, eastern Wisconsin, USA." Hydrogeology Journal **8**: 161-176.

Schwertmann, U. and R. M. Cornell (2000). Iron oxides in the laboratory : preparation and characterization. Weinheim ; New York, Wiley-VCH.

Shackelford, C. D. (1994). "Critical Concepts for Column Testing." Journal of Geotechnical Engineering-Asce **120**(10): 1804-1828.

Sharma, S., B. Petrusevski, et al. (2005). "Biological removal of iron from groundwater: a review." Journal of Water Supply, Research and Technology: Aqua.

Silvester, E., L. Charlet, et al. (2005). "Redox potential measurements and Mossbauer spectrometry of Fe-II adsorbed onto Fe-III (oxyhydr)oxides." Geochimica Et Cosmochimica Acta **69**(20): 4801-4815.

Singer, P. C. (1972). "Anaerobic control of phosphate by ferrous iron." Journal of the Water Pollution and Control Federation **44**(4): 663-669.

Singer, P. C. and W. Stumm (1970). "Acid mine drainage - the rate-limiting step." Science **167**(3921): 1121-1123.

Smedley, P. L. and D. G. Kinniburgh (2002). "A review of the source, behaviour and distribution of arsenic in natural waters." Applied Geochemistry **17**(5): 517-568.

Smith, R. M. and A. E. Martell (2001). NIST critically selected stability constants of metal complexes. Gaithersburg, Md., U.S. Dept. of Commerce National Institute of Standards and Technology Standard Reference Data Program.

Solozhenkin, P. M., E. A. Deliyanni, et al. (2003). "Removal of As(V) ions from solution by akaganeite β-FeO(OH) nanocrystals." Journal of Mining Science **39**(3): 287-296.

Sposito, G. (1989). The Chemistry of Soils. New York, Oxford University Press.

Stollenwerk, K. G., G. N. Breit, et al. (2007). "Arsenic attenuation by oxidized aquifer sediments in Bangladesh." Science of the Total Environment **379**(2-3): 133-150.

Stookey, L. L. (1970). "Ferrozine - a new spectrophotometric reagent for iron." Analytical Chemistry **42**(7): 779-781.

Strathmann, T. J. and A. T. Stone (2001). "Reduction of the carbamate pesticides oxamyl and methomyl by dissolved Fe-II and Cu-I." Environmental Science and Technology **35**(12): 2461-2469.

Strathmann, T. J. and A. T. Stone (2002). "Reduction of the pesticides oxamyl and methomyl by Fe-II: Effect of pH and inorganic ligands." Environmental Science and Technology **36**(4): 653-661.

Stumm, W. (1992). Chemistry of the Solid-Water Interface. New York, Wiley.

Stumm, W. and G. F. Lee (1961). "Oxygenation of ferrous iron." Industrial & Engineering Chemistry **53**(2): 143-146.

Stumm, W. and J. J. Morgan (1996). Aquatic Chemistry: Chemical Equilibria and Rates in Natural Waters. New York, Wiley.

Stumm, W. and B. Sulzberger (1992). "The Cycling of Iron in Natural Environments - Considerations Based on Laboratory Studies of Heterogeneous Redox Processes." Geochimica Et Cosmochimica Acta **56**(8): 3233-3257.

Su, C. M. and R. W. Puls (2001). "Arsenate and arsenite removal by zerovalent iron: Effects of phosphate, silicate, carbonate, borate, sulfate, chromate, molybdate, and nitrate, relative to chloride." Environmental Science and Technology **35**(22): 4562-4568.

Sun, X. H. and H. E. Doner (1998). "Adsorption and oxidation of arsenite on goethite." Soil Science **163**(4): 278-287.

Sung, W. and J. J. Morgan (1980). "Kinetics and Product of Ferrous Iron Oxygenation in Aqueous Systems." Environmental Science and Technology **14**(5): 561-568.

Tamura, H., K. Goto, et al. (1976). "The effect of ferric hydroxide on the oxygenation of ferrous ions in neutral solutions." Corrosion Science **16**: 197-207.

Tamura, H., S. Kawamura, et al. (1980). "Acceleration of the oxidation of Fe-2+ ions by Fe(III)-oxyhydroxides." Corrosion Science **20**(8-9): 963-971.

Tyrrel, S. F. and P. Howsam (1997). "Aspects of the occurrence and behaviour of iron bacteria in boreholes and aquifers. Quarterly Journal of Engineering Geology 30, 161-169." Quarterly Journal of Engineering Geology **30**: 161-169.

USEPA (1998). Mineralogical Study of Borehole MW-206, Asarco Smelter Site, Tacoma, Washington. Seattle, WA, USEPA.

USEPA (2000). Arsenic in drinking water rule: Economic analysis. Washington, D.C., USEPA.

USEPA (2001a). Laboratory study on the oxidation of arsenic III to arsenic V. Washington, D.C., USEPA.

USEPA (2001b). National Primary Drinking Water Regulations; Arsenic and Clarifications to Compliance and New Source Contaminants Monitoring; Final Rule. 40 CFR Parts 9, 141 and 142. Federal Register / Vol. 66, No. 14 / Monday, January 22, 2001 / Rules and Regulations.

van Geen, A., A. P. Robertson, et al. (1994). "Complexation of Carbonate Species at the Goethite Surface - Implications for Adsorption of Metal-Ions in Natural-Waters." Geochimica Et Cosmochimica Acta **58**(9): 2073-2086.

Vikesland, P. J. and R. L. Valentine (2000). "Reaction pathways involved in the reduction of monochloramine by ferrous iron." Environmental Science and Technology **34**(1): 83-90.

Vikesland, P. J. and R. L. Valentine (2002). "Iron oxide surface-catalyzed oxidation of ferrous iron by monochloramine: Implications of oxide type and carbonate on reactivity." Environmental Science and Technology **36**(3): 512-519.

Villalobos, M. and J. O. Leckie (2000). "Carbonate adsorption on goethite under closed and open CO_2 conditions." Geochimica Et Cosmochimica Acta **64**(22): 3787-3802.

Voigt, D. E., S. L. Brantley, et al. (1996). "Chemical fixation of arsenic in contaminated soils." Applied Geochemistry **11**(5): 633-&.

Wang, K. J. and B. S. Xing (2004). "Mutual effects of cadmium and phosphate on their adsorption and desorption by goethite." Environmental Pollution **127**(1): 13-20.

Waychunas, G. A., J. A. Davis, et al. (1995). "Geometry of Sorbed Arsenate on Ferrihydrite and Crystalline FeOOH - Reevaluation of EXAFS Results and Topological Factors in Predicting Sorbate Geometry, and Evidence for Monodentate Complexes." Geochimica Et Cosmochimica Acta **59**(17): 3655-3661.

Waychunas, G. A., C. C. Fuller, et al. (1996). "Wide angle X-ray scattering (WAXS) study of "two-line" ferrihydrite structure: Effect of arsenate sorption and counterion variation and comparison with EXAFS results." Geochimica Et Cosmochimica Acta **60**(10): 1765-1781.

Waychunas, G. A., B. A. Rea, et al. (1993). "Surface-Chemistry of Ferrihydrite .1. EXAFS Studies of the Geometry of Coprecipitated and Adsorbed Arsenate." Geochimica Et Cosmochimica Acta **57**(10): 2251-2269.

Wehrli, B. (1990). Redox reactions of metal ions at mineral surfaces. Aquatic chemical kinetics: reaction rates of processes in natural waters. W. Stumm. New York, Wiley**:** 311-336.

Weiss, J. (1935). Naturwissenschaften **23**.

Welch, A. H., K. G. Stollenwerk, et al. (2000). Preliminary evaluation of the potential for in situ arsenic removal from groundwater. Pre-Congress Workshop, Arsenic in Groundwater of Sedimentary Aquifers. 31st International Geological Congress, Rio de Janeiro, Brazil.

Welch, A. H., K. G. Stollenwerk, et al. (2003). In situ arsenic remediation in a fractured, alkaline aquifer. Arsenic in Ground Water: Geochemistry and Occurrence. A. H. Welch and K. G. Stollenwerk. Boston, Kluwer.

Welch, A. H., D. B. Westjohn, et al. (2000). "Arsenic in ground water of the United States: Occurrence and geochemistry." Ground Water **38**(4): 589-604.

WHO (2001). Environmental Health Criteria 224: Arsenic and Arsenic compounds, WHO.

WHO (2004). Guidelines for drinking-water quality, 3rd edition. Geneva, World Health Organization.

Wijnja, H. and C. P. Schulthess (2001). "Carbonate adsorption mechanism on goethite studied with ATR- FTIR, DRIFT, and proton coadsorption measurements." Soil Science Society of America Journal **65**(2): 324-330.

Wilkie, J. A. and J. G. Hering (1996). "Adsorption of arsenic onto hydrous ferric oxide: effects of adsorbate/adsorbent ratios and co-occurring solutes." Colloids and Surfaces A: Physicochemical and Engineering Aspects **107**: 97-110.

Wilkie, J. A. and J. G. Hering (1998). "Rapid oxidation of geothermal arsenic(III) in streamwaters of the eastern Sierra Nevada." Environmental Science and Technology **32**(5): 657-662.

Williams, A. G. B. and M. M. Scherer (2004). "Spectroscopic evidence for Fe(II)-Fe(III) electron transfer at the iron oxide-water interface." Environmental Science and Technology **38**(18): 4782-4790.

Yu, Q. Y., A. Kandegedara, et al. (1997). "Avoiding interferences from Good's buffers: A contiguous series of noncomplexing tertiary amine buffers covering the entire range of pH 3-11." Analytical Biochemistry **253**(1): 50-56.

Zachara, J. M., D. C. Girvin, et al. (1987). "Chromate Adsorption on Amorphous Iron Oxyhydroxide in the Presence of Major Groundwater Ions." Environmental Science & Technology **21**(6): 589-594.

Zhang, Y., L. Charlet, et al. (1992). "Adsorption of protons, Fe(II) and Al(III) on lepidocrocite (γ-FeOOH)." Colloids and Surfaces **63**(3-4): 259-268.

Zheng, Y., M. Stute, et al. (2004). "Redox control of arsenic mobilization in Bangladesh groundwater." Applied Geochemistry **19**(2): 201-214.